The Pennsylvania State University

The Graduate School

Department of Energy and Mineral Engineering

EVALUATION OF ULTRASONIC CAVITATION TREATMENT EFFECTS ON THE BENEFICIATION OF BITUMINOUS COAL

A Thesis in

Energy and Mineral Engineering

by

Branden Barry

Submitted in Partial Fulfillment
of the Requirements
for the Degree of

Master of Science

August 2014

The thesis of Branden Barry was reviewed and approved* by the following:

Mark S. Klima
Associate Professor of Mineral Processing
and Geo-Environmental Engineering
Thesis Advisor

Jeremy Gernand
Assistant Professor of Industrial Health
and Safety

Richard Hogg
Professor Emeritus of Mineral Processing
and Geo-Environmental Engineering

Luis F. Ayala H.
Associate Professor of Petroleum and Natural Gas Engineering
Associate Department Head for Graduate Education

*Signatures are on file in the Graduate School

ABSTRACT

Laboratory testing was conducted to evaluate the effects of hydroacoustic cavitation (HAC) treatment on two bituminous coal slurries and the performance of various subsequent separation processes. Separation process units studied were the hydrocyclone, spiral concentrator, froth flotation, and plate filter press. The pilot-scale HAC circuit consisted of a stainless-steel ultrasonic resonator chamber and in-line flow reduction cavitation orifice.

The two materials processed were nominal -1-mm and -0.15-mm Illinois Basin bituminous coal slurries. The -1-mm material (Sample A) was the feed stream to a coal preparation plant classifying hydrocyclone while the -0.15-mm material (Sample B) was the overflow stream from the same hydrocyclone. Laboratory analyses showed that Sample A had an value of 34.44±2.28% and was 4.16% total sulfur while Sample B had an ash value of 53.39±1.16% and was 2.3% total sulfur. Over 70% of the total sulfur was pyritic sulfur for both samples. Heating values were 8,656 Btu/lb and 6,423 Btu/lb for Sample A and Sample B, respectively.

HAC treatment of Sample A demonstrated that 100% power sonication (Son) and 100% power sonication with all slurry flow through the cavitation orifice (SonCav) reduced feed particle size and ash values of coarser size intervals (+150 μm). After only 5 s of treatment, the 50% cumulative passing size was reduced by about 50 μm with ash values for certain size fractions decreasing over 5% between untreated and SonCav tests. Extending treatment time led to greater degradation of the +1180-μm material with increases in the -25-μm material and reductions in ash values of central size fractions (-850+150 μm).

Utilizing the hydrocyclone at an inlet pressure of 20 psi, solids splits to the underflow stream of about 90% and 40% were achieved for Sample A and Sample B, respectively. HAC treatment concentrated sulfur in the underflow stream while reducing underflow ash values and increasing heating values as compared to the feed material. From untreated to SonCav treatment,

ash was reduced by about 16% for Sample A and 25% for Sample B while heating value increased 7% and 33% for Sample A and B, respectively.

Hydrocyclone desliming of Sample A followed by spiral concentration of the underflow stream was effective at reducing ash and total sulfur values of the feed material. SonCav treatment prior to hydrocyclone desliming and spiral concentration produced a yield of nearly 70% with reductions in ash value of almost 60% and total sulfur by 6%. The spiral negated the effect of hydrocyclone concentration of sulfur in the product stream.

Desliming Sample B by hydrocyclone followed by froth flotation reduced yields about 33% despite HAC treatment, but reduced ash values by almost 40% in some instances. Decreasing flotation time led to more dramatic reductions in product ash values (>70%) but yields were poor (~10%). The effects of desliming were more prominent than treatment in reducing ash and sulfur values for the froth product.

Pressure filtration of Sample B by plate filter press was minimally affected by HAC treatment in terms of cake moisture content as treatment caused high levels of feed stream dispersion and surface fine liberation. Reduction of filter press feed slurry pH to 4 and flocculation by a high molecular weight polymer had more noticeable effects, decreasing final cake moisture. Test runs for an untreated and 5-min SonCav treated feed stream which was flocculated and pH reduced exhibited the best performance, reaching a final cake moisture of about 36%.

TABLE OF CONTENTS

LIST OF FIGURES

LIST OF TABLES

ACKNOWLEDGEMENTS

I would like to thank my professor, advisor, and friend, Dr. Mark S. Klima for convincing me of the worth and knowledge gained through graduate studies and granting me this opportunity to further my education. His guidance and passion for this field have helped to affirm my interest in the mineral industries and have molded my skills to place me in the position I am today. I also want to thank Dr. Richard Hogg who personally ensured that I understood many of the very fundamental concepts related to my graduate work. I would also like to extend my thanks to Dr. Jeremy M. Gernand for serving on this committee despite our acquaintanceship. It is much appreciated.

Though he was unable to review this work, I want to thank Dr. M. Thaddeus Ityokumbul who helped me immensely during my undergraduate studies. Not to be forgotten, I would like to thank Tom Motel for all his help in the laboratory whether assisting in experimentation, offering advice, or making repairs. In addition, I would like to thank Furness Newburge for fabricating the hydroacoustic cavitation circuit as well as the Illinois Clean Coal Institute for providing all funding.

Though I am unsure they understood what I was doing all this time, my loving family, especially my father and mother, were continually there for support and guidance throughout my education at Penn State. Lastly, I am very grateful for my girlfriend, Rebecca Bruning, who is one of the most sincere and loving people I have ever met. She is a source of motivation and I am always reassured by the confidence she has in me.

CHAPTER 1

INTRODUCTION AND LITERATURE REVIEW

1.1 Coal Usage

Coal accounted for 37.4% of U.S. electricity generation in 2012 (EIA, 2013b) and 93% of the 890 million tons of coal consumed in the U.S. in 2012 were utilized by the electricity sector that year (EIA, 2013c). Projected to provide 40.1% of U.S. electricity generation in 2013 and 2014 (EIA, 2013d), it is predicted coal will remain the largest electricity generation source through 2040 (EIA, 2013a). However, due to increasingly stringent regulation of pollution resulting from burning coal, the Clean Air Act and imposition of legislation such as National Ambient Air Quality Standards and New Source Performance Standards threaten the existence of coal-fired power generation. Because of this, by 2015 it is estimated that over 90% of U.S. coal-fired electricity generating facilities will have installed clean coal technologies and criteria pollutant emission controls (Smith et al., 2012). In order to understand the concomitant pollution generation problem associated with burning coal and offer economic control methods, it is important to present background on this energy source.

Coal is a heterogeneous, organic rock largely consisting of carbon but also containing hydrogen, oxygen, sulfur, nitrogen, and additional inorganic components such as minerals and absorbed water (Radovic and Schobert, 1997). Moisture in coal reduces heating value and increases cost of transportation but the most undesirable components are high levels of inorganic mineral matter, which inhibit coal usage due to their incombustibility. Ash-related problems stemming from the presence of these deleterious minerals in coal are one of the primary causes of plant outages and are responsible for decreasing process efficiency (Borio and Levasseur, 1986). Examples include ash deposition in boilers and slagging, or the fusion and hardening of mineral matter on the surfaces of furnaces and boilers. Such occurrences reduce heat transfer, lead to high

furnace exhaust gas temperatures, damage metal components, and increase maintenance costs. Though rare, coal ash is occasionally beneficial such as in coal liquefaction where the gasification rate is improved by pyrite and alkalies, which act as catalysts (Vorres, 1986). Also, whether existing as components of minerals or in elemental form, heavy metals and nonmetals such as sulfur in coal combust to form polluting byproducts or remain in ash, adding toxicity. For instance, sulfur oxides such as SO_2 form during combustion in air leading to the formation of sulfuric acid in rainwater (acid rain). According to EPA Air Market Program Data from the Acid Rain Program, almost 3.3 million tons of SO_2 were emitted from coal-fired power plants in the U.S. in 2012 alone. Also, combustion products may become contaminated with toxic substances but, due to the heterogeneity of coal, these are widely variable. In bituminous coals, common trace elements include boron, beryllium, bromine, germanium, antimony, and vanadium (Gluskoter et al., 1977; Kuhn et al., 1980). Following combustion, these elements concentrate in the fly and bottom ash, which has led to a substantial increase in leaching protocol and regulations related to ash disposal and waste thresholds (Izquierdo and Querol, 2012). Leachates containing arsenic and selenium have been of particular interest due to the high environmental mobility of these substances at basic pH (Wang et al., 2009).

In 2012, the United States produced nearly 110 million tons of coal combustion products (ACAA, 2012). While about 47% of this material was used beneficially, almost 58 million tons were disposed of into open waste pits and surface waste ponds (ACAA, 2012). Though coal ash has a wide array of applications from building materials and structural fill to production of geopolymers (Izquierdo and Querol, 2012), constituents of environmental concern can make reuse infeasible. Therefore, coal beneficiation prior to combustion is necessary to decrease negative products and byproducts.

1.2 Coal Beneficiation

Upon being mined, coal is processed in a preparation facility to generate a product that is high in organic content and reduced in mineral matter and polluting constituents. Density separation processes are primarily utilized to reduce deleterious material content. Improvements in processing have made upgrading of coal increasingly efficient. However, more stringent regulations have forced facilities to upgrade, augment, and implement new processes.

Characterization of plant feed material is necessary to design a preparation plant properly. This can be accomplished through a variety of techniques including optical and scanning electron microscopy to determine shape and surface properties, sieve analysis and light scattering for size, float-sink testing for density, and ultimate and proximate analysis to determine properties related to combustion as well as mineral and elemental components.

Elimination of pollution forming minerals improves heating value, reduces harmful emissions, and allows for waste disposal at the mine, which minimizes transport and off-site disposal costs incurred by power plants. Initially, run-of-mine coal is crushed to control the top size of the feed and to achieve liberation of the organic material from the mineral matter. This is especially true if mineral matter comprises at least 15% of the coal (Vorres, 1986). The particles are then partitioned into several size fractions, and each fraction is subjected to a separation process to maximize yield and combustible recovery. For coarser material (e.g., > 1mm), density-based processes such as dense-medium vessels and cyclones are used, while the -1 mm+0.15 mm fraction is usually processed using spiral concentrators. For -0.15 mm material, the difference in constituent surface properties are often exploited using a flotation process. After processing, the streams are dewatered, typically using screens and centrifuges for the clean coal concentrate, screens for coarser refuse, and a thickener, often followed by a pressure filtration device such as a belter filter press or plate filter press for fine and ultrafine refuse. In some cases, the thickened refuse slurry is disposed into an impoundment.

Despite beneficiation, some fine mineral matter particles often remain with the coal including fine clay particles on the surface of coarser coal particles, creating separation difficulties. In addition, poorly consolidated surface clays can hinder separation by gravity- and surface-controlled cleaning processes and increase media viscosity in dense-medium systems if liberated. Also, materials may be very strongly bound or dispersed in the rock matrix of the coal generating excessive expense for full liberation by comminution. Also, physical methods alone may simply be unable to achieve separation. This is often the case with sulfur.

Sulfur exists in three forms in coal. These are organic sulfur, which is chemically bonded to carbon, pyritic sulfur or grains of mineral pyrite (FeS_2), and sulfate sulfur, which appears as iron or calcium sulfates (Radovic and Schobert, 1997). Of these forms, pyritic sulfur is most easily removed as it can be liberated by physical methods because it is mechanically and not chemically incorporated into the coal. In fact, density separation processes are effective at decreasing pyritic sulfur content. Chemical techniques such as use of strong caustic reagents are needed to remove sulfate and organic sulfur (Vorres, 1986). However, they are not practical except for specialized applications. If a sufficient quantity of sulfur cannot be removed prior to combustion, then a post-combustion capture process such as flue-gas desulfurization must be used. Examples include sorbent injection and wet and dry scrubbing.

In an attempt to improve clean coal recovery, various studies have been conducted using ultrasonic sound to improve coal processing performance. It is a novel approach capable of liberating ash forming minerals and sulfur from coal, but its full capabilities have yet to be explored.

1.3 Ultrasonic Cavitation

Ultrasound of 20-1000 kHz, known as power ultrasound, consists of high energy waves, which when used to irradiate liquids can create zones of compression and expansion (Frederick, 1965; Leighton, 1994; Mason and Lorimer, 1988). This generates varying pressure regions

leading to acoustic cavitation or the formation, growth, and near immediate collapse of microscopic voids (Frederick,1965; Leighton, 1994; Mason and Lorimer, 1988). These voids, commonly referred to as bubbles, are created in a process called homogeneous nucleation if formed in liquid, or heterogeneous nucleation if formed at a solid/liquid interface such as a particle surface in a suspension or at the wall of a containing ultrasonic vessel (Brennen, 1995). Bubble collapse produces high local temperatures of ~5000 ºC and pressures around ~1000 atm as well as large thermal and pressure gradients leading to high-energy chemical reactions (Suslick et al., 1999). Oxidation occurs as a result of sonolysis (i.e., ultrasonic treatment) in water due to the production of OH radicals, H_2O_2, and ozone stemming from the thermal dissociation of water vapor and subsequent reactions (Ambedkar et al., 2011). Collapse occurs when the bubble reaches critical size and cannot absorb additional sound field energy (Shchukin, 2011). This size is governed by the ultrasound frequency (Shchukin, 2011).

In suspensions, bubbles that collapse at solid surfaces do so in a non-spherical manner, forming high-speed liquid microjets, generating shockwaves that can damage the surface of (i.e., pitting) and even fragment solids (Shchukin, 2011; Suslick and Price, 1999). These impinging forces are responsible for ultrasonic cleaning, which dislodge unwanted surface particles and expose fresh surfaces. Shockwaves resulting from bubble collapse in the aqueous medium, away from solid surfaces, can propel proximate particles causing high-velocity interparticle collisions (Suslick and Price, 1999) and generate shear forces producing mechanical stirring (Ambedkar et al., 2011). In addition, for microjet effects to occur requires a particle surface area several times larger than the bubble size. For example, particles less than ~200 μm will be unaffected by microjet damage at an ultrasonic frequency of ~20 kHz (Suslick and Price, 1999). Submission to low-frequency (<100 kHz) ultrasound predominantly produces cavitation phenomena causing particle breakage while high-frequency (>200 kHz) ultrasound generates mainly streaming phenomena (i.e., fluid flow currents produced by sound absorption) so leaching is prevalent

(Ambedkar et al., 2011). Moreover, these ultrasonic effects may be enhanced by maintaining material "near-field" or in close vicinity to the resonating transducer generating ultrasonic waves (Frederick, 1965). This optimal zone is determined by wavelength (Frederick, 1965).

Buttermore et al. (1989) tested an Illinois No. 6 coal of 5.8% moisture, 27.8% ash, and 5.1% total sulfur by weight. A near-field sonic array processor operating at 10 kHz and consisting of two ~645-mm^2 sonic radiator panels facing one another and separated by 16 mm was used for treatment. Following grinding and screening, a suspension consisting of -2400+150-µm particles and deionized water was enclosed between the radiators with a 75-µm (200 mesh) screen and issued ten, 5 s long pulses of sonication while a continuous desliming rinse of deionized water flowed through the unit to allow -75-µm material to pass. Timed samples were taken and ash value was determined. Treatment was able to reduce ash of the -600+300-µm size fraction by 31.1% and reduce ash ~20% in the -2400+1200-µm and -300+150-µm fractions. Selectivity was very high and nearly 100% of the coal was recovered.

In addition, Hallimond tube microflotation was performed on the Illinois No. 6 at a loading of 1.3% solids by weight, with and without sonication. The -212+150-µm size fraction and particles >1.45 specific gravity were used as feed. Flotation was also highly selective but, only after sonically dislodged particles were removed with a rinse (i.e., desliming) prior to flotation. It was concluded that sonic exposure promotes not only dispersion of minerals but separation of coal-mineral composite particles as demonstrated by microflotation results. The sonically treated flotation tests exhibited an increased recovery of lower ash product, indicating that the treatment enhanced the selectivity. In addition, separate testing demonstrated that sonication can reduce the hydrophobic elemental sulfur on the surface of oxidized pyrite. This suggests that sonication may depress flotation of pyrite. Sonication was also shown to restore the floatability of oxidized coal to levels similar to coal with fresh, nonoxidized surfaces.

Tao and Parekh (2000) conducted ultrasonic testing using a DAGER Inc. ultrasonic system with 2-L capacity, operating at 20 kHz and loaded at 5% solids by weight. A 12-L Ken-Flote column was used for flotation of the treated material with reagent loadings of 0.7-kg/t of #2 fuel oil and 0.45 kg/t of MIBC. A -150-μm size fraction South African coal with an ash value of 28.7% was used as the feed material. Treatment with a retention time of 30 s increased combustible recovery from 50.1% to 57.2% and lowered the product ash value from 9.4% to 8.6%. Also, the same ultrasonic treatment improved flotation of the -150-μm fraction of another South African coal. Product ash was reduced from 32.2% to 26.6% but combustible recovery increased only 0.36%. It was demonstrated for this higher ash coal that greater residence time of 1 min and 4 min only marginally improved product ash (23.2 % at 4 min) and even decreased combustible recovery.

Sedimentation testing of the treated -150-μm flotation tailings was conducted in 1000-mL graduated cylinders and improved the settling rate by 10 mm/min. In addition, vacuum filtration of a -150-μm low-rank Thailand coal sonicated in the same manner (30 s at 5% solids by weight) reduced cake moisture from 60% to 49%. Increasing treatment time did not improve results. At higher solids concentration of 15% during both treatment and filtration, the feed required 5-min of treatment to achieve even ~9% reduction in moisture. Across all tests, SEM microphotographs of the coal before and after treatment demonstrated sonication removed surface slime coatings. It was concluded that it is more convenient and cost-effective to treat prior to filtration and/or dewatering.

Wen-ze et al. (2007) conducted experiments on samples of a Chinese No. 10 coal (9.36% ash, 3.82% total sulfur) at 25% solid by weight with 20-kHz ultrasound at 200-W power for 10 min. Comparison of size distribution of untreated and treated samples following wet screening into five size fractions (+500, -500+250, -250+125, -125+75, -75+45, -45 μm) demonstrated that ultrasonics have a crushing effect on particles. This led to liberation of pyrite mineral matter from

the coal as determined by comparison of interval ash and total sulfur data before and after treatment. Furthermore, data were gathered concerning the contact angle and heat of wetting of ground -200-µm coal and pyrite at ~7% solids by weight loading as conditioning time increased. Following 1 min of treatment the coal contact angle increased by 2.07º, indicating increased hydrophobicity. Extended treatment up to a total of 7 min increased this angle by only 0.46 º. After 3 min of treatment, the pyrite contact angle decreased by 9.01º, and only 2.38º more after 2 min of additional treatment. Also, 3 min of ultrasonic conditioning of the -20-µm fraction of the sample coal decreased the wetting heat of coal and water by an average of 17.72%. The wetting heat for coal and kerosene increased by 45.85% and thus coal hydrophilicity decreased and oleophilicity increased. Experimentation on -20-µm pyrite and refuse showed that the wetting heat of pyrite and refuse with water increased by 38.52% and 93.66%, respectively, while that with kerosene decreased by 36.43% and 9.02%, respectively. These results indicate ultrasonics cause pyrite and refuse to become more hydrophilic and oil-repellent. Overall, testing demonstrated ultrasonic conditioning improved de-sulphurization and de-ashing by flotation.

Additional ultrasonic testing was carried out by Wen-ze et al. (2008) utilizing the same sample material. Separate ultrasonic testing was performed on -500-µm and -500+150-µm size fractions of raw coal and pure pyrite with 3 min of treatment at ~7% solids. Scanning electron microscopy (SEM) results demonstrated that ultrasonics cleaned the coal and pyrite surfaces as well as exposed fresh surfaces. X-ray fluorescence (XRF) spectroscopy showed that the coal particle composition shifted after treatment, increasing elemental carbon content by ~5%, though sulfur and iron decreased only minimally. Elemental oxygen decreased 4% as ultrasonics denuded the oxidizing layer on the coal surface. Treatment increased the iron and sulfur elements of the pyrite indicating increase in purity. Flotation rate tests were conducted on -500-µm coal before and after 3 min preconditioning with ultrasonic treatment. Flotation was carried out over 3 min with a 100-mL float cell loaded at a solids concentration of 50 g/L with 1.3-kg/t reagent

loading of both a kerosene collector and secondary octyl alcohol frother. Depending on froth sample collection time, treatment increased yield over 10% and the froth product was shown to have lower ash and sulfur content by over 1% and 1.5%, respectively. Also, flotation under optical microscopy showed greater attachment of bubbles to coal following ultrasonic conditioning.

Ambedkar et al. (2011) tested a high-sulfur lignite coal (18.9% ash, 5.03% total sulfur, 2.45% sulfate sulfur, 2.59% organic and pyritic sulfur) ground to -212 μm. Ultrasonic treatment was performed in an ultrasonic tank at 500 W over frequencies of 20, 25, and 430 kHz with one 58/192-kHz simultaneous frequencies test. Treatment was performed over 60 min on ~4% solid by weight slurries consisting of coal and water. All tests were able to remove at least 90% of sulfate sulfur from the coal and at least ~50% of total sulfur with >60% removal being achieved by the dual frequency test. Pyritic and organic sulfur (not speciated; determined as total sulfur less sulphate) were removed to a lesser extent with the 58/192-kHz test removing almost 40% while the others removed <20%. Sizing by particle counter demonstrated that after just 2 min of 20 kHz, 25 kHz, 58/192 kHz, and 430 kHz frequency treatment, the untreated mean particle size decreased from 28 μm to 11, 9.5, 19, and 26 μm, respectively. At 5 min of treatment mean particle size decreased further, most so at the 58/192-kHz frequency. Also, sphericity of particles increased with sonication time.

Ozkan (2012) tested a German (Ruhr Region) coal slime, which was floated both fresh from a preparation facility and after being aged 4 years. This material, both before and after aging, exhibited similar attributes with a heating value of ~9000 Btu/lb, ash value of ~35%, and ~1.1% total sulfur. Testing was performed in a Wemco flotation unit with a stainless steel cell equipped with four 50-W ultrasonic transducers operating at a 40-kHz frequency. Treatment was conducted at 10-15% solids with 5 min of conditioning for the Montanol-531 (collector-frother combination) reagent and 5 min of aeration time. The slurry was subjected to ultrasonics

throughout conditioning and aeration. Results showed that reagent consumption largely decreased and combustible recovery increased when ultrasonic treatment was utilized. This was primarily attributed to surface cleaning allowing for greater reagent contact with the coal. The ash value of the froth product did not improve as a result of treatment. Also, it was found that surface oxidation as a result of aging can be removed by ultrasonics.

Fairbanks et al. (1990) conducted testing in a 3-ft wide by 8-ft long stainless steel ultrasonic processing trough, treating coal slurry at 20% solids by weight. Following treatment, the slurry was diverted into a screen for size separation and removal of fine refuse material from the coarser coal product. Utilization of the treatment device on ponded coal-waste material liberated clays and silica and reduced clean coal moisture content. It is stated that moisture decreased by reduction of water absorbed by fine surface films. Also, it is reported that a pilot-scale demonstration plant reduced water retainment of coal piles by 33-50%.

1.4 Objectives

The objectives of this study were to determine the effects of hydroacoustic cavitation treatment on the separation and dewatering of fine and ultrafine coal. Two Illinois Basin bituminous samples, one of -1 mm and the other -0.15 mm in size, were tested. The effects on several separation unit processes were studied including the hydrocyclone, spiral concentrator, froth flotation cell, and plate filter press. The results of size, ash, sulfur and proximate analyses were determined.

CHAPTER 2

LAB SAMPLING AND MATERIAL CHARACTERIZATION

2.1 Introduction

Despite decreased national popularity due to the Clean Air Act of 1970 and declining production overall, coal is still a key fuel in electricity generation due in part to advances in scrubbing technology (Miller, 2014). In fact, some mining areas such as the Illinois Basin, have seen increased coal production by up to 10% in 2012 (Miller, 2014). The Illinois Basin contains high volatile bituminous coals, which increase in rank from high volatile C to high volatile A over geographic progression in a southeastern direction (Archer, 1979). These coals are characteristically 5-20% moisture, 6-14% ash, 2-4% sulfur, and possess a heating value of 11,000-14,000 Btu/lb (Archer, 1979). Principal minerals found in Illinois Basin coals are kaolinite, calcite, pyrite, marcasite (pyrite polymorph), and gypsum (Archer, 1979).

2.2 Material Splitting

Representative samples of nominal -1-mm and -0.15-mm Illinois Basin bituminous coal slurries were supplied in twelve 55-gal drums (6 drums per sample). The -1-mm material (Sample A) was obtained from the preparation plant's classifying hydrocyclone circuit feed stream. The -0.15-mm material (Sample B) was obtained from the overflow stream of the same hydrocyclone circuit. This stream was considered a waste material and was being sent to the plant's refuse thickener. The slurry samples were concentrated by plant personnel using a combination of settling and decanting. This process was repeated multiple times to increase the volume of solids in each drum.

Each 55-gal drum sample was split into 5-gal bucket samples using the following procedures. For Sample A, each drum was decanted and the wet solids were split into eight 5-gal buckets by scooping in layers in a downward, clockwise fashion within the drum to minimize

effects of settling and stratification. The decanted supernatant was then evenly distributed among the bucket samples.

Similarly, for each drum of Sample B, the supernatant was decanted and saved. The solids were then split into eight, 5-gal buckets but by rapidly mixing an approximately 6-in layer of the material with a scoop by hand. Because of the fineness and lower solids content of the material, it was possible to homogenize a layer in this way. This layer was then evenly distributed into the buckets with a 2-L beaker. This approach was repeated in a downward fashion until the drum was empty. The decanted supernatant was then evenly distributed among the bucket samples.

2.3 Sample Characterization

2.3.1 Solids Concentration

After a 55-gal drum of Sample A was divided into a set of representative 5-gal bucket samples, a single bucket of the set was selected and slowly introduced into a closed-loop recirculatory sump/pump system consisting of a 10-gal sump with side-mounted variable-speed Lightnin Labmaster (1600 RPM, 1/15 HP) mixer, Moyno progressive cavity pump (MOD 35601) with 0.75-hp variable-speed Emerson motor (1750 RPM, 7 V, MOD G639), and US Gearmotors Series 3000 reducer having a 1.6 ratio, and a Focus 1 DC drive Emerson variable-speed controller (Fig. 2.1). After 1 min of mixing and recirculation to ensure the material had homogenized, an approximately 1-L sample of the slurry was taken. The sample was dried in a 215°F oven for 24 h and the solids concentration by weight, S_w, was calculated by

$$S_w = 100\frac{m_o}{m_p} \tag{2.1}$$

where m_o is the mass of the dry solids and m_p is the mass of the pulp or slurry. This procedure was repeated for Sample B.

Figure 2.1. Sampling circuit

2.3.2 Size Analysis

For Sample A, an additional 1-L sample was taken and dried as described in Section 2.3.1. From the dried material, a 5-g head sample was riffled for ash analysis and a 150-g sample for size analysis. The 150-g sample was first wet screened by hand at 25 µm on a 500 U.S. mesh sieve. The -25-µm and +25-µm fractions were then separately oven-dried at 215 °F for 24 h. The +25-µm material was then dry screened by loading a stack of sieves into a Tyler Ro-Tap Model B testing sieve shaker and operating the unit for a total of 20 min. Eight-inch diameter sieves with square opening sizes of 1180, 850, 600, 425, 300, 212, 150, 106, 75, 53, 38, and 25 µm (16, 20, 30, 40, 50, 70, 100, 140, 200, 270, 400, and 500 U.S. mesh) were used for screening the material. The sieves were deblinded after 5 min by brushing the woven-wire mesh undersides. Following screening, the material in each size interval was weighed and bagged.

The -25-µm material was sized via a Microtrac S3500 particle size analyzer loaded with distilled water. Due to the small portion of material required for size analysis by the device, three replicates were performed and the size % passing values averaged to ensure that the results were

consistent. Triplicates were performed for all Microtrac results throughout this thesis and all data were shifted downward by a $\sqrt{2}$ to compensate for oversizing by this light scattering technique. For example, 12% passed 18.5 μm, following adjustment 12% passed 18.5 μm/$\sqrt{2}$ = 13.1 μm. Moreover, sieving and Microtrac data were joined after the last sieve size of 25 μm as if sieving was utilized for sizing the entire sample. Additionally, afterward the +1180-μm material was dry screened for 5 min at 3350, 2360, 1700 μm (6, 8, and 12 U.S. mesh) solely to determine the material top size. These sieves were not included initially as the Ro-Tap sieve stack holding height was inadequate to hold all sieves.

For Sample B, a 10-mL sample was taken per Section 2.2.1 but not dried. This material was then sized via a Microtrac S3500 loaded with distilled water as the material was very fine (-0.15 mm), so no sieving was used. An additional 10-mL sample was taken and dried to serve as a head sample for ash analysis.

2.3.3 Ash Analysis

Ash analyses were carried out on head samples and individual size fractions of Sample A and Sample B using a LECO TGA701 thermogravimetric analyzer. Prior to analysis, head samples and all +100-μm size fractions of Samples A and B were individually ground in a Fritsch Analysette Type 03501 vibratory micro ball mill.

2.3.4 Short Proximate and Sulfur Forms Analyses

A 750-g slurry sample of Sample A and a 250-g slurry sample of Sample B were obtained using the approach indicated in Section 2.3.1. Sample A was first wet screened by hand at 106 μm after which the -106-μm size fraction was wet screened at 25 μm. This generated +106-μm, -106+25-μm, and -25-μm size fractions, which were oven-dried at 215 °F for 24 h. The same procedure was followed for Sample B but the material was only screened into +25-μm and -25-μm size fractions. For both samples, a 20-g head sample and 20-g portion of each size fraction

was riffled. Head samples and size fraction samples were sent to Standard Laboratories, Inc. (Cresson, PA) for short proximate (i.e., moisture, ash, heating value, and total sulfur) and sulfur forms (i.e., pyritic, sulfate, and organic) analyses. Ash analysis was performed via ASTM D3174, total sulfur by ASTM D4239 Method B, heating value (Btu/lb) by ASTM D5865, and sulfur forms by ASTM D2492.

2.4 Results and Discussion

The average solids concentration and ash value across each 55-gal drum set of samples were determined. Sample A was 66.86±2.64% solids and 34.44±2.28% ash, while Sample B was 43.54±1.23% solids and 53.39±1.16% ash. Dry screening results revealed that Sample A possessed a nominal top size of 2360 µm, while Microtrac data showed Sample B had a nominal top size of 296 µm. Complete size distribution data can be found in Table 2.1. It is evident that Sample B was much finer as would be expected of hydrocyclone overflow when compared to hydrocyclone feed.

Table 2.1. Sample size distribution

Size, µm	Cumulative % passing		Size, µm	Cumulative % passing	
	Sample A	Sample B		Sample A	Sample B
2360	100.00	100.00	4.62	5.46	33.04
1180	90.68	100.00	3.27	4.25	26.41
850	79.82	100.00	2.31	3.17	20.39
600	68.85	100.00	1.63	2.23	14.96
425	57.31	100.00	1.16	1.46	10.36
300	47.82	99.82	0.82	0.91	6.81
212	39.52	98.88	0.58	0.51	4.08
150	32.76	97.35	0.41	0.23	1.89
106	27.14	95.21	0.29	0.05	0.41
75.0	22.60	92.13			
53.0	19.04	87.42			
38.0	15.86	80.59			
25.0	14.17	72.49			
18.5	12.00	64.25			
13.1	10.07	56.05			
9.25	8.19	47.87			
6.54	6.74	40.21			

Table 2.2 shows that the ash value increased as particle size decreased. Also, aside from the -25-μm material, direct weight percentage increased down to 425 μm and then gradually dropped off. The -25-μm size fraction had the largest direct weight percentage and ash value, presumably because very fine clays were concentrated in this material.

Table 2.2. Direct size distribution and ash data, Sample A

Size interval, μm	Wt., %	Ash, %
+1180	9.32	14.14
-1180+850	10.86	14.36
-850+600	10.97	19.26
-600+425	11.54	25.53
-425+300	9.49	29.02
-300+212	8.30	33.34
-212+150	6.76	37.87
-150+106	5.63	38.24
-106+75	4.53	39.99
-75+53	3.57	43.16
-53+38	3.18	48.67
-38+25	1.69	59.14
-25	14.17	74.71
Total (Calculated)	100.00	34.65

Additional sample data have been provided in Table 2.3. Sample A contained 63.82% +106-μm particles, which had an ash value of 27.76%, heating value of 10,242 Btu/lb, and a total sulfur value of 4.14%. Sample B contained 32.68% +25-μm particles, which had an ash value of 24.35%, heating value of 10,963 Btu/lb, and a total sulfur value of 3.78%. For both samples, the -25-μm material had very high ash, low sulfur, and low heating values.

Table 2.3. Sample attributes

			Sulfur				Heating Value
Stream	Direct wt., %	Ash, %	Total, %	Pyritic, %	Sulfate, %	Organic, %	Btu/lb
Sample A							
+106 µm	63.82	27.76	4.14	3.46	0.03	0.65	10,242
-106+25 µm	15.30	38.79	4.78	4.37	0.03	0.38	8,519
-25 µm	20.88	71.75	2.82	2.62	0.09	0.11	3,542
Total	100	38.63	3.96	3.42	0.04	0.50	8,579
Head	-	37.56	4.16	3.38	0.08	0.7	8,656
Sample B							
+25 µm	32.68	24.35	3.78	3.06	0.03	0.69	10,963
-25 µm	67.32	66.95	1.56	1.31	0.12	0.13	4,398
Total	100	53.03	2.29	1.88	0.09	0.31	6,543
Head	-	51.88	2.3	1.72	0.16	0.42	6,423

2.5 Conclusion

It was apparent that Sample B consisted of a low quality stream that was essentially refuse due to its high ash and low heating value. The sulfur across all samples and size fractions was mostly pyritic, which demonstrated that physical removal may be possible. In addition, coarser size fractions were of high heating value for both sample types so liberation of mineral matter and sulfur by treatment with subsequent size separation may produce a high quality product.

CHAPTER 3

HYDROACOUSTIC CAVITATION CIRCUIT

3.1 Introduction

Section 1.3 details the background and theory of ultrasonic cavitation and so it will not be discussed further here. The focus of this chapter is on the installation and operation of the hydroacoustic cavitation (HAC) circuit.

3.2 Experimental Circuit

The HAC circuit (Fig. 3.1) functions as a recirculatory system capable of several flow options depending on valve placement. The circuit offers two forms of treatment: cavitation due to flow through an ultrasonic resonator chamber or enhanced cavitation by initial flow reduction through a punched plate orifice (Fig. 3.2) then flow into the ultrasonic chamber. The hexafoil-shaped flow reduction orifice is incorporated into the circuit prior to entry to the ultrasonic chamber. The shape of the punched plate orifice has been carefully designed to maximize pressure drop and enhance cavitation in the ultrasonic chamber by generating a larger quantity of impinging air bubbles. Also, the impact of slurry solids on the plate is capable of shattering particles. The circuit, fabricated by Furness-Newburge, Inc., is a pilot-scale test platform designed to replicate the function of the FNI Sonoperoxone blackwater and sand reclamation system (Wang et al., 2006). It consists of a 60-gal polyethylene conical inductor feed tank (24-in diameter by 42-in height) supported by a stand, a Goulds 1.25-in by 1.5-in by 6-in centrifugal pump, a 5 hp (208-230/460 V, 3450 rpm) Bluffton fixed-speed motor, a tankside-mounted variable speed Lightnin (MOD EV5P75) with 1-ft diameter 3-pronged mixer, an ultrasonic generator operating at 25 kHz equipped with an automatic frequency controller maintaining a range of 24-26 kHz with an AC 230 V/50/60 Hz power supply, a 4.5-ft high by 6-in inside diameter by 6.5-in outside diameter stainless steel ultrasonic resonator chamber (Volume ~7 gal),

a 4-in by 4-in by 0.25-in stainless steel orifice plate secured between two flanges with punched 0.75-in outside diameter hexafoil-shaped flow reduction orifice, and a main control panel. The circuit is piped with 1.5-in diameter PVC Schedule 80 piping. All system electronics are powered by a 200-240 VAC 3-phase cable, which is connected to the control panel electrical enclosure. The ultrasonic controller offers amplitude adjustment from 10-100% of the nominal generator amplitude through alteration of power output and the option to run only in "sweep" mode, which when enabled, issues pulsing versus continuous vibration from the ultrasonic resonator. Valving and parallel circuit piping enables flow to be diverted around or entirely through the cavitation plate. All tests involving ultrasonics were performed in sweep ultrasonication at the recommendation of Furness-Newburge's engineer. Also, the stopcock ball valve at the top of the resonator chamber running from the chamber to the feed tank was left open at all times to avoid pressure build up. The circuit contains an ozone generation system and diffuser but it was not utilized for testing.

3.3 Experimental Procedures

A T-port 3-way valve in the recirculation line running from the chamber to the feed tank was used for all sample collection. In addition, an L-port 3-way valve at the exit of the resonator chamber was left positioned as to maintain recirculatory flow without any diversion to the hydrocyclone. Initially, circuit flow rate was determined to be ~90 gpm by loading the system with water and collecting timed samples with the T-port 3-way valve fully open.

HAC testing was conducted to quantify the effects of recirculation within the circuit as well as ultrasonic treatment, with and without flow through the cavitation plate, on particle size and size interval ash values. The amount of dilution water required to reduce a single 5-gal bucket of Sample A to 10% solids by weight was calculated. This solids concentration corresponded to that of the preparation plant hydrocyclone feed from which the samples were provided and was chosen to maximize treated volume without overloading the circuit and

clogging the pump. The calculated volume of dilution water was then added to the circuit feed tank and circulated throughout the system while the sample was added.

To ensure slurry homogenization, 64-oz samples were first taken after 1 min of recirculation from the start of solids introduction. These samples will be referred to as 0-min. Recirculation was allowed to continue, and 64-oz samples were taken following 1, 5, and 10 min of additional recirculation. Utilizing separate 5-gal samples, this process was repeated but with HAC treatment. Treatments included 100% power ultrasonication with (i.e., SonCav) and without (i.e., Son) all flow being diverted through the cavitation plate. Treatment was initiated approximately 5 s before gathering the first 64-oz samples. At a 90-gpm flow rate, 5 s is approximately the amount of time required to pump 7 gal of slurry through the resonator chamber. The samples were screened and analyzed for ash as given in Section 2.3.

3.4 Results and Discussion

Across the 3 treatments (i.e., Untreated, Son, SonCav) and 4 samples collected over time for each treatment (i.e., 0 , 1, 5, 10 min), the average sample weight for screening was 159.39±16.66 g and average calculated head ash value was 33.52±1.41%. Observing Figure 3.3, the effects on size by recirculation alone were not completely negligible as shown by the untreated bar plots. After 1 min of recirculation, the weight percentage of material in the seven +150-µm size intervals was reduced by an average of 0.45%, while the -25-µm material increased 1.55%. The weight percentage of +1180-µm particles decreased by more than an additional 2% from 1 to 5 min and again from 5 to 10 min due to circuit recirculation alone. Also, the -25-µm material weight percentage increased 2.66% from 1 to 5 min, and then 1.75% from 5 to 10 min. Overall, the untreated size distribution became finer as recirculation time increased (Fig. 3.4) due to the degradation caused by the pump impeller. Furthermore, Figure 3.5 indicates that Son and SonCav treatments degraded particle size to a greater extent than untreated recirculation.

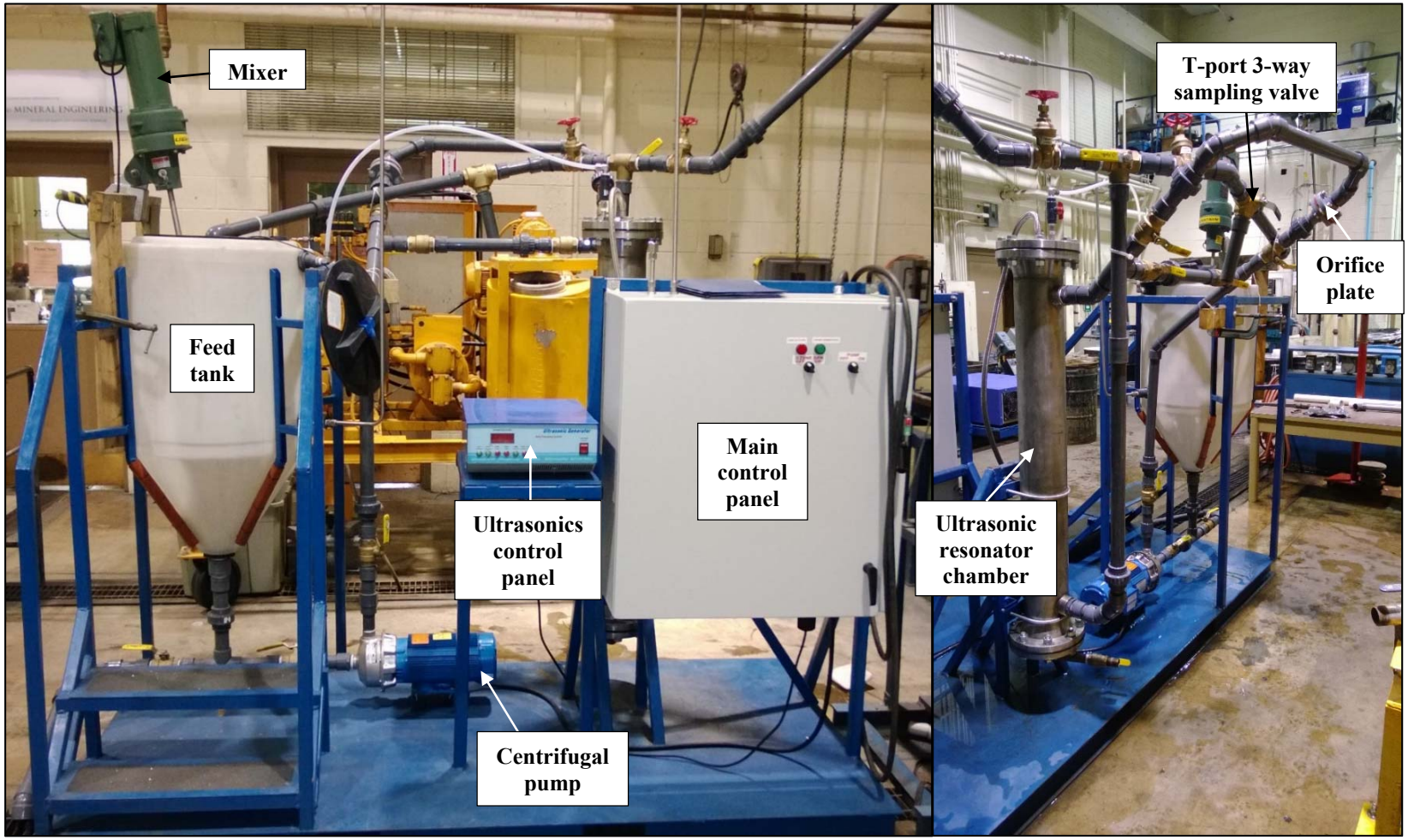

Figure 3.1. HAC Circuit

Figure 3.2. Flow reduction orifice (cavitation plate)

While at 0 min the Son and SonCav curves are nearly indistinguishable, by 10 min the curves indicated that flow through the cavitation plate (SonCav) more significantly reduced particle size. After only 5 s of Son or SonCav treatment, the 50% cumulative passing size (x_{50}) was reduced by about 50 μm from the untreated condition.

It has already been established that ash values increased with decreasing size for Sample A (Table 2.2) and this is also evident in Figure 3.6. Breaking and fragmentation of particles was evident as ash values sporadically shifted up and down with time for many size intervals. For example, the untreated -425+300-μm material was 29.02% ash at 0 min and 20.16% ash at 5 min but then 25.07% ash at 10 min. Also, over time the ash value of the -25-μm particles shifted very little. This indicated that though fines may have been liberated, carbon-rich particles were reduced in size so it appeared that there were no treatment effects. In addition, at 0 min, interval ash values between the Untreated- and Son-treated material varied 0.13-5.6%. Between the Son- and SonCav-treated material, interval ash values varied 0.06-5.38%. This variation demonstrated that even 5 s of treatment altered the composition of the size intervals in terms of ash value. Thus, ash-bearing minerals and/or clays may be being liberated. Also, increasing circuit recirculation

time of the untreated samples from 0 to 1 min created interval ash variation of 0.38-4.86% and so, not only was residence time a factor but extended exposure to treatment generated some change in the material. After 1 min, ash values varied from 0.4-11.64% between Untreated and Son treatment and 0.45-5.32% between Son and SonCav treatment.

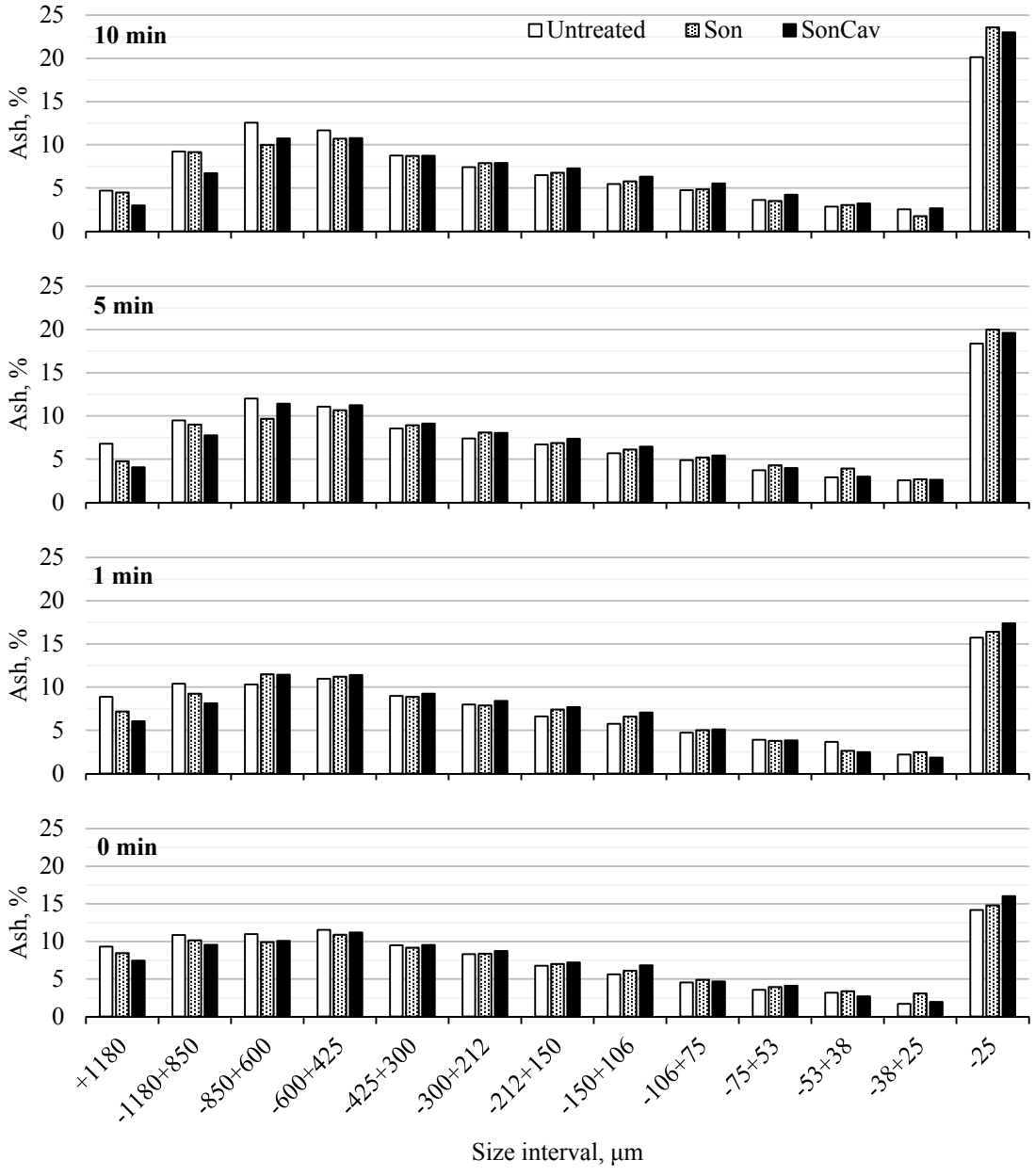

Figure 3.3. Direct weight percentage by size interval for various recirculation times

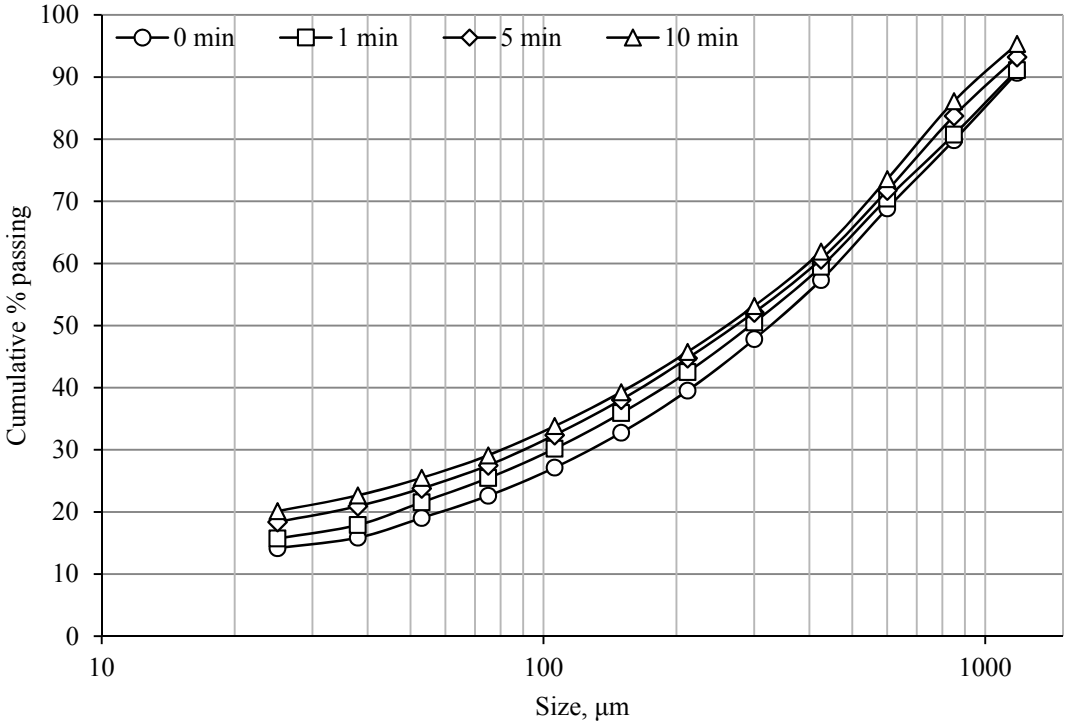

Figure 3.4. Untreated size distributions for various recirculation times

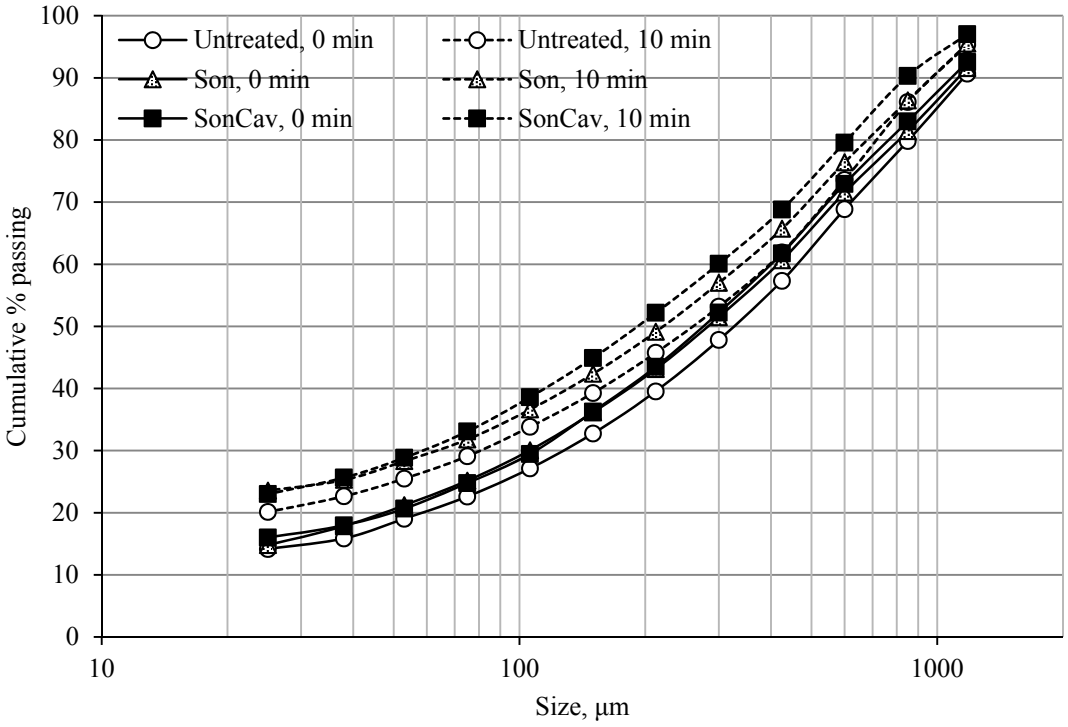

Figure 3.5. Treatment size distributions at 0 and 10 min of recirculation

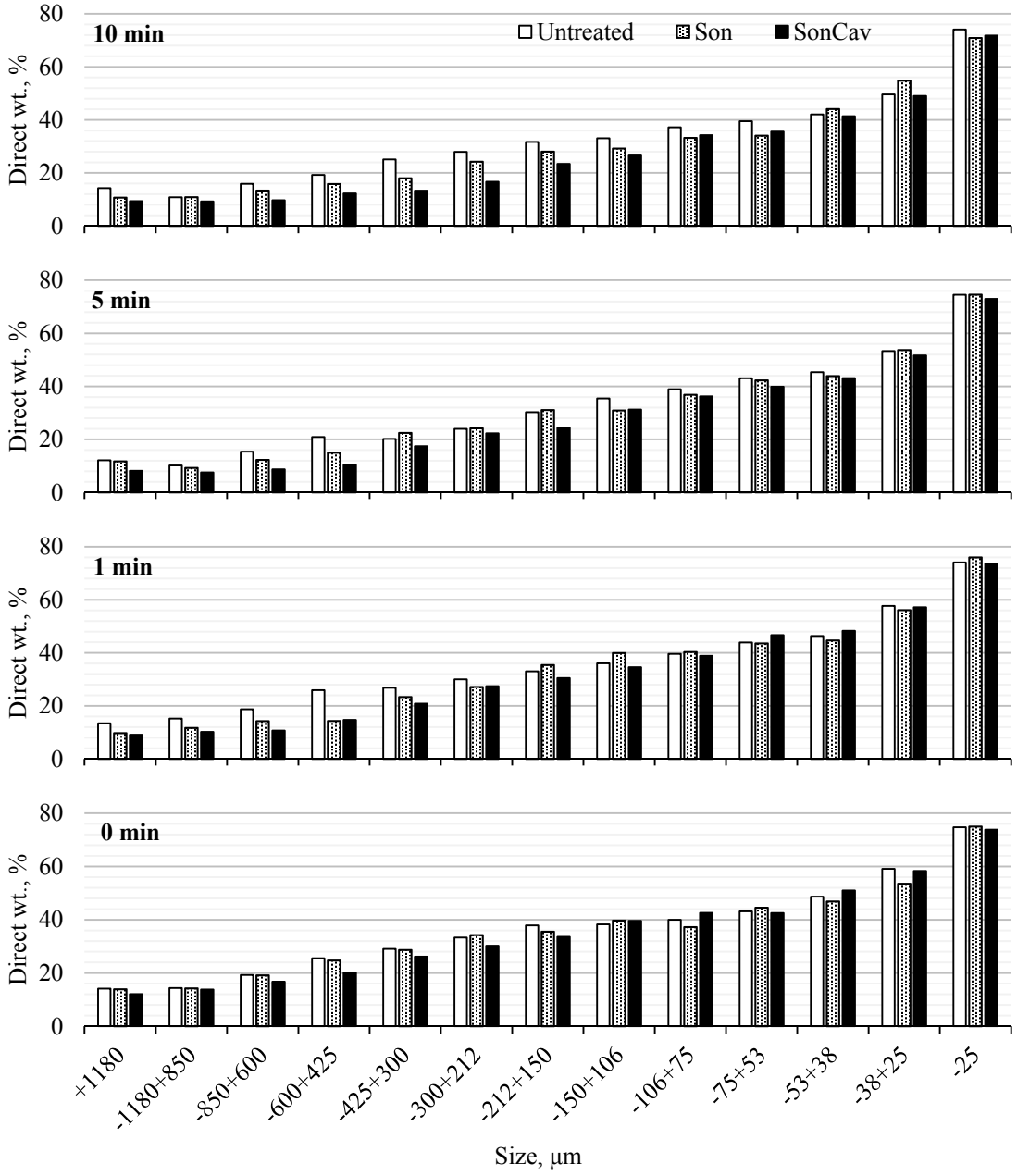

Figure 3.6. Direct ash % by size interval for various recirculation times

3.5 Conclusion

Testing of residence time in the circuit with continuous recirculation demonstrated that pumping through the piping circuit is capable of nonselectively degrading the size of the sample material. Also, with increasing time the effects became more prominent and breaking and fragmentation of particles likely occurred. Generally, it appeared that intensifying treatment from Son to SonCav progressively reduced the ash value of most size intervals. This was especially true as residence time within the circuit increased. Also, extended treatment seemed to reduce the ash value in coarser size intervals and increased the ash value in finer size intervals.

Because the goal of this study was to explore the effects of HAC treatment while maintaining an economical and potentially industry applicable approach, short residence time was more desirable. For the results defined as 0 min, which apply to 5 s of treatment time, the Son and SonCav condition exhibited a finer size distribution than the untreated condition (Fig. 3.5). Son and SonCav treatment were essentially the same despite some variation at finer sizes. Figure 3.6 shows that SonCav treatment reduced ash most in coarser intervals, with increase in ash in finer intervals. For these reasons, SonCav appeared most beneficial in terms of de-ashing.

CHAPTER 4

HYDROCYLONE SEPARATION

4.1 Introduction

Hydrocyclones are used extensively in the coal and mineral industries for their ability to classify and sort solids by size and density allowing for the classification, concentration (thickening), desliming, and degritting of slurries. These units maintain popularity due to their affordability and ease of installation and use with low space requirements (Svarovsky, 1984; Wills, 2006). There are many variants of hydrocyclones depending on the industry and intended separation, but they are governed by the same design parameters and operating conditions. The most pertinent of these parameters include diameters of the cyclone vortex finder, inlet, and apex, vortex finder length and shape, cyclone length and cone angle, and internal roughness (Majumder and Barnwal, 2011; Slechta and Firth, 1984; Svarovsky, 1984). A dense-medium suspension may also be used to allow separations to be made primarily on the basis of density differences.

There are a number of theories concerning how separation occurs within a cyclone, which vary greatly namely because they are tailored to specific experimental results and are not comprehensive (Svarovsky, 1984). These include the theory of equilibrium orbit (Driessen, 1951; Criner, 1950), residence time (Rietema, 1961a), crowding (Fahlstrom, 1960), and turbulent two-phase flow (Rietema, 1961b) to name several. However, the major forces particles are subjected to, which lead to separation, are generally agreed upon. Centrifugal forces are generated within a cono-cylindrical cyclone by tangentially introducing a suspension through an inlet located at the top cover. This creates a vortex directed toward the apex characterized as outer helical flow with circular symmetry. The high shear forces in this vortex tend to break agglomerates and disperse solids. Suspension particles move radially outward if their solid density exceeds that of the suspending liquid. The coarsest particles generally enter a boundary layer existing on the internal surface of the cyclone wall where their radial movement is opposed by a drag force defined by

Stokes' law. There is opposition to movement in the tangential but not axial and radial directions and gravity has no significant effect (Svarovsky, 1984). Particles in this layer generally exit at the apex while the remaining flow, consisting largely of the suspending fluid and fine particles, is carried upward by inner helical flow out of the vortex finder. This upward flow is known as a water core (or air core) and is generated due to the central low pressure region of the vortex. It is desirable and indicative of vortex stability (Bradley, 1965). In addition, the vortex finder protrudes into the cyclone to prevent short-circuiting of flow or exit out of the overflow immediately following entry from the inlet. Between the vortices lie circulation eddies and re-entrainment of boundary layer particles as well as movement between vortices due to turbulence is possible, thus particle residence time may vary.

4.2 Experimental Circuit

The hydrocyclone was incorporated into the HAC circuit as discussed in Section 3.2. A Krebs urethane cyclone (MOD U4-in-10º) was mounted to the steel frame of an adjacent mineral spiral (Fig. 4.1). The device has a 4-in diameter barrel, apex (spigot) fitted with a 0.5-in diameter insert, and a vortex finder which may be fitted with a 1-, 1.25-, or 1.6-in diameter insert to adjust overflow diameter. An Ametek diaphragm seal 0-60 psi pressure gauge was piped to the 1.5-in diameter hydrocyclone inlet as well as the 1.5-in diameter PVC line stemming from an L port 3-way valve of the HAC circuit. Depending on valve position, partial to all circuit flow can be diverted to the cyclone. In addition, there is a siphon break in the cyclone overflow line.

4.3 Experimental Procedures

Volumetric flow rate testing was performed after filling the HAC circuit feed tank with water and then collecting simultaneous, timed samples of the overflow and underflow streams. Samples were gathered under different operating conditions when the unit was fitted with the 1-, 1.25-, and 1.6-in diameter overflow inserts at various inlet pressures of 5, 10, 15, 20, and 25 psi. Similar testing was then performed when the circuit was loaded with Sample A slurry at 10%

solids by weight. Simultaneous, timed overflow and underflow samples were gathered when the cyclone was fitted with the 1-, 1.25-, and 1.6-in diameter overflow inserts at inlet pressures of 10 and 20 psi. The 1-in diameter overflow insert and inlet pressure of 20 psi were utilized for subsequent testing (See Section 4.4).

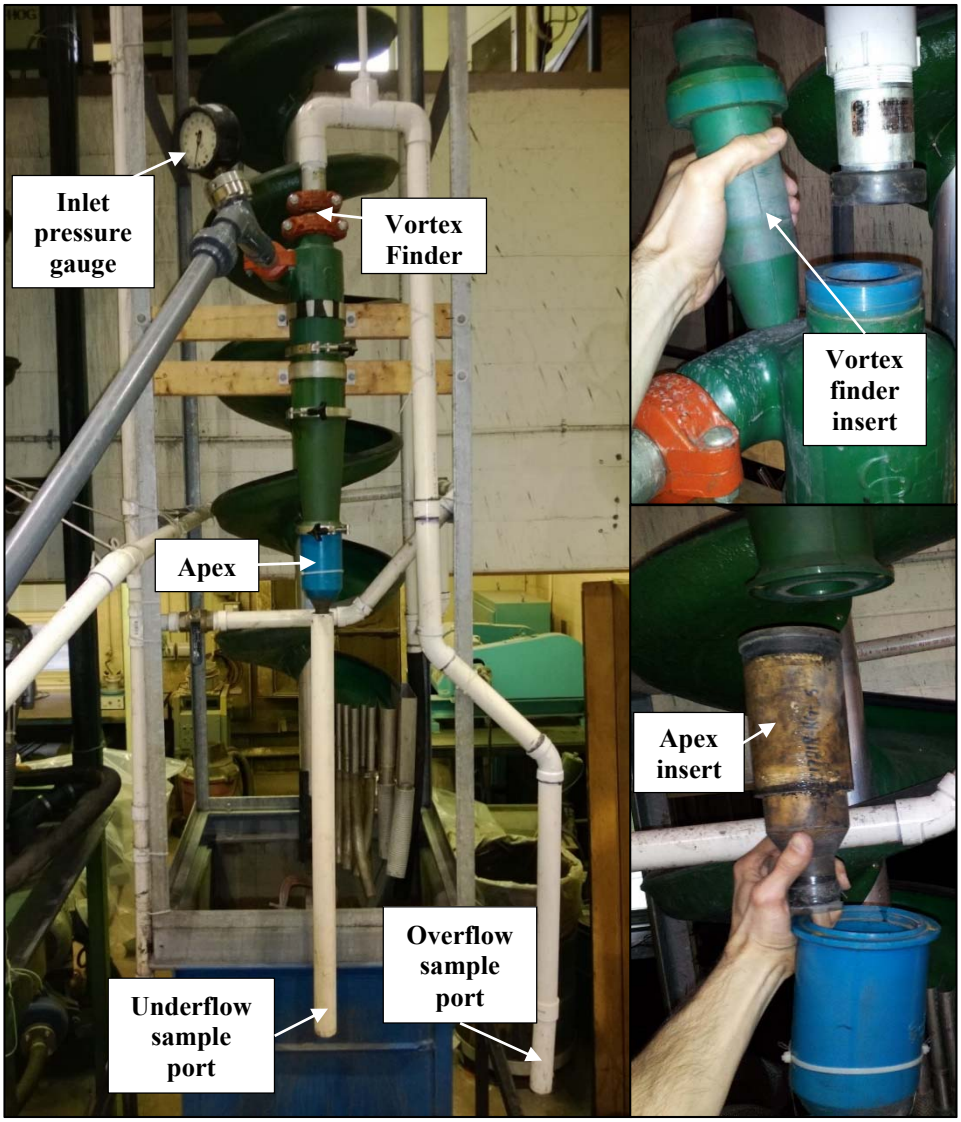

Figure 4.1. Laboratory hydrocyclone

In order to determine the treatment effects on size, ash, and sulfur values of the overflow and underflow streams as well as yield, simultaneous samples were gathered at various treatment conditions. The circuit was loaded at 10% solids by weight with Sample A and flow was diverted

to the hydrocyclone to achieve an inlet pressure of 20 psi after 1 min of recirculation from the start of solids loading. Conditions included no treatment, Son, and SonCav. Treatment was initiated 5 s before diversion of flow and separation by the hydrocyclone. An inlet pressure of 18 psi was the maximum achievable for the SonCav condition. Approximately 1-quart samples of the underflow and 5-gal samples of the overflow were collected. Underflow samples were dried and riffled down to 150 g, which was wet and dry screened as described in Section 2.3.2. Overflow samples were not sieved but sized by the Microtrac along with the -25-μm underflow material as discussed in Section 2.3.2. Head samples of both streams were riffled, ground, and analyzed for ash along with the interval fractions as described in Section 2.3.3. Short proximate and sulfur forms analyses were conducted on 20-g head samples of both streams as discussed in Section 2.2.4. This procedure was repeated with Sample B; however, the circuit was loaded at 4% solids by weight, which is the approximate solids concentration of the overflow stream at the preparation plant. Because of the fineness of the material (-0.15 mm) no sieve screening was conducted on either product stream so interval ash analysis was not performed. Both streams were sized with the Microtrac and short proximate and sulfur forms analyses were performed on head samples.

4.4 Results and Discussion

As expected, increasing inlet pressure increased flow to both the underflow and overflow streams (Table 4.1). Also, increasing overflow diameter increased the overflow flow rate while reducing the underflow flow rate. These observations are reflected in the cyclone data when fed with the 10% solids by weight slurry (Table 4.2), as increasing overflow diameter increased solids split to the overflow while decreasing overflow solids concentration. Solids split to the overflow increased with increasing inlet pressure, as well. For these experiments, the hydrocyclone was to function as a separator of fine mineral matter from the organic-rich coal while increasing the solids concentration of this stream. Of all tests, the solids split to the

underflow was greatest (79.4%) and underflow solids concentration near highest (62.2% by weight) at 20-psi inlet pressure when the cyclone was fitted with the 1-in diameter overflow insert. Also, higher inlet pressure generates higher throughput and yield to the underflow, and increased pressure drop offers finer cut size (Svarovsky, 1984). For these reasons, the 1-in diameter overflow insert and an inlet pressure of 20 psi was used for subsequent hydrocyclone testing.

Table 4.1. Hydrocyclone stream flow rates, gpm (water)

	Overflow insert diameter, in								
	1.0			1.25			1.6		
Inlet pressure, psi	UF	OF	Total	UF	OF	Total	UF	OF	Total
5	6.5	18.3	24.8	3.3	29.7	33.0	1.5	43.3	44.8
10	6.9	31.9	38.8	2.8	46.6	49.4	1.7	61.8	63.5
15	13.0	43.3	56.3	3.1	63.4	66.5	1.9	77.3	79.2
20	15.0	44.0	59.0	2.8	65.9	68.7	2.1	82.1	84.2
25	15.9	57.9	73.8	3.4	78.3	81.7	*	*	*

*25-psi inlet pressure unachievable

Table 4.2. Hydrocyclone stream data with Sample A feed (10% solids by weight)

		UF		OF	
Inlet pressure, psi	OF diameter, in	% Solids by wt.	Solids split, wt. %	% Solids by wt.	Solids split, wt. %
10	1	62.3	79.4	3.3	20.6
	1.25	61.3	59.4	2.7	40.6
	1.6	60.4	55.4	2.6	44.6
20	1	62.2	79.4	3.0	20.6
	1.25	62.2	54.2	3.0	45.8
	1.6	60.5*	52.3*	3.1*	47.7*

*Maximum of 17-psi inlet pressure achieved

The hydrocyclone mass balance is given by

$$PA_P = TA_T + QA_Q \tag{4.1}$$

where P, T, and Q are the solid mass flow rates of the feed, underflow, and overflow, respectively and A_P, A_T, and A_Q are an attribute (e.g., ash value) of those respective streams. Feed attributes may be reconstituted by rearranging this equation. In order to estimate yield to reconstitute feed

attributes for comparison to direct measurements and generate size selectivity (partition) curves to characterize the hydrocyclone separations, the least absolute sum method (Klimpel, 1979) was utilized. Using the least absolute sum method, circulation ratio (T/Q) was estimated by

$$C = \frac{\sum_{i=1}^{n-1}|p(x_i)-q(x_i)|}{\sum_{i=1}^{n-1}|t(x_i)-p(x_i)|} \tag{4.2}$$

where $p(x_i)$, $t(x_i)$ and $q(x_i)$ represent the weight fractions of those streams for size interval x_i and n is the total number of size intervals. The coarse yield would then be $\frac{C}{1+C}$.

The feed size distribution was reconstituted by

$$p'(x_i) = \frac{q(x_i)+t(x_i)C}{1+C} \tag{4.3}$$

and the actual size selectivity values were calculated by

$$s_a(x_i) = \frac{t(x_i)C}{(1+C)p'(x_i)} \tag{4.4}$$

In order to correct for apparent bypass, fitted size selectivity values were generated by

$$s_f(x_i) = (1 - a - b\,)c(x_i) + a \tag{4.5}$$

where a is the fraction of bypassed fine material in the underflow stream, b is the fraction of bypassed coarse material in the overflow stream, and $c(x_i)$ are the corrected size selectivity values. Normal cyclone operations exhibit a-bypass due to water in the underflow while b-bypass indicates abnormal operating conditions. The corrected values were fitted to the log-logistic function given by

$$c(x_i) = \frac{1}{1+e^{\left[\left(\frac{2.1972}{\ln\kappa}\right)\ln\left(\frac{x_i'}{d_{50}}\right)\right]}} \tag{4.6}$$

where x_i' is the geometric mean of size interval x_i, d_{50} is the particle size that has a 50% chance of reporting to both the underflow and overflow (i.e., cut size or equiprobable size). The sharpness index, κ, is defined by

$$\kappa = \frac{d_{25}}{d_{75}} \tag{4.7}$$

where d_{25} and d_{75} are the particle sizes at which the chance of the feed reporting to the underflow are 25% and 75%, respectively. Parameters a, b, κ, and d_{50} were estimated using the Solver add-in for Microsoft Excel by minimizing the sum of squares (SSQ) as defined by

$$SSQ = \sum_{i=1}^{n-1}[s_a(x_i) - s_f(x_i)]^2 \quad (4.8)$$

This approach was utilized to generate size selectivity curves for Sample A and Sample B across all 3 treatment conditions.

Size analysis results for Sample A (Fig. 4.2) demonstrated that the untreated overflow was slightly coarser than the Son and SonCav overflow, which exhibited nearly the same size distribution. At 18.5 μm, the SonCav underflow shifted from being finer than the untreated underflow to coarser. For all sizes, a greater cumulative percentage passing was expected for the SonCav condition and not the untreated condition, due the SonCav treatment intensity. The lower inlet pressure at this condition (17 psi vs 20 psi) may be a factor. The Son treatment underflow distribution resembled that of the SonCav condition at +18.5-μm sizes but more closely resembled the untreated condition at finer sizes. After reconstituting the feed distributions, it was evident that the feed material which received treatment was initially finer (Fig. 4.3). However, the actual (i.e., not reconstituted) untreated feed material size distribution was finer than the reconstituted untreated feed size distribution in -18.5-μm size fractions. As stated in Section 2.3.2, all -25-μm material was sized with a Microtrac and the output size was adjusted downward a $\sqrt{2}$ size interval, so this discrepancy should not be due to this adjustment. Also, the difference is only 1.67-3.08% for -18.5-μm size intervals and merely appears larger when graphically depicted as the axis is logarithmic. Minor sample size variation is likely a result of sampling error in collecting material at high flow rate (i.e., 90 gpm) from the T port 3-way valve.

Sample B size analysis results (Fig. 4.3) indicated that there was much less difference in size distribution between the streams across the respective treatments. The size distributions of the

underflow and overflow streams were almost identical across treatments.

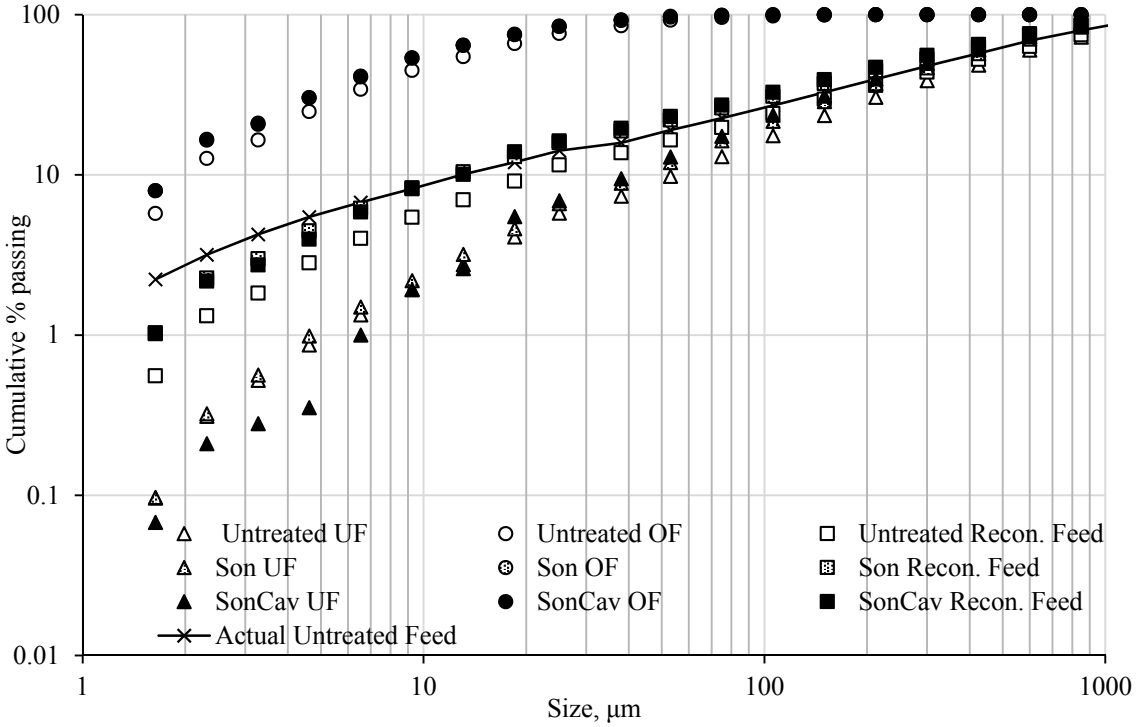

Figure 4.2. Hydrocyclone stream size distributions, Sample A

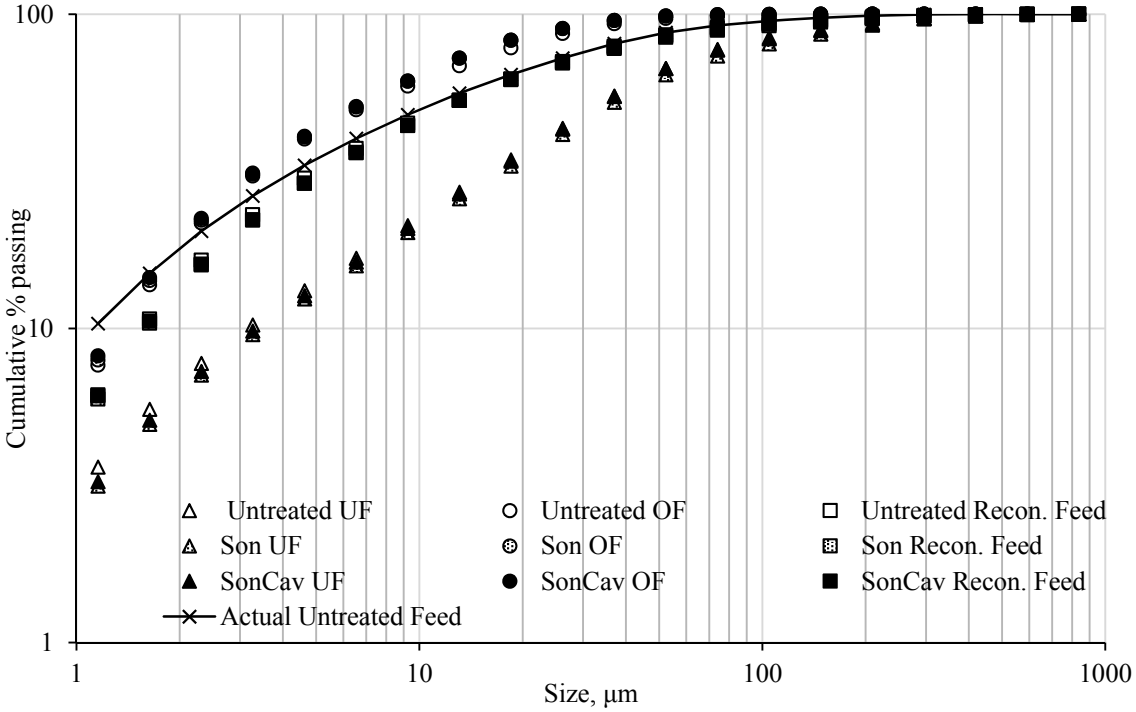

Figure 4.3. Hydrocyclone stream size distributions, Sample B

A similar observation was made for the feed streams but again, it appeared there was more -18.5-μm material in the actual untreated feed than the reconstituted feed. As previously explained, discrepancy was likely caused by sampling error resulting from sample collection from a high flow rate stream.

Size selectivity and separation efficiency are dependent on the size distribution of the feed coal and the particle density distribution (Hsu et al., 2011; Lynch and Bush, 1977). The particle specific gravities in run-of-mine coal range from 1.2 for pure bituminous coal to 2.6 for shale and 5.0 for pyrite. Hence, liberation of dense fines from the surface and solid matrix of coarse coal particles could affect the separation. Figure 4.4 shows that the a-bypass somewhat decreased with an increase in the intensity of HAC treatment. Because the inlet pressure for the SonCav condition was only 17 psi versus 20 psi for the other two tests, this size selectivity curve is not directly comparable to the untreated and Son treatment curves. The size selectivity curves for Sample B (Fig.4.5) were even less variable than those for Sample A. The b-bypass was zero for all tests. A summary of yield and size selectivity data has been provided in Table 4.3.

For Sample A, excluding SonCav data due to reduced inlet pressure, the cut size was ~21-μm. Considering the coarseness of the feed, a high coarse yield (i.e., ~90%) was obtained, though the sharpness index was quite low at 0.23 when untreated and 0.29 for Son treatment. Higher sharpness index values and selectivity curves that resemble a step function are ideal and represent high separation efficiency.

For Sample B, the cut size decreased from about 36 μm when untreated to 29 μm after SonCav treatment. Also, HAC treatment increased the sharpness index. In addition, the a-bypass was approximately constant over all treatments and because Sample B was much finer than Sample A, the coarse yield was lower at ~40%. It has been shown that an increase in feed solids concentration generally leads to a coarser cut size and reduced sharpness of separation (Braun and

Bohnet, 1990). Experimentation produced the opposite result but, this slight change is likely attributable to the size and composition (density) differences between the two sample types.

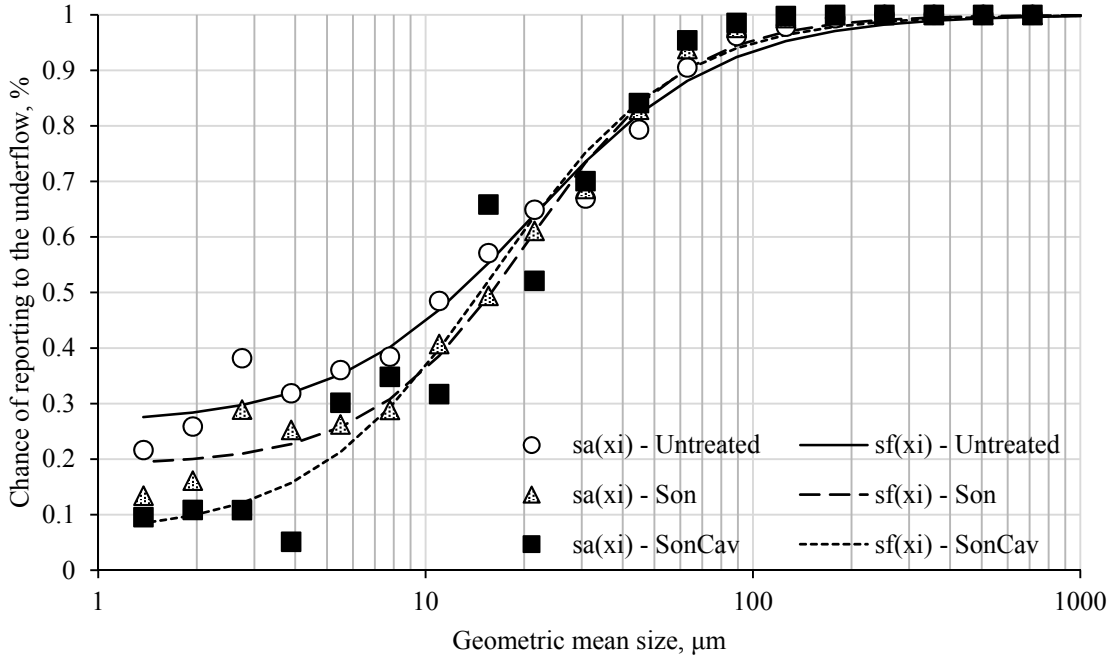

Figure 4.4. Size selectivity curves, Sample A

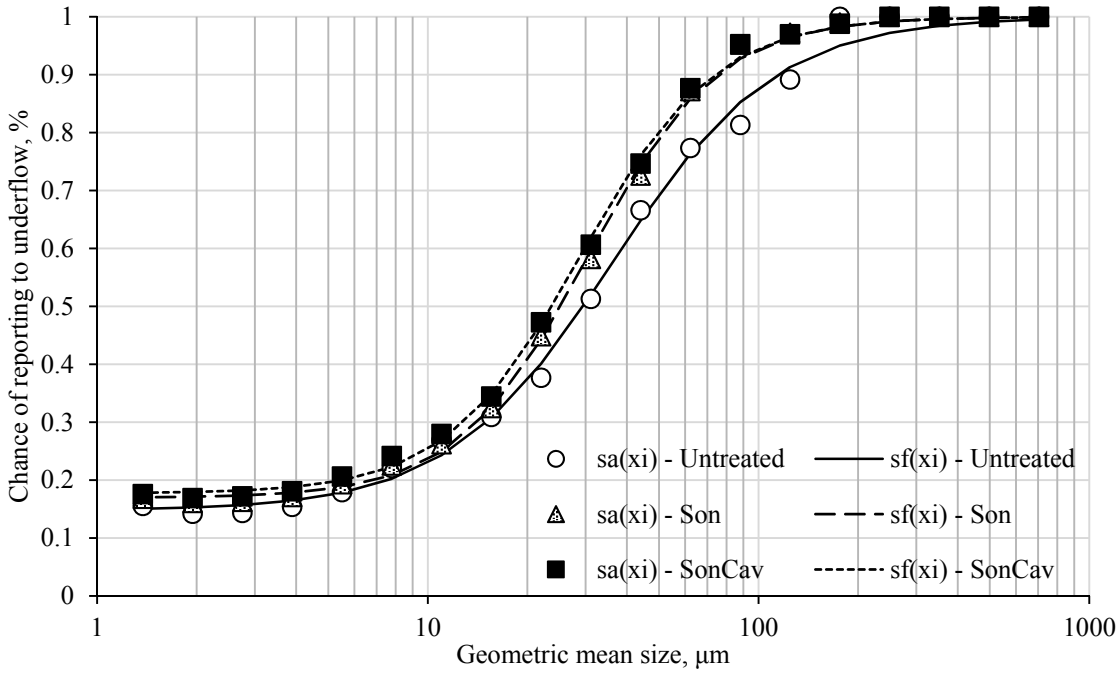

Figure 4.5. Size selectivity curves, Sample B

Table 4.3. Size selectivity parameters

	Sample A (Feed ~10% solids)			Sample B (Feed ~5% solids)		
	Untreated	Son	SonCav	Untreated	Son	SonCav
a	0.26	0.19	0.07	0.15	0.17	0.18
κ	0.23	0.29	0.25	0.29	0.37	0.36
d_{50} (cut size), μm	20.8	20.7	16.1	36.0	30.4	29.0
Coarse yield, %	92	88	88	37	41	42

Figure 4.6 shows the variation of cumulative ash values of the hydrocyclone underflow product with cumulative weight percentage (i.e., cumulative percentage retained). It can be seen that the ash value increased with decreasing size. Also, it is evident that treatment and desliming reduced the interval and total ash values of the underflow. This occurred without decreasing the underflow solids yield as shown in Tables 4.4-4.6. These tables illustrate the solids split and attribute effects of treatment on the hydrocyclone streams for both Sample A and B.

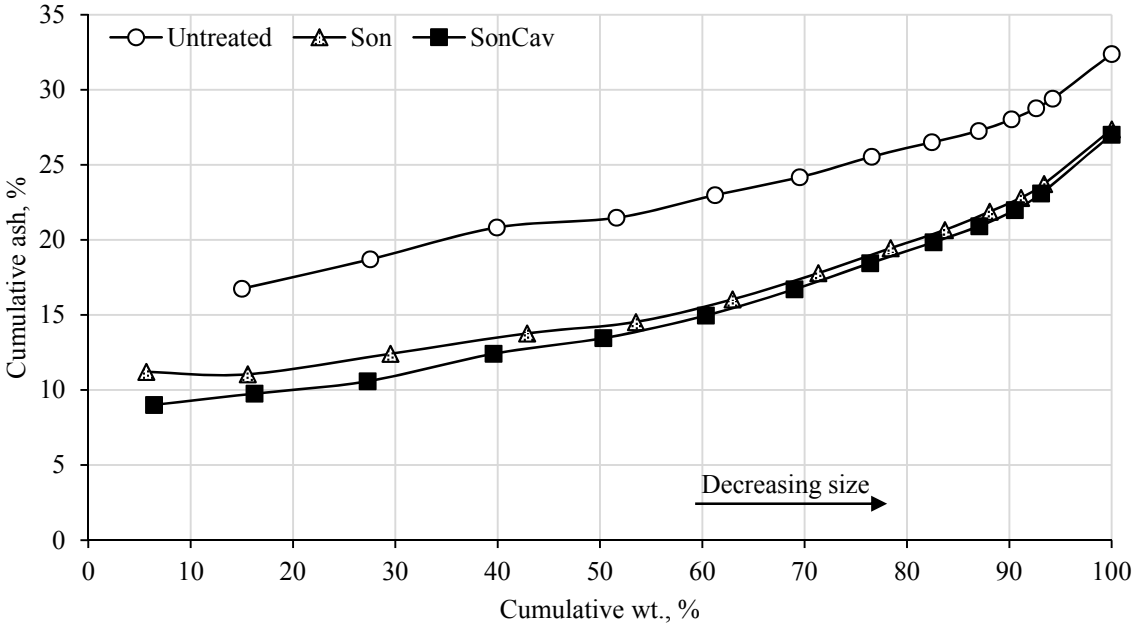

Figure 4.6. Hydrocyclone underflow ash-yield curves, Samples A

Table 4.4 Hydrocylone results, Untreated

			Sulfur				Heating Value
Stream	Solids Split, %	Ash, %	Total, %	Pyritic, %	Sulfate, %	Organic, %	Btu/lb
Sample A							
Overflow	8.15	56.82	1.4	0.96	0.04	0.4	5,009
Underflow	91.85	29.59	4.17	2.59	0.11	1.47	9,436
Feed (reconstituted)	100	35.67	3.94	2.46	0.10	1.38	9,075
Sample B							
Overflow	62.83	61.28	1.36	0.81	0.17	0.38	5087
Underflow	37.17	39.34	3.38	1.86	0.11	1.41	8397
Feed(reconstituted)	100	53.12	2.11	1.20	0.15	0.76	6,317

Table 4.5. Hydrocyclone results, Son

			Sulfur				Heating Value
Stream	Solids Split, %	Ash, %	Total, %	Pyritic, %	Sulfate, %	Organic, %	Btu/lb
Sample A							
Overflow	11.91	63.01	1.37	0.96	0.04	0.37	4,747
Underflow	88.09	24.24	3.55	2.07	0.08	1.40	10,388
Feed(reconstituted)	100	31.64	3.29	1.94	0.08	1.28	9,716
Sample B							
Overflow	58.74	60.88	1.07	0.66	0.02	0.39	5194
Underflow	41.26	39.92	3.08	1.62	0.06	1.4	8612
Feed(reconstituted)	100	52.23	1.90	1.06	0.04	0.81	6,604

Table 4.6. Hydrocyclone results, SonCav

			Sulfur				Heating Value
Stream	Solids Split, %	Ash, %	Total, %	Pyritic, %	Sulfate, %	Organic, %	Btu/lb
Sample A							
Overflow	12.04	62.19	1.39	0.98	0.02	0.39	4,910
Underflow	87.96	24.47	3.58	2.16	0.07	1.35	10,295
Feed(reconstituted)	100	31.38	3.32	2.02	0.06	1.23	9,646
Sample B							
Overflow	57.73	62.06	1	0.63	0.03	0.34	5056
Underflow	42.27	39.19	2.55	1.37	0.05	1.13	8900
Feed(reconstituted)	100	52.39	1.66	0.94	0.04	0.67	6,681

There is some variation between the reconstituted feed values across treatments for both Sample A and Sample B. This variability is substantial enough that data cannot be directly compared between treatments. Therefore, the relative percentage difference between the reconstituted feed and its respective underflow was calculated (Table 4.7). For both Samples A and B, the hydrocyclone underflow product was upgraded from the feed by ash reduction and heating value improvement. These two attributes are associated in that the presence of less ash-forming material increases the heating value per unit mass. However, sulfur was more concentrated after treatment. The treatment effects were more pronounced for Sample B, which was a finer, higher ash and lower sulfur material.

Table 4.7. Percentage difference between hydrocyclone reconstituted feed and respective underflow for different HAC treatment options

	Sample A				Sample B			
Condition	Ash	Total sulfur	Pyritic sulfur	Heating value	Ash	Total sulfur	Pyritic sulfur	Heating value
Untreated	-7.0	+5.7	+5.4	+4.0	-25.9	+60.1	+55.0	+32.9
Son	-16.0	+7.9	+6.8	+6.9	-23.6	+62.2	+53.4	+30.4
SonCav	-15.7	+8.0	+7.0	+6.7	-25.2	+54.1	+45.3	+33.2

4.4 Conclusion

Initial testing of the hydrocyclone with and without solids demonstrated that increasing the inlet pressure and diameter of the vortex finder increased the volumetric flow and solids split to the overflow, as suggested by theory. Also, increasing the inlet pressure produced a more concentrated underflow. In pairing HAC treatment with hydrocyclone separation, the size reducing effects of sonication and cavitation were apparent from the stream size distributions. Overall, HAC treatment had a slight effect on the size selectivity curves. These effects were more prominent for Sample A, which was a coarser material than Sample B. Sample B was essentially unaffected by treatment in terms of size degradation. HAC treatment increased the sharpness index and decreased the cut size (d_{50}) for both sample types. This was likely due to the liberation of dense surface fines and particle dispersion effects resulting from sonication and cavitation.

Coarse yield decreased for Sample A and increased for Sample B after treatment, though only minimally. The ash value of the underflow was more greatly reduced with intensifying treatment for Sample B, and SonCav treatment offered the greatest ash reduction for both sample types. Because sulfur, namely pyritic sulfur, was more concentrated in the underflow, HAC treatment followed by hydrocyclone separation would not be sufficient to produce a higher quality coal.

CHAPTER 5

SPIRAL CONCENTRATION

5.1 Introduction

The first coal spirals were developed in 1945 by Humphrey and consisted of 6 turns with an experimentally determined pitch and standard mineral spiral trough length (Thompson and Welker, 1990). Upon decline of the coal fines market, interest in the spiral subsided but regained popularity in the 1980's in Australia where the spiral was redesigned with urethane/fiberglass construction and the high capacity coal spiral was developed (Holland-Batt, 1995). Today, spiral concentrators are desirable separation devices because they possess low capital and operating costs and a general insensitivity to changes in the feed rate (Zeilinger and Deurbrouck, 1976).

Spiral concentration is a form of flowing-film concentration allowing for progressive stratification of particles as they descend by gravity down turns of a vertically-oriented, helical pitched trough. Stratification occurs similar to sluicing (i.e., fluidized bed) and is governed by hindered settling, interstitial trickling, dispersive Bagnold forces, and centrifugal forces (Sivamohan and Forssberg, 1985). Primary design variables are the helix pitch, trough profile (i.e., trough length), and trough radius with major variables affecting performance and operation being feed grade and size distribution, solids concentration, and flow rate (Sivamohan and Forssberg, 1985). Comparative sedimentation rates of feed particles are particularly important (Holland-Batt, 1995). It is also necessary to ensure even distribution of feed across the trough, which is controlled by a feed box and first turn geometry as well as repulpers (Holland-Batt, 1995).

As mentioned, stratification of the feed is dependent on several factors. Because coal spirals are typically fed with suspensions at solids concentrations exceeding 10% by weight, hindered settling occurs where particles no longer settle independently but in zones. This leads to

reduced settling velocity due to crowding and upward liquid flow as a result of liquid displacement by particles. When hindered, as slurry solids concentration increases, the settling velocity generally decreases. Also, due to variety in particle specific gravity and size, differential acceleration and interstitial trickling leads to the migration of dense fines to the bottom of the film and less dense, coarse particles at the free surface. This is also a result of Bagnold forces, which arise from particle-particle collisions in a layer submitted to shear forces (Bagnold, 1954). These forces increase with volumetric solids concentration as well as particle diameter and shear rate. The forces lift coarse, lower specific gravity particles to the high velocity free surface (Bagnold, 1954). Furthermore, rising current at the inner spiral radius and falling current at the outer radius tends to lift fines (Sivamohan and Forssberg, 1985). Though the stratification process is complex, inevitably the highest specific gravity particles will progress toward the bottom of the film with the lower specific gravity particles situated near the free surface. Centrifugal forces cause this stratified film to shift outwardly. Thus, the lower specific gravity particles in the upper film move outwardly in the trough while the denser lower layers, subject to lower centrifugal force and greater inward radial velocity, flow towards the inner side of spiral (Sivamohan and Forssberg, 1985).

Spirals are used widely throughout the coal and mineral industries, and the spiral design is modified accordingly. For example, steeper pitch offers higher capacity and higher product grade but lower recovery, while flatter pitch is often used for fines, coals, and feed particles with little specific gravity difference (Sivamohan and Forssberg, 1985; Holland-Batt, 1995). Additionally, greater trough radius and length are useful in treating fines (Sivamohan and Forssberg, 1985; Atasoy and Spottiswood, 1995). Greater length increases residence time causing particles to more evenly distribute by size (Atasoy and Spottiswood, 1995).

Much testing has been performed concerning spiral separation of coal. Utilizing a Humphreys spiral, Geer et al. (1950) demonstrated with a variety of coals that a -2380-μm feed

material, containing -595+149-μm impurities (e.g., pyrite), achieved maximum ash reduction and organic recovery. In addition, Holland-Batt (1995) concluded that coal spirals should employ the lowest number of turns to achieve separation, which is typically 4-7 turns. Lastly, Zeilinger and Deurbrouck (1976) analyzed sulfur reduction potential of a Humphrey coal spiral on a crushed Middle Kittanning bed coal. Loading the spiral with a -420-μm feed at 10-30% solids by weight over various feed rates, 78-85% reductions in pyritic sulfur were observed in the +75-μm clean coal at over 86% yield. However, pyrite reduction was poor in the -75-μm fraction. Also, feed rate minimally affected product quality. When loaded over a range of 10-40% solids by weight with a -1410-μm feed, 76-90% pyritic sulfur reduction with 68-85% coal recovery was achieved in the +75-μm clean coal. The middling and -75-μm clean coal showed reduced pyritic sulfur but required retreatment to lower the ash.

5.2 Experimental Circuit

A Multotec SX7 single-start two-stage spiral concentrator (Fig. 5.1) was incorporated into a closed-circuit consisting of 2-in by 1.5-in centrifugal pump (Ash, MOD 5 ME), 15-hp motor (Westinghouse, 460 V, 1760 rpm) with variable frequency controller (ABB), 100-gal stainless steel sump, and variable-speed mixer (Lightnin MOD EV5P75). The spiral trough has a 38-cm radius and is comprised of seven turns. After four turns there is an auxiliary splitter where the densest material, primarily mineral matter, is diverted into the center column, while the remaining slurry continues flowing downward on the outer 28 cm of the trough. This material enters a repulper, which mixes the slurry through contact with internal baffles and then exits down three more turns. At the base of the trough is a splitter box, which partitions the slurry into six streams. For sample collection, the clean coal (i.e., CC) stream was considered splitter box ports 1 and 2, which are within 11 cm of the outer rim. Middlings (i.e., MID) were defined as ports 3 and 4 from 11 to 23.5 cm from the outer rim and refuse (i.e., REF) as the center column as well as ports 5, 6 and 7, from 23.5 to 38 cm from the outer rim. The 14-L urethane-lined, steel

head tank at the top of the spiral possesses an overflow port and discharge orifice, which may be fitted with different diameter urethane inserts. There is also a flexible bypass line for slurry recirculation when changing head tank orifices or filling and emptying the sump.

5.3 Experimental Procedures

Spiral volumetric flow rate testing was performed with water for the 23-, 32-, and 35-mm diameter head tank discharge line orifices. Samples from the clean coal, middling, and refuse ports were collected simultaneously and timed. Three replicate samples from each stream were collected and averaged to determine mean flow rate. A motor frequency of 21 Hz was maintained to ensure constant overflow from the head tank for feed flow rate testing.

To determine the combined effects of treatment, desliming, and spiral concentration, three separate spiral tests were conducted where the feed was untreated or treated by Son or SonCav. For each test series, the HAC circuit was loaded with 55 gal of slurry consisting of Sample A and sufficient water for dilution to 10% solids by weight. The water was added and recirculated, and then the undiluted drum sample material was added. After 1 min of slurry recirculation from the time of sample introduction, flow was diverted by the L port 3-way valve to the hydrocyclone, which was fitted with 1-in diameter overflow and 0.5-in diameter underflow inserts. Desliming was performed at a hydrocyclone inlet pressure of 20 psi. When utilized, treatment was initiated 5 s prior to desliming.

The hydrocyclone underflow was collected and weighed. Because the HAC circuit is a batch process, this operation was performed several times until sufficient material was collected to load the spiral sump to ~70 gal at 25-30% solids by weight. Following underflow collection, dilution water was recirculated within the spiral sump and the collected material was then added. Once recirculated for 5 min to achieve homogenization, the slurry was diverted to the head tank using an L port 3-way valve.

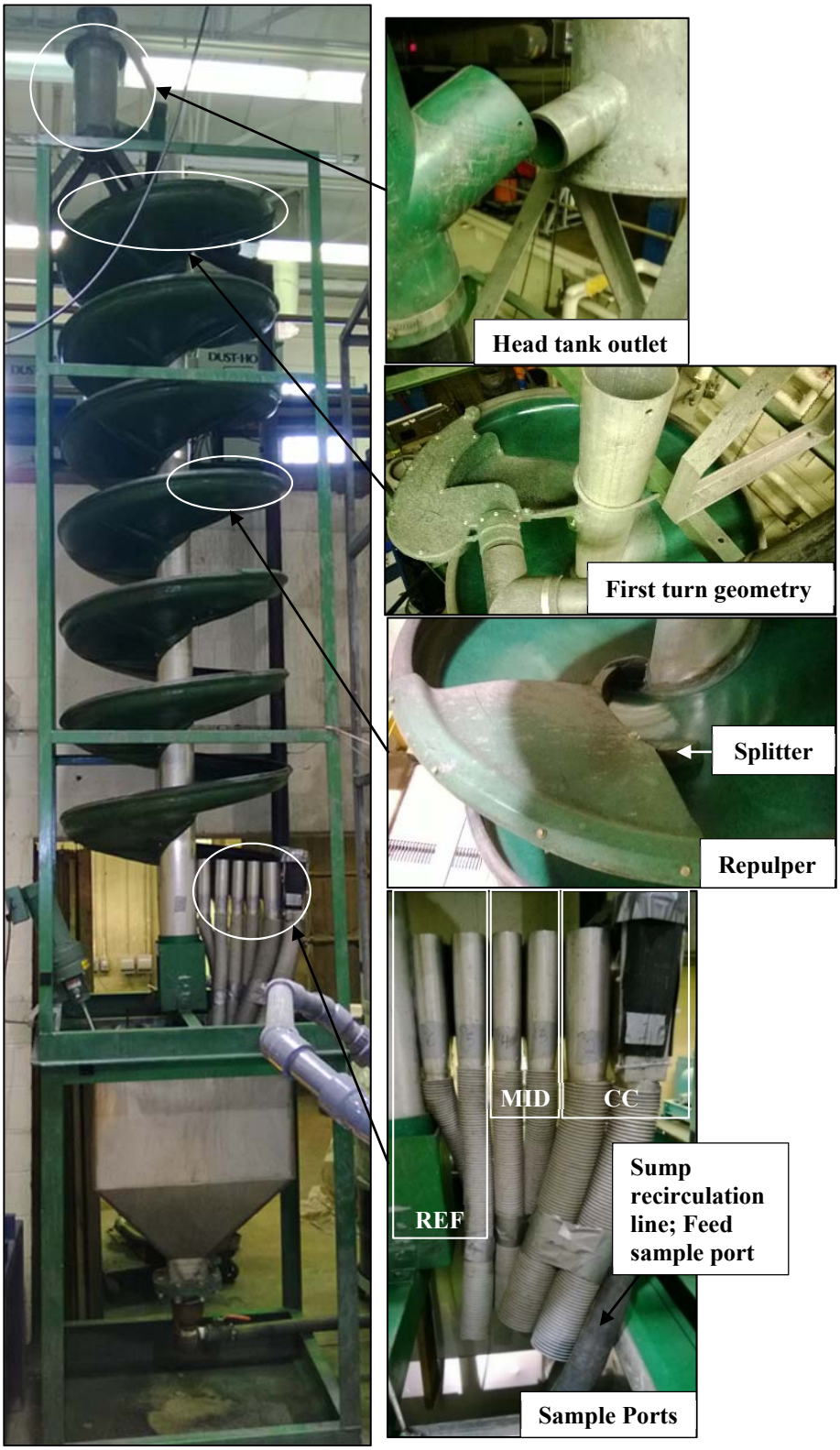

Figure 5.1. Spiral concentrator and select components

Timed simultaneous samples of the clean coal, middlings, and refuse were gathered for the three head tank discharge orifices while maintaining a motor frequency of 21 Hz. A feed sample was also taken from the sump recirculation line (Fig. 5.1). No replicate samples were gathered due to material quantity constraints. Per the procedures in Section 2.3, samples were dried for solids concentration, sized, and head and size intervals analyzed for ash. When using the 32-mm head tank outlet, a 5-g and 30-50-g sample of each stream was obtained by riffling for each test condition. The 30-50-g sample was wet screened at 300 and 106 μm and all samples were analyzed for total sulfur.

5.4 Results and Discussion

Flow rate testing with water showed that there was a linear relationship between outlet area and volumetric flow rate (Fig. 5.2), which was previously demonstrated for this unit (Benusa, 2007).

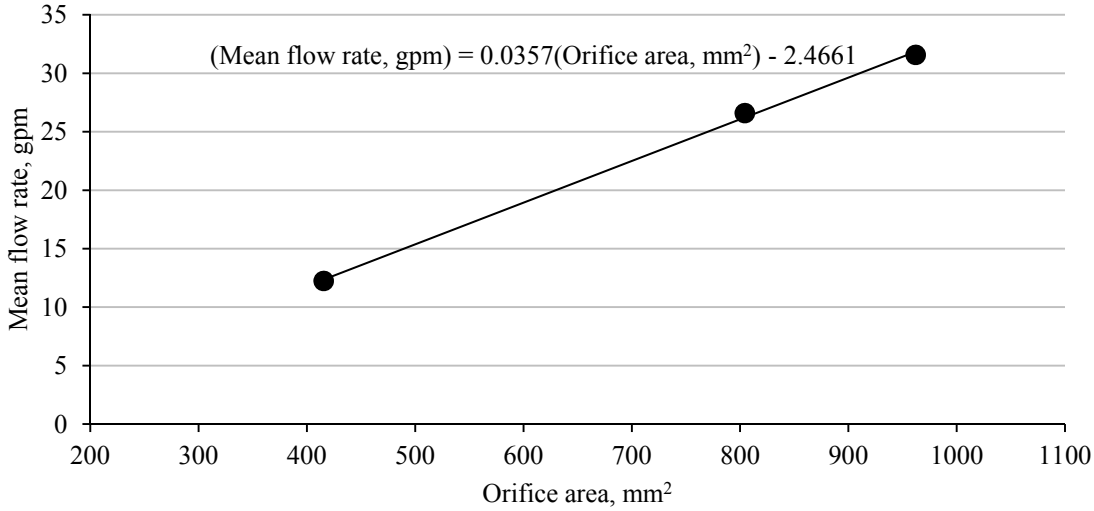

Figure 5.2. Spiral volumetric flow rate (water-only)

The mean flow rates for the 23-, 32-, and 35-mm diameter outlets were 12.2, 26.6, and 31.6 gpm, respectively. Outlet size will be referred to by flow rate from this point forward.

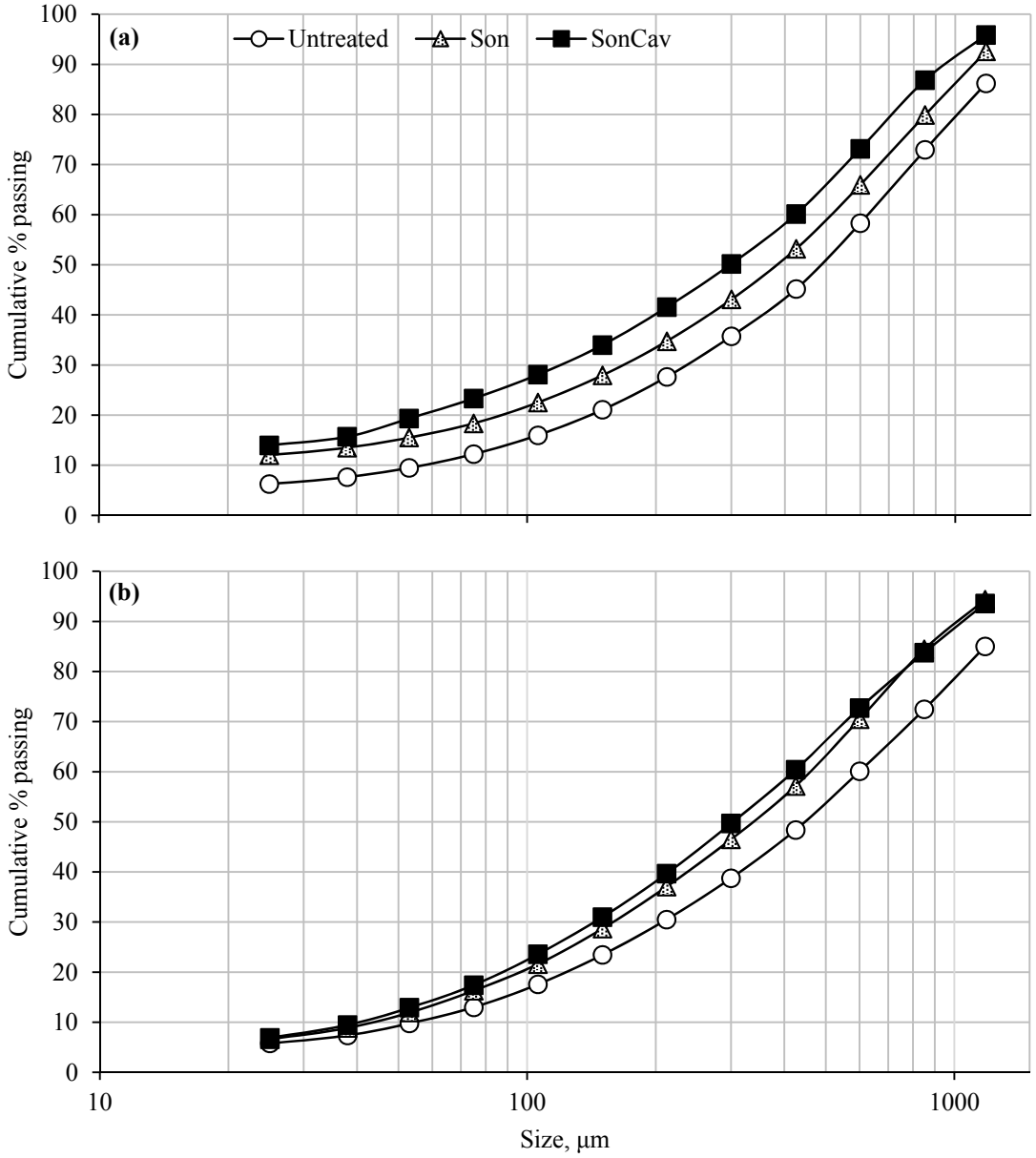

Figure 5.3. Hydrocyclone underflow (a) and spiral feed (b) size distributions

The spiral feed, which corresponds to the hydrocyclone underflow, is finer with treatment across all size intervals. This is evident as the size distribution curves (Fig. 5.3) shifted upward as treatment intensified from untreated to Son then SonCav. This is a result of the combined effects of size degradation and surface fines liberation due to treatment and subsequent removal of fines from the spiral feed by the hydrocyclone (i.e., desliming). Across all size intervals, cumulative %

passing values increased 5.8-8% from untreated to Son then 1.96-6.96% from Son to SonCav. Again observing Fig. 5.3 (a), the hydrocyclone underflow size distribution curves exhibit a similar trend. However, differences between the Son and SonCav curves are very slight and the cumulative % passing value at 25 μm was ~6%, regardless of treatment. It is possible that some settling occurred within the spiral head tank causing the finest particles to appear more prominent in the feed samples than they truly were as they did not rapidly settle in the head tank and were collected in the head tank overflow stream.

Figure 5.4 indicates that the +1180-μm size interval was most degraded by treatment, decreasing in direct weight percentage from 13.8% when untreated, to 7.41% for Son treatment, and 4.15% for SonCav treatment. SonCav treatment also caused moderate size reduction of the -1180+850-μm material, reducing direct weight percentage from 13.26% when untreated to 9.00% for SonCav treatment. Despite hydrocyclone desliming, the -25-μm fraction increased most, from 6.24% when untreated, to 12.01% for Son treatment, and 13.97% for SonCav treatment. Similar results were also demonstrated in Figure 4.3. In addition, the ash value of the size fractions increased as size decreased. Figure 5.4 indicates that after treatment, ash values were lower for each respective size interval. Because treatment largely degraded the +1180-μm and 1180+850-μm material and not other size intervals, yet ash values were lower for all size intervals after treatment, selective liberation of high ash value material must be occurring.

Table 5.1 displays attribute data for all spiral tests. It should be noted that some data for Son treatment at 31.6 gpm were unavailable due to sampling error as apparent from markedly higher solids split and inconsistent ash value for the middlings stream. Increasing flow led to higher ash values in all streams for all treatments. Also, greater flow led to a significant increase in solids split to the clean coal but, beyond 26.6 gpm, there was very little difference. Furthermore, solids concentration decreased with increasing flow but only substantially from 12.2 to 26.6 gpm.

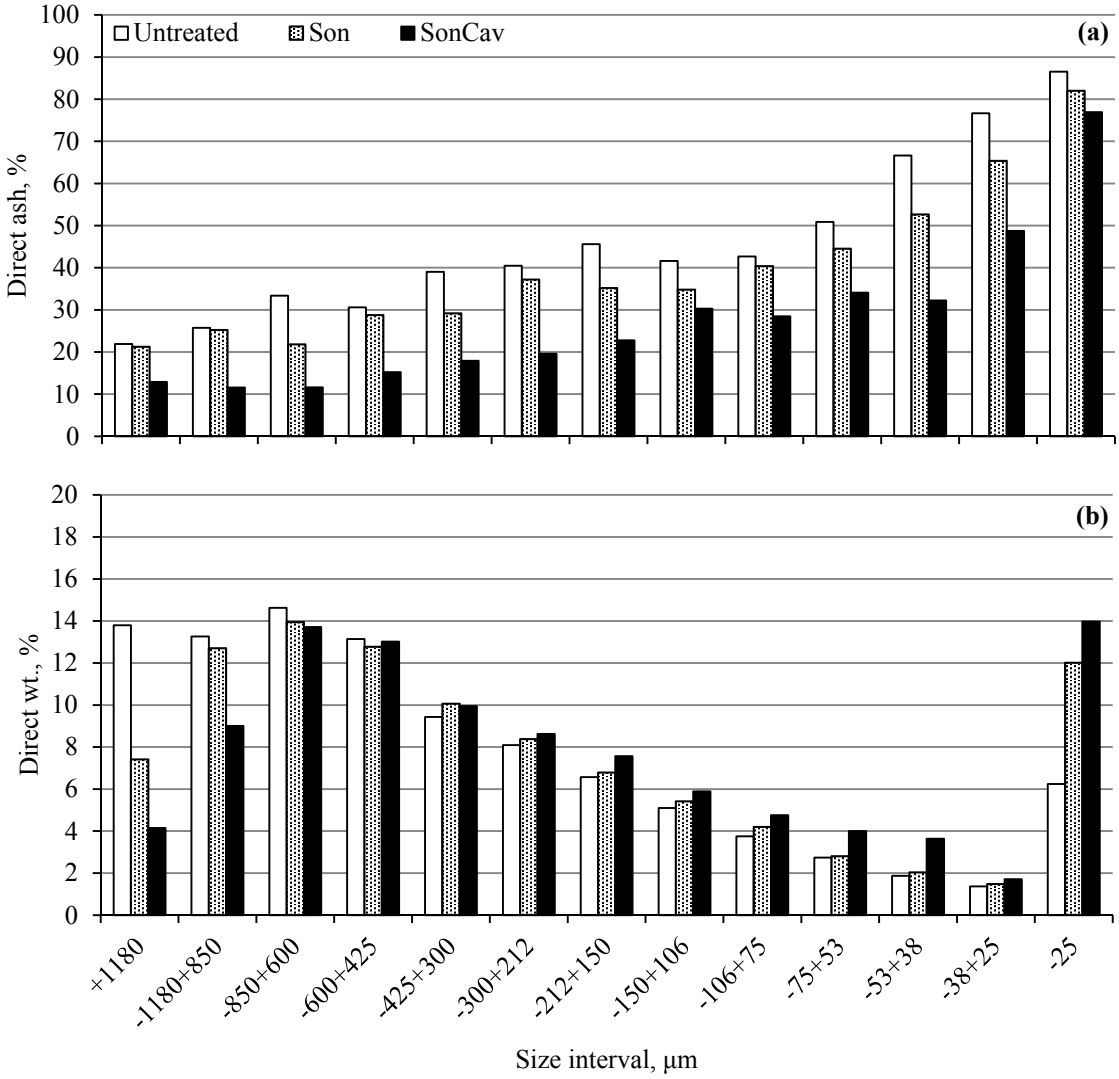

Figure 5.4. Spiral feed direct ash (a) and weight (b) percentages

In terms of HAC effects on the clean coal, the solids split increased as treatment intensified. In terms of other attributes, ash value was lowest for SonCav treatment and highest for Son treatment. Solids concentration was lowest for Son treatment and highest for SonCav treatment.

Table 5.1. Direct measurement attributes

		Flow rate, gpm								
		12.2			26.6			31.6		
Condition	Stream	Solids, % by wt.	Solids split, %	Ash, %	Solids, % by wt.	Solids split, %	Ash, %	Solids, % by wt.	Solids split, %	Ash, %
Untreated	CC	27.4	49.85	15.6	22.3	59.4	17.9	22.4	60.3	20.7
	MID	29.3	13.55	35.3	31.4	7.7	45.1	32.1	7.0	46.8
	REF	33.6	36.60	79.0	55.2	32.9	83.3	55.7	32.7	83.2
	FEED	25.8	-	37.6	-	-	-	-	-	-
Son	CC	22.0	52.88	18.3	20.4	63.2	20.4	21.6	*	20.9
	MID	27.8	13.48	31.2	31.1	8.3	40.6	*	*	*
	REF	44.2	33.64	69.9	49.2	28.6	76.0	50.1	*	77.2
	FEED	24.2	-	35.6	-	-	-	-	-	-
SonCav	CC	31.0	67.2	15.2	26.8	78.9	15.4	26.9	78.2	16.0
	MID	30.1	11.6	23.7	30.5	6.6	32.3	30.7	6.3	37.0
	REF	37.6	21.2	61.3	40.7	14.6	70.2	43.5	15.6	70.2
	FEED	26.7	-	26.5	-	-	-	-	-	-

*Values unavailable due to middlings (MID) sampling error

To assess the accuracy of sampling, the feed ash and solids concentration were reconstituted for each treatment condition across all flow rates using

$$\mathrm{Ff_a} = \mathrm{Cc_a} + \mathrm{Mm_a} + \mathrm{Rr_a} \tag{5.1}$$

where F, C, M, and R are the mass flow rates of the feed, clean coal, middlings and refuse streams, respectively, and f_a, c_a, m_a, r_a represent an attribute (e.g., ash %, sulfur %) of each respective stream. Averaging the values across the 3 flow rates for each treatment, calculations indicated that the feed was 28.93±0.64% solids by weight with 41.98±0.84% ash when untreated, 26.38±1.38% solids by weight with 37.66±0.42% ash for Son treatment, and 29.78±2.00% solids by weight with 25.39±0.81% ash for SonCav treatment. There was some discrepancy between reconstituted feed values and feed head values but overall, accuracy was relatively high.

Plotting cumulative weight percentage against cumulative ash percentage by size for the clean coal (Fig. 5.5), distinct trends by flow rate and treatment are revealed. Increasing the cumulative product weight percentage by incorporating finer size intervals resulted in a lower ash

value product. Including material less than approximately 106 μm caused product ash to begin increasing. By excluding the -106-μm material (i.e., the rightmost five points on each curve), the ash percentage dropped by up to 12% with loss of only 10-15% of product weight. This indicates the importance of an efficient desliming process. Also, intensifying treatment generated a lower ash clean coal product, evident by the downward shift of the curves from untreated to Son and SonCav. Despite minor discrepancies in the coarser size intervals, it appeared that the lowest flow rate produced the lowest cumulative ash clean coal as finer size intervals are incorporated. However, because 26.6-gpm flow leads to a more favorable solids split to the clean coal with only moderate increase in ash value from 12.2 gpm and without sacrificing capacity, the remaining discussion will focus on the 26.6-gpm results.

The impact of treatment with hydrocyclone desliming on the spiral separation for the 26.6 gpm flow rate is apparent from Figures 5.6 and 5.7. Across all streams, the size distribution data (Fig. 5.6) showed a consistent trend of decreasing weight percentage in coarser size intervals with increasing weight percentage in those that were finer as treatment went from untreated to Son and SonCav. In addition, Figure 5.7 shows that ash value decreased with treatment for nearly all size intervals across all streams. From untreated to Son, size intervals that showed reduced ash values declined 0.34-17.84% for clean coal, 0.43-12.46% for middlings, and 2.33-8.4% for refuse. From Son to SonCav, the size interval ash values again declined 0.4-16.9% for clean coal, 0.46-13.32% for middlings, and 4.04-12.99% for refuse.

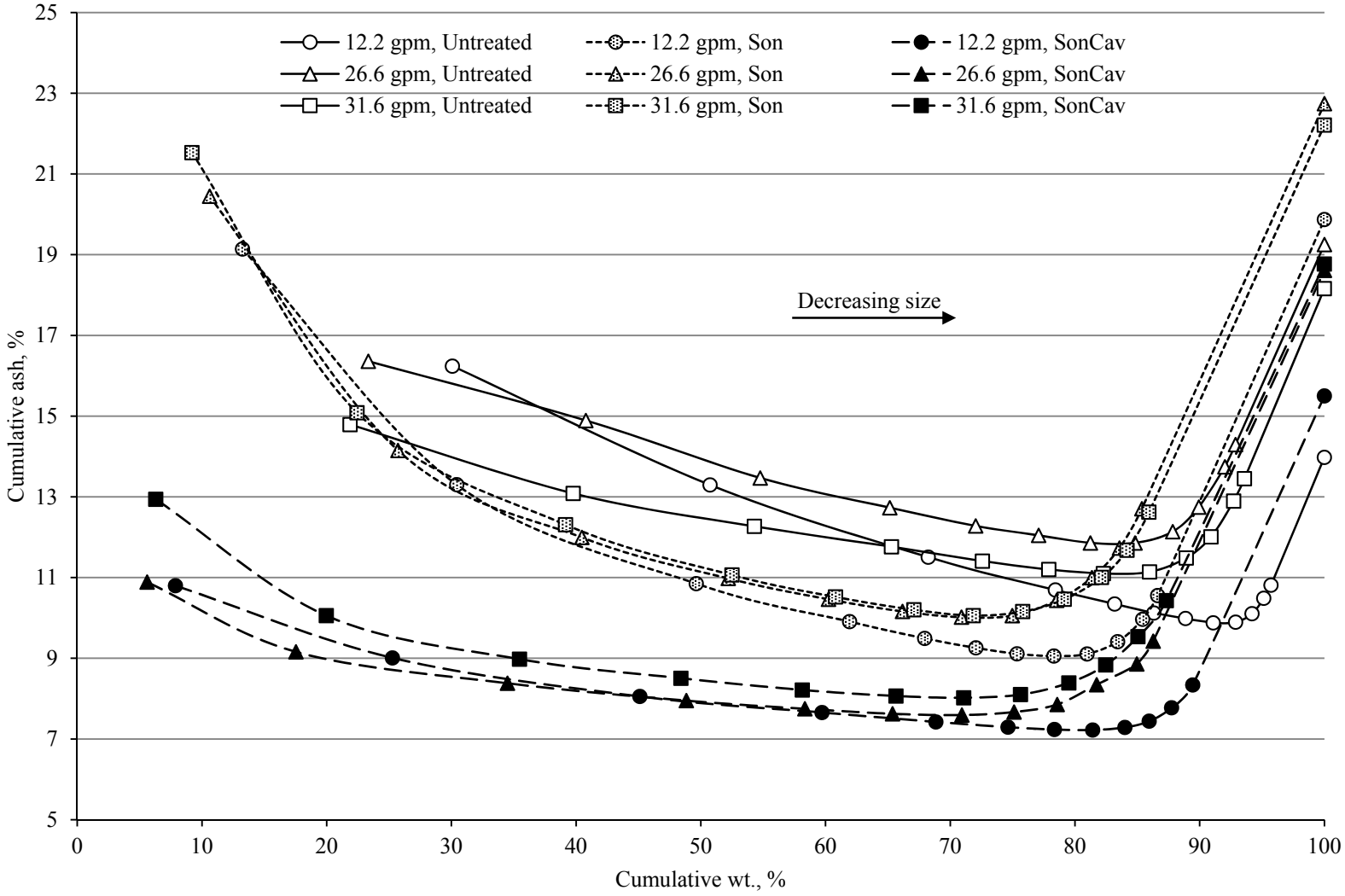

Figure 5.5. Clean coal cumulative yield vs. cumulative ash

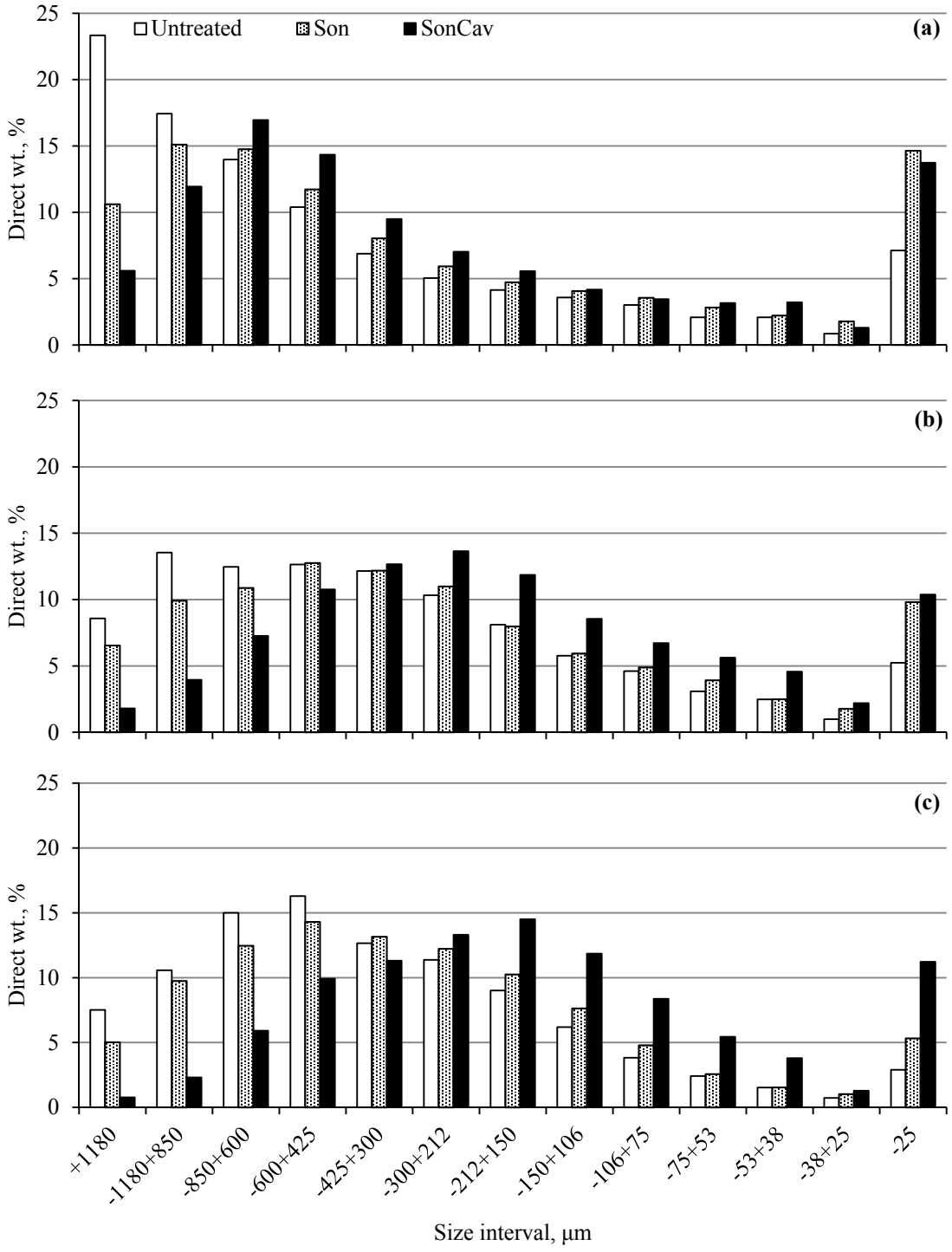

Figure 5.6. Size interval direct weight percentage of the clean coal (a), middlings (b), and refuse (c) at 26.6 gpm

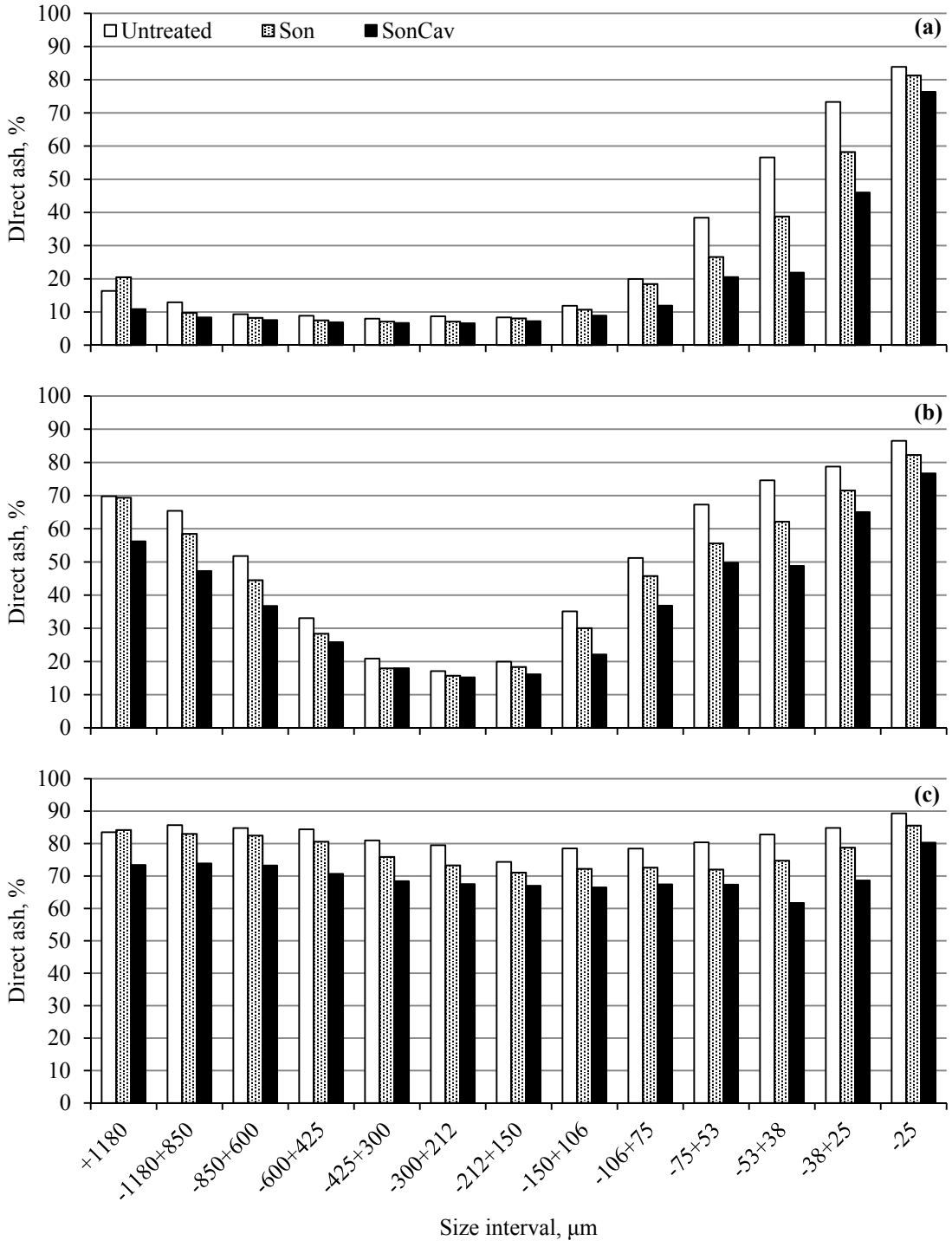

Figure 5.7. Direct ash weight percentage of the clean coal (a), middlings (b), and refuse (c) at 26.6 gpm

To further characterize the streams, the total sulfur of three size intervals (i.e., +300, -300+106, -106 μm) was experimentally determined. As evidenced by the curves (Fig. 5.8), for all treatments the clean coal had the lowest sulfur, ranging from 3.00-3.30%, followed by the middlings at 4.39-4.72% and then the refuse at 7.62-8.27%. The calculated total sulfur of the feeds were 4.91%, 4.63%, and 3.83% for the untreated, Son, and SonCav spiral feeds, respectively. As expected, spiral separation following hydrocyclone desliming reduced the overall sulfur content of the streams. Across treatments, each respective stream possessed a similar sulfur content.

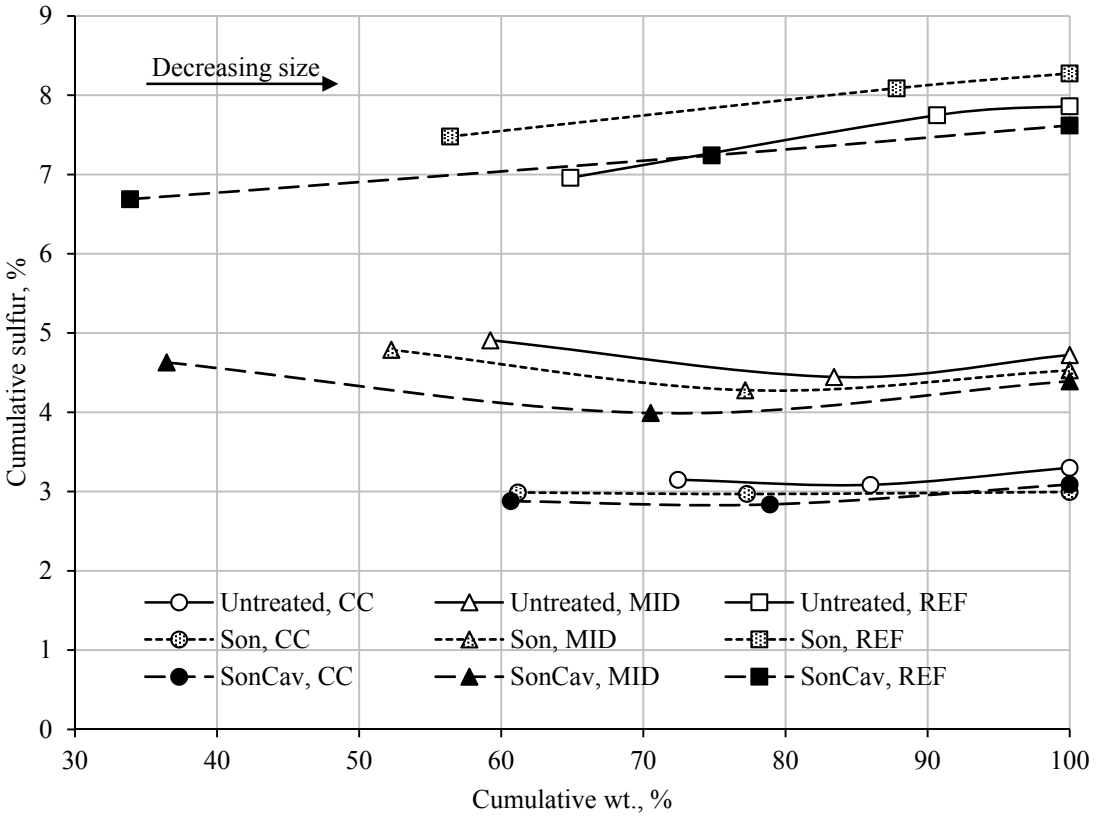

Figure 5.8. Total sulfur content of the spiral streams

5.5 Conclusion

Spiral separation of the hydrocyclone deslimed Sample A material offered considerable ash and sulfur reduction in the clean coal product. Results indicated that optimum performance

was achieved at 26.6 gpm as that condition offered the greatest clean coal yield (78.9%) with an ash value of 15.4%, nearly the lowest observed throughout the testing, and a high clean coal stream solids concentration of 26.8%. Also, regardless of size interval, the SonCav treatment essentially outperformed the untreated and Son conditions in terms of sulfur reduction, producing lower sulfur streams overall. The clean coal contained 3.09% total sulfur compared to 3.83% in the feed stream (reconstituted). Spiral processing was responsible for this reduction as it was shown in Chapter 4 that the hydrocyclone actually concentrated the feed sulfur in the underflow stream.

The overall clean coal yield relative to the hydrocyclone feed was (0.8796)(78.87%)=69.37%. Table 5.2 illustrates that when the Sample A feed received SonCav treatment and was deslimed by the hydrocyclone (20 psi inlet pressure, 1-in diameter overflow, and 0.5-in diameter underflow), then separated into a clean coal stream by the spiral (26.6 gpm), for the ash and sulfur values were reduced by 57.68% and 5.74%, respectively.

Table 5.2. Yield and attribute effects for SonCav treatment at 26.6 gpm

Unit	Yield, %	Ash effects, %	Total sulfur effects, %
Hydrocyclone	87.96	-15.66	7.95
Spiral	78.87	-42.02	-13.70
Total	69.37	-57.68	-5.74

Thus, when SonCav treatment is paired with the hydrocyclone and spiral, substantial ash reduction with moderate sulfur reduction and minimal loss of material to the refuse is possible. Treatment positively affects density separation.

CHAPTER 6

FROTH FLOTATION

6.1 Introduction

Froth flotation is a separation process exploiting the differences in surface properties of particles in a suspension, specifically their wettability, to promote selective attachment of air bubbles. The most hydrophobic particles, which possess a high contact angle between the solid-liquid and liquid-vapor interface (i.e., low wettability), will be carried to the suspension surface within the flotation cell via adhered air bubbles and enter the froth. The froth can then be rinsed with wash water to reduce hydraulically entrained fine, unwanted particles and then removed from the suspension surface, typically reporting to a product launder. However, froth washing is more often industrially used for column flotation rather than conventional flotation using mechanical cells. In coal separations, ash-forming minerals tend to be more hydrophilic and thus remain in the cell to be collected as tailings, while the froth product contains the organic-rich coal. Non-polar substances such as hydrocarbons are naturally hydrophobic. Polar substances such as pyrite (unless after partial oxidation or under acidic conditions where pH<4) are naturally hydrophilic (Kawatra and Eisele, 2001).

The flotation process is controlled by a combination of interdependent variables including chemical (e.g., pH, collector, frother), operational (e.g., particle size, pulp density, temperature), and cell design factors (e.g., air flow, agitation, equipment configuration) (Klimpel, 1995). Higher rank coals of a size range -595+45 μm are often sent to froth flotation for cleaning (Arnold, 1989). In addition, fine coal (-500 μm) is frequently floated to achieve solid/solid separation of organic material from ash and pyritic sulfur (Tao and Parekh, 2000). However, the presence of ultrafine coal (-63 μm) can severely limit the amount of collector available to adhere

to the coarse particles, particularly the +250-μm fraction, which leads to the consequent loss of coarse coal (Smitham and Firth, 1982).

Clay particles are a major inhibitor of effective flotation to produce a high purity coal product due to electrostatic attachment to coal and carry-over with the froth. Because fine coal is typically floated and there exists a low probability of air bubble attachment to small particles, cleaning is difficult and further complicated by clay slime surface coatings, which can reduce hydrophobicity (Reinecke et al., 2003; Tao and Parekh, 2000). To combat these issues, wash water flow rate is increased to decrease ash-producing particle entrainment and produce a cleaner froth product, but at the cost of lower combustible recovery due to increased particle drop-back in the froth zone (Lynch et al., 1981; Tao and Parekh, 2000). Studies related specifically to this topic have shown that kaolinite and illite do not significantly depress coal flotation but that bentonite can, even with moderately hydrophobic coals (Arnold and Aplan, 1986). Because bentonite particles are extremely fine, they are more prone to coat coal particles and even flotation bubbles, preventing particle attachment (Arnold and Aplan, 1986). It has been shown that removal of slime coatings can increase coal flotation recovery (Arnold and Aplan, 1986; Celik, 1989).

6.2 Experimental Circuit

Flotation testing was conducted on Sample B in order to determine treatment effects on froth product yield, ash value, and sulfur content. To carry out the various treatment conditions, the HAC circuit (Section 3.2) and hydrocyclone (Section 4.2) were utilized prior to flotation. For flotation testing, a Wemco laboratory flotation machine (MOD 71260-01) was used (Fig. 6.1). This batch unit is comprised of a single 4-L plexiglass cell with a 3-L effective volume and a forward facing weir for manual removal of froth with a plexiglass paddle. The system has a 2-in diameter, 6-pronged impeller housed within a 4-in diameter and 2-in high stator and a manual (open/closed) air valve. A faucet hose was used to add wash water, as necessary, to maintain cell slurry level. Reagents utilized included a nonpolar collector (fuel oil #2) and a heteropolar frother

(methyl isobutyl carbinol [MIBC] or 4-methyl-2-pentanol). Stainless steel pans were used for froth collection.

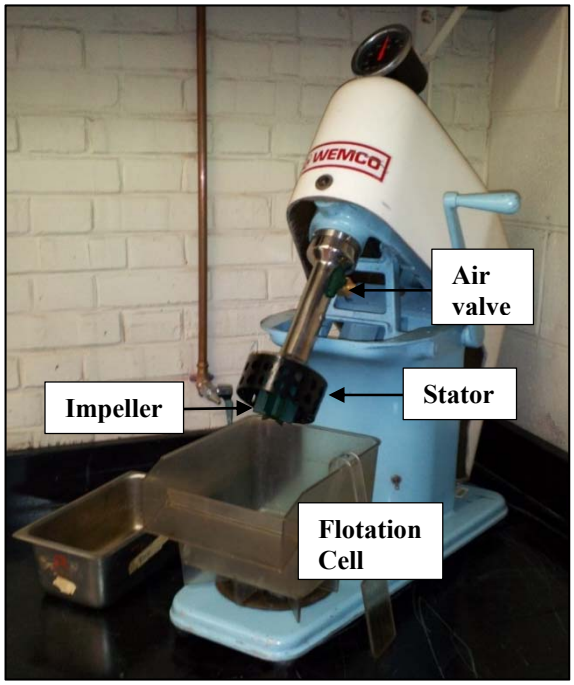

Figure 6.1. Wemco flotation unit

6.3 Experimental Procedures

Initial testing was used to establish a standard flotation procedure. Because initial sample characterization demonstrated Sample B was approximately 4% solids by weight at the preparation plant, it was decided that treatment and flotation would be conducted near this solids concentration (125 g coal/3 L water). A variety of treatment conditions were utilized including 50% and 100% power sonication (i.e., 50Son and 100Son), cavitation without sonication by diverting all flow through the orifice plate (i.e., Cav) and 50% and 100% power sonication with all flow through the orifice plate (i.e., 50SonCav and 100SonCav). All treatment was engaged 5 s prior to sampling and the samples floated within 1 hr of treatment. Deslimed samples were collected from the hydrocyclone underflow and undeslimed samples retrieved from the HAC circuit T-port 3-way valve. Samples were always introduced to the flotation cell in slurry form

and diluted by manually adding tap water with a faucet hose if deslimed. Pulp level was maintained at 0.5 in below the discharge lip (3 L) with the impeller submerged for the entirety of each individual test. Pulp pH was recorded with an Oakton WD-35634-20 pH tester. Cell pulp was mixed for 3 min at 1100-rpm impeller speed prior to reagent addition and conditioned for 1 min after frother addition and 4 min after collector addition. Frother and collector were introduced using separate Hamilton Co. #725 Microliter syringes (250-µL syringe, 5-µL smallest increment). During flotation, the air valve was opened fully. Air was only introduced to the cell following reagent conditioning and immediately shut off following completion of froth collection. Collection was performed using a constant scraping technique. The products were dried at 215°F for 24 h in the 5.5-in by 9.5-in by 4-in stainless steel collection pans for the froth products and in 18-in by 18-in by 3-in stainless steel pans for tailings.

Qualitative testing was initially conducted to determine adequate frother and collector dosages. Based on the previously determined solids concentration, a sufficient mass of Sample B slurry was acquired per Section 2.3.1 and diluted to 4% solids by weight without exceeding the 3-L effective cell volume. Following mixing, 40 µL of MIBC was added and conditioned. The air valve was opened and the froth collected. The air was then shut off and the process repeated for several 40-µL MIBC additions. After determining the appropriate MIBC dosage of 120 µL, another pulp of 4% solids was mixed, 120 µL of MIBC added and conditioned, and #2 fuel oil then added in 50-µL increments and conditioned. The froth was collected between each incremental #2 fuel oil addition. At 4% solids by weight cell loading, 40 µL of MIBC is ~0.5 lb MIBC/ton coal and 50 µL of #2 fuel oil is ~0.7 lb #2 fuel oil/ton coal.

Following these tests, two types of flotation tests were performed. The first type was an ultimate flotation recovery test where, following treatment and/or desliming depending on test condition, slurry was introduced to the cell and diluted, if necessary, to approximately 4% solids by weight though the actual solids concentration was not known until the samples were dried.

Following mixing, the reagents were added and the froth product was collected until minimal solids were observed in the froth (Fig. 6.2). At this point, aeration was stopped and additional reagent added to the same pulp batch, conditioned, and froth product collected. This was repeated so that a single ultimate recovery test produced four froth products of cumulative dosages 40-µL MIBC, 80-µL MIBC, 120-µL MIBC, and 120-µL MIBC with 50-µL #2 fuel oil as well as tailings. All froth products and the tailings were oven-dried at 215°F for 24 h. The ash values were determined per Section 2.3.3.

The second type of testing was based on the flotation rate. After the solids were added to the cell and mixed as previously described, 120 µL of MIBC was added to the pulp and conditioned. Because this coal was readily floatable, #2 fuel oil was not used. Following conditioning, the air valve was opened and the froth allowed to build until spilling onto the collection weir. This time, which elapsed from the start of aeration until the froth reached the weir, was recorded as induction time. Following induction, the froth product was continuously collected in separate pans for time intervals 0-15, 15-30, 30-45, 45-60, 60-90, 90-120, 120-180, and 180-240 s. Each test produced eight froth products and tailings, which were dried and analyzed in the same manner as the ultimate recovery tests. In addition, for the undeslimed untreated, 100Son, and 100SonCav tests, the time interval froth products and tailings were wet screened by hand at 25 µm, and ±25-µm material was analyzed for ash and total sulfur per Section 2.3.4. Proximate analysis was performed on a head sample of the tailings from those tests, as well.

Figure 6.2. Ultimate recovery flotation before (a) and after (b) froth scraping

6.4 Results and Discussion

The ultimate flotation recovery tests had an average cell solids loading of 195.1±23.9 g of coal (5.4-6.8% solids by weight). The feed ash of each test was reconstituted using the product and tailings weights and their respective ash value. For the ultimate recovery tests, the average feed ash value was 51.86±0.89% for the undeslimed tests, 39.50±2.66% for the hydrocyclone deslimed tests, and 26.06% for the single wet screened +25-µm test. For the recovery rate tests, the average cell solids loading was 159.7±20 g of coal (4.3-5.6% solids by weight). Average ash values were 53.87±1.05% for the undeslimed tests, 40.33±0.77% for the hydrocyclone deslimed tests, and 16.05% for the single wet screened +25-µm test. The slurry pH and induction time were recorded only for the rate recovery tests and were an average of 8.06±0.08 and 11.9±5.2 s, respectively.

The effects of desliming prior to flotation are readily apparent from Figures 6.3 and 6.4. Desliming removes the high ash, ultrafine particles and so for equivalent yield, the deslimed tests possess lower cumulative ash than their undeslimed counterparts by a difference of over 20% in some cases. From the +25-µm wet screened curves, the removal of the -25-µm material resulted

in superior flotation, independent of treatment. Focusing on Figure 6.3, among deslimed curves, except at the higher reagent dosages, it appears that treatment essentially worsened flotation performance, exhibiting higher ash values in the product at equal yields. Also, 100Son and 100SonCav exhibited the best flotation behavior of the treated deslimed conditions. Wen-ze et al. (2007) demonstrated that refuse hydrophilicity increased with sonication, which seemed to occur for the 100Son and 100SonCav tests after desliming but, was not true for the undeslimed test. This suggests that perhaps surface fines were liberated by the more intense HAC treatment and subsequently removed by the hydrocyclone. Thus, these fine particles would not be present in the flotation feed (i.e., hydrocyclone underflow) to carryover and increase the ash values of the froth products. Weaker sonication and cavitation alone may have failed to liberate fines and only dispersed the material leading to increased carryover. Interestingly, the undeslimed, untreated flotation had a more desirable low ash value recovery than the undeslimed tests with treatment likely due to treatment dispersion effects. Also, the undeslimed 100Son and 100Soncav tests exhibited the worst performance, reinforcing the idea that fines were liberated by these stronger treatments and without desliming, led to a poor flotation.

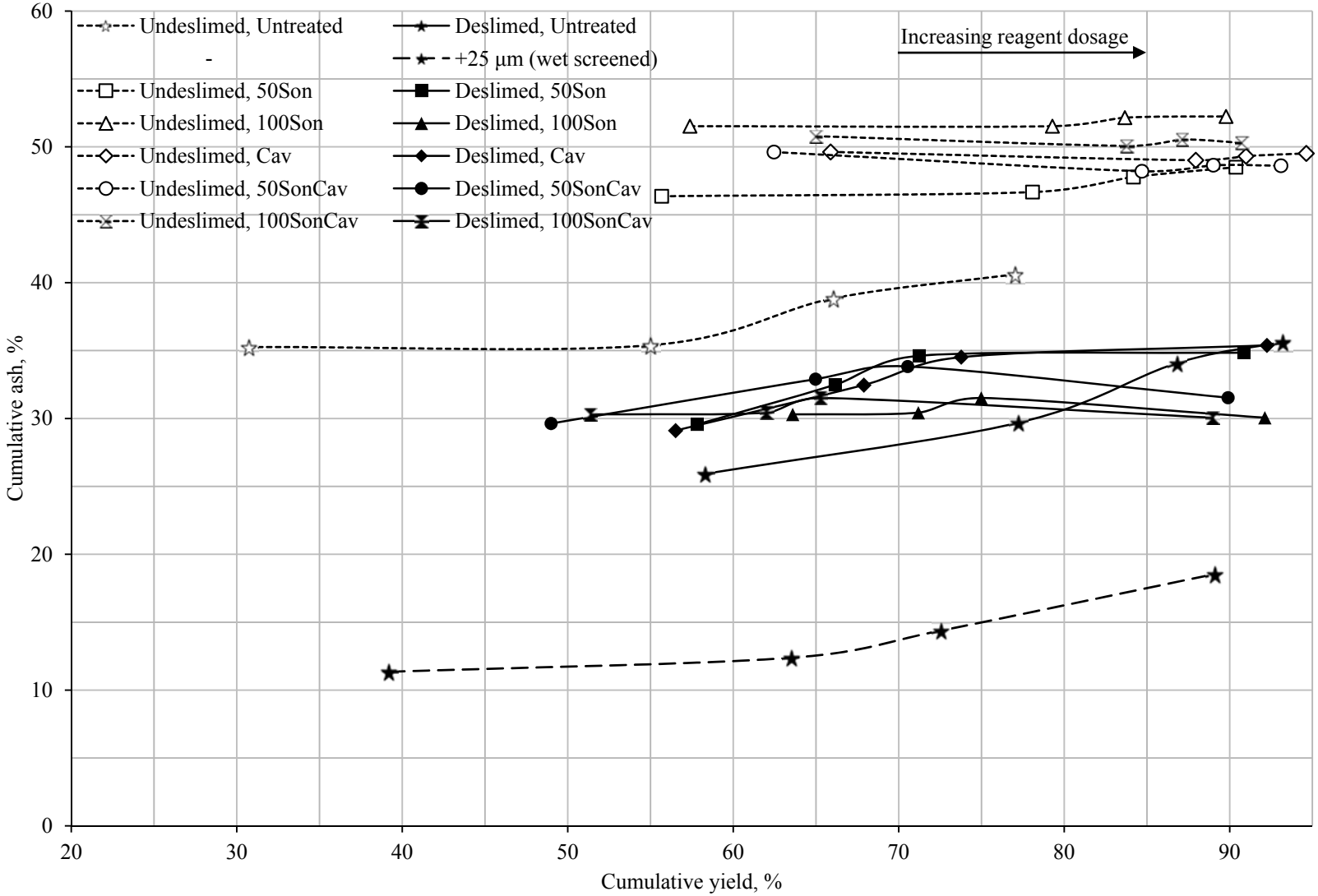

Figure 6.3. Ultimate recovery flotation tests

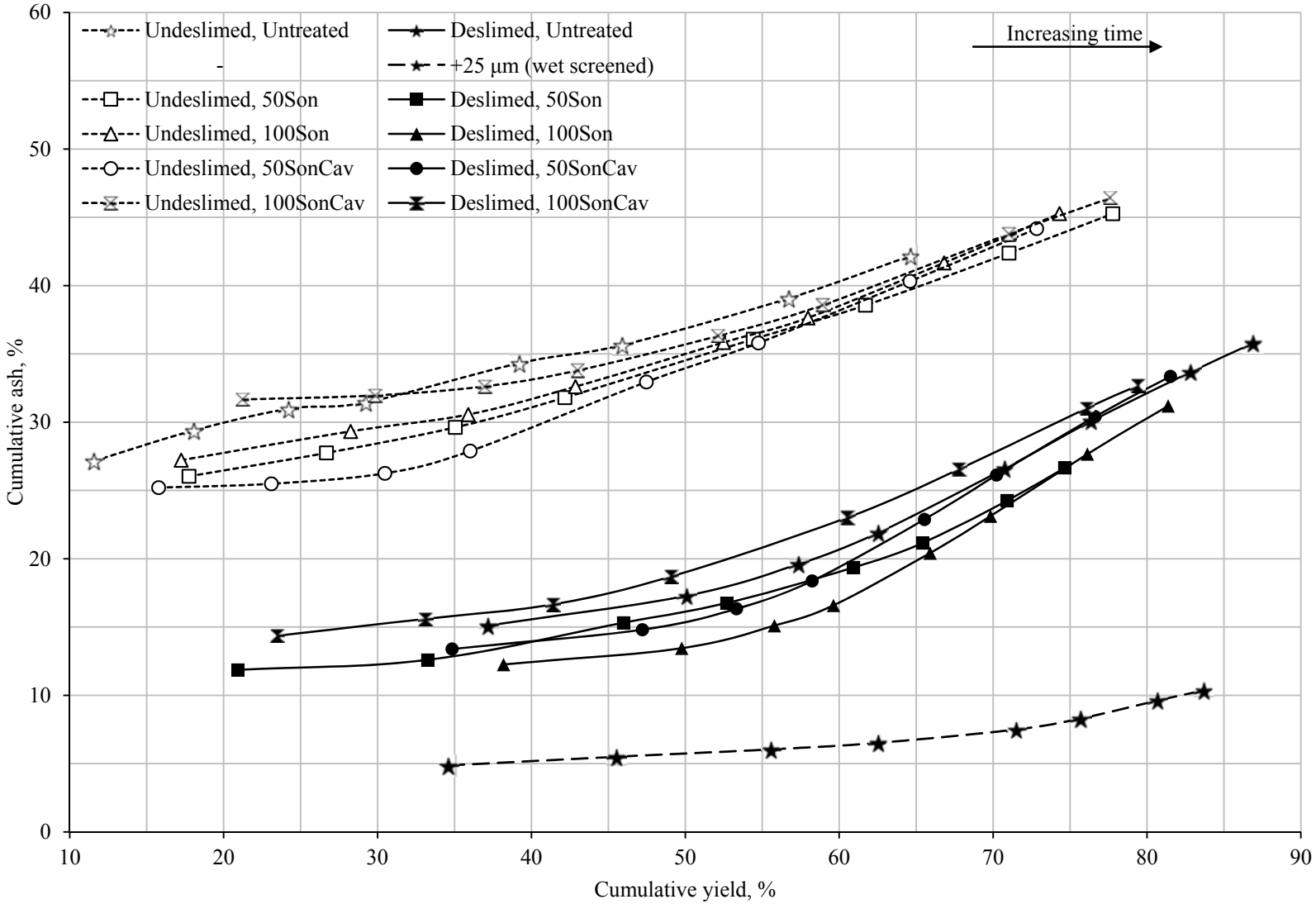

Figure 6.4. Recovery rate flotation tests

Figure 6.4 shows the results from the flotation rate tests. Because testing was carried out in fixed time intervals at a fixed reagent dosage, the results are not necessarily directly comparable to the ultimate recovery testing. The effects of hydrocyclone desliming are again very obvious, increasing initial (i.e., 0-15 s collection time) yield by up to 25.6% at 12.1% lower ash value for the untreated condition. The hydrocyclone deslimed curves (Fig. 6.4) show that 50Son, 50SonCav, and 100Son treatment showed some improvement in flotation performance over the untreated condition. When undeslimed, essentially all treatments were effective at reducing product ash values.

The ash rejection and combustible recovery were calculated for the flotation tests. First, the ash balance is defined as

$$\mathrm{FA_F} = \mathrm{CA_C} + \mathrm{TA_T} \tag{6.1}$$

where F, C, and T are the mass of feed, concentrate (i.e., froth product) and tailings, respectively, and A_F, A_C, and A_T represent the respective ash values (%) of those streams. Ash rejection is then calculated by

$$\text{Ash rejection}, \% = 100 * \frac{\mathrm{TA_T}}{\mathrm{FA_F}} \tag{6.2}$$

and combustible recovery calculated by

$$\text{Combustible recovery}, \% = 100 * \frac{\mathrm{C}(100-\mathrm{A_C})}{\mathrm{F}(100-\mathrm{A_F})} \tag{6.3}$$

To calculate cumulative values, froth products that were collected following the reagent addition or time of collection of interest were considered tailings. For example, if the cumulative ash rejection was determined for up to 60 s of collection for the rate recovery testing, froth products from 60-240 s (i.e., 60-90, 90-120, 120-180, 180-240 s) would be incorporated into the tailings using the mass and ash value for each interval.

For the ultimate recovery (Fig. 6.5), the untreated material possessed better flotation performance than any treated samples when both undeslimed and deslimed. That is, greater

combustible recovery was observed at higher ash rejection. Treatment negatively affected flotation as a result of dispersion, which caused carryover of the high ash value material. For the rate recovery tests (Fig. 6.6), the undeslimed flotation curves show that all treatment essentially increased combustible recovery and ash rejection. Observing the deslimed rate curves, the 50Son and 100Son treatments most distinctly improved flotation as well as the 50SonCav treatment in froth products sampled within the first minute (i.e., 0-15, 15-30, 30-25, 45-60 s).

As previously mentioned, the undeslimed untreated, 100Son, and 100SonCav treatment flotation products and tailings for rate recovery testing were wet screened at 25 μm and analyzed for ash and total sulfur. As shown in Figure 6.7, HAC treatment had a minor effect on flotation for both size fractions. For equivalent cumulative weight percentage at a given collection time, the treated -25-μm material had higher ash values. Sample B displayed minimal size reduction effects after 5 s of treatment and 1 min of recirculation in the HAC circuit (Fig 4.4) so this was not attributable to size degradation. However, as collection time increased, a substantially larger amount of inorganic material is present in the treated +25-μm material of later froth products and tailings. Overall, the treated +25-μm material had higher ash values. Thus, liberation of inorganic surface fines with greater carryover may not be occurring, but this perhaps was masked by the slight variation in feed solids composition.

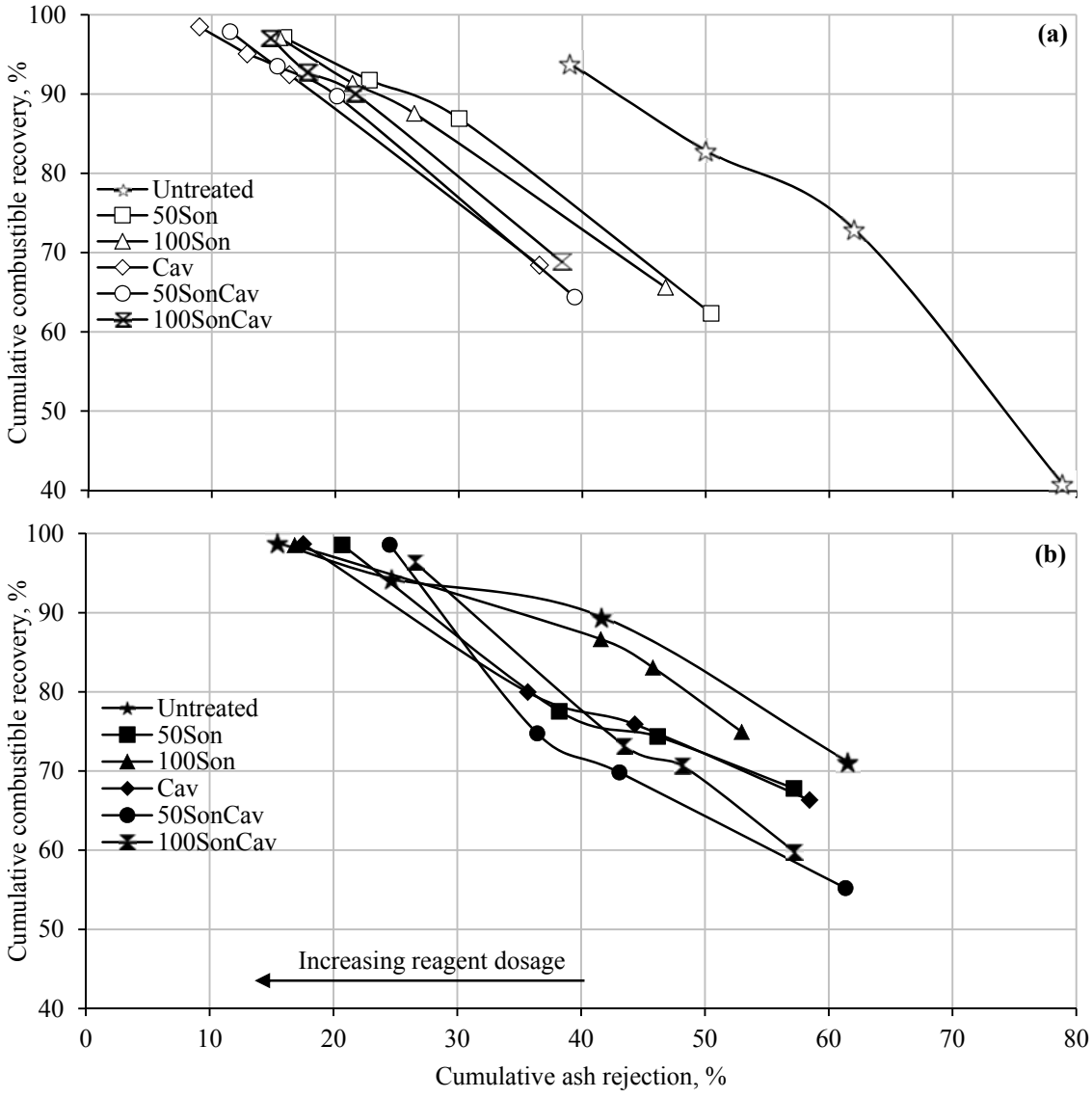

Figure 6.5. Undeslimed (a) and deslimed (b) ultimate recovery flotation

Total sulfur analysis of these same size fractions by collection time indicated that there was no substantial effect on total sulfur by treatment (Fig. 6.8). Only the +25-µm tailings showed any significant difference generated by HAC treatment. Because sonication and cavitation have been shown to more strongly affect pyritic sulfur rather than organic sulfur, and size reduction potentially leading to pyrite liberation was minimal after only 5 s of either treatment, sonication

and cavitation may have increased the hydrophilicity of pyrite as found previously (Wen-ze et al., 2007).

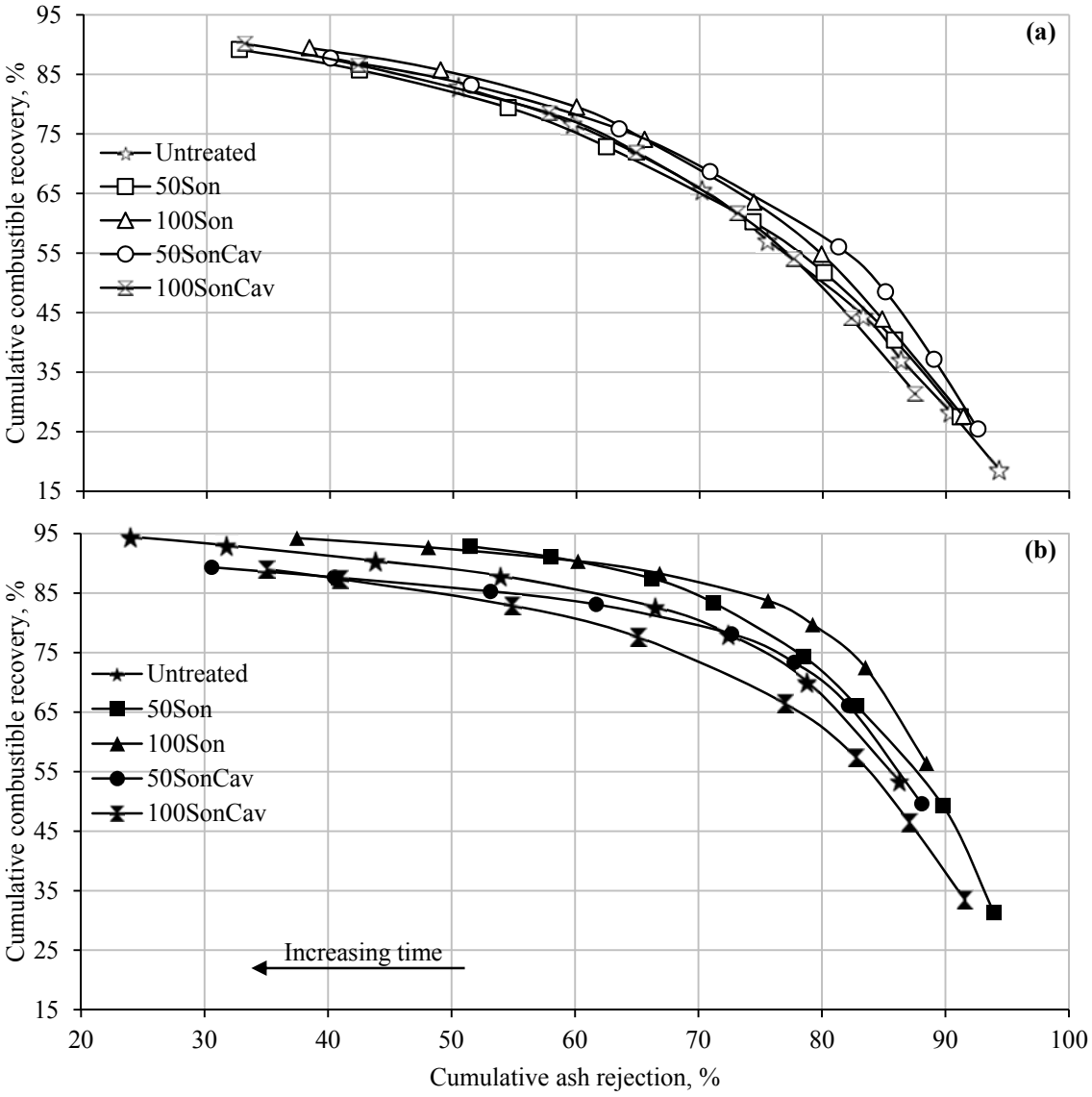

Figure 6.6. Undeslimed (a) and deslimed (b) recovery rate flotation

Proximate analysis of tailings head samples and calculation of combined product (0-240 s) attributes reveals more about the undeslimed rate tests (Table 6.1). It was assumed that the cell feed characteristics were equivalent to those of the Sample B head (Table 2.3) for these calculations. Sulfur was minimally affected by the treatment and as the treatment intensified,

product yield (i.e., solids split) and ash values increased by more than 13% and 6%, respectively, while the heating value declined. Again, dispersive effects and carryover are directly apparent from these results.

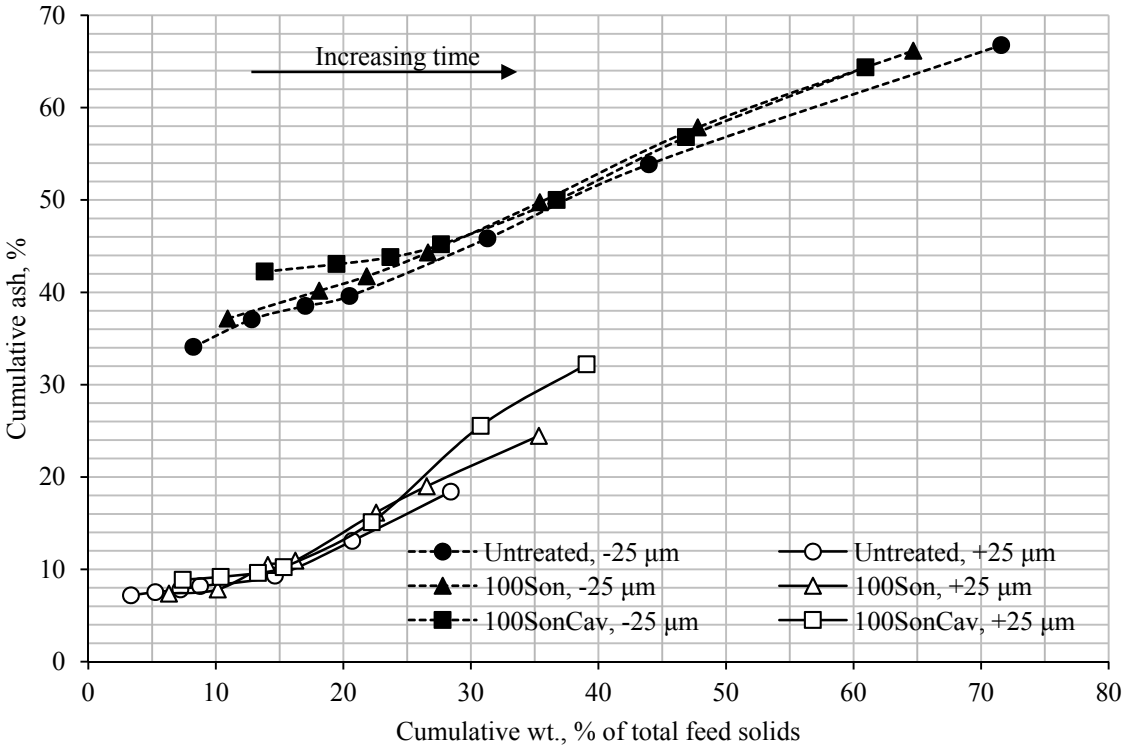

Figure 6.7. Undeslimed rate test cumulative yield vs. cumulative ash by size

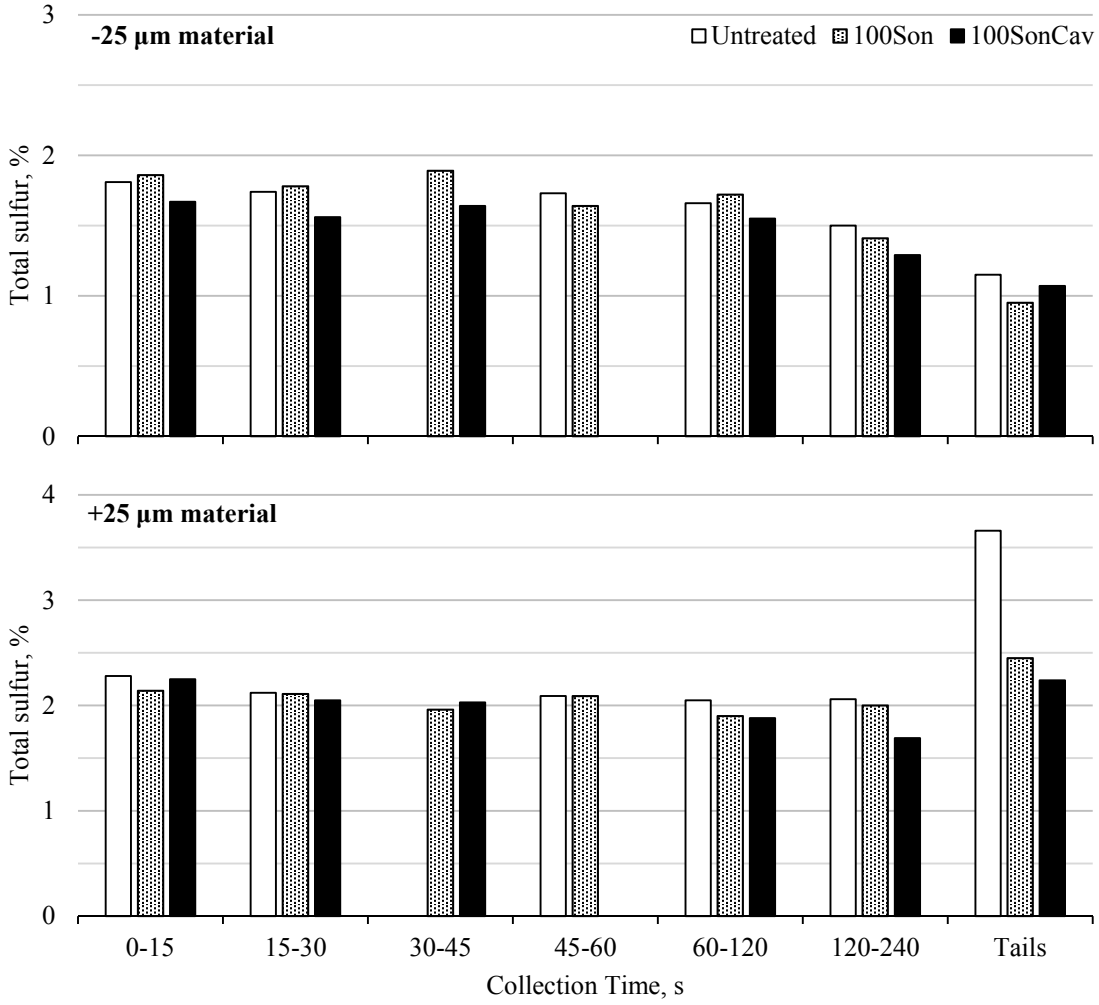

Figure 6.8. Rate recovery total sulfur by time and size (30-45 s and 45-60 s data unavailable for certain conditions)

Table 6.1. Proximate analysis of undeslimed rate recovery tailings

			Sulfur				Heating Value
Condition	Solids Split, %	Ash, %	Total, %	Pyritic, %	Sulfate, %	Organic, %	Btu/lb
Total Product (Calculated)							
Untreated	62.9	38.4	2.68	1.93	0.23	0.51	8497
100Son	74.2	43.7	2.54	1.92	0.19	0.43	7724
100SonCav	76.6	44.6	2.54	1.86	0.19	0.49	7548
Tails (Head)							
Untreated	37.1	74.8	1.66	1.36	0.04	0.26	2909
100Son	25.8	75.3	1.62	1.15	0.07	0.40	2685
100SonCav	23.4	75.7	1.51	1.26	0.05	0.20	2735

The effects of pairing desliming and flotation are illustrated in Tables 6.2 and 6.3. Desliming by hydrocyclone or screening had minimal effects on cumulative yield following 15 s of flotation when compared to undeslimed testing. However, cumulative reduction in feed ash values were over 20% greater after 15 s of flotation when the sample was deslimed. Overall, it appeared that as time of flotation increased, cumulative yield among deslimed tests was nearly the same with greater cumulative ash value reduction for tests that received HAC treatment. Undeslimed tests which received HAC treatment had higher cumulative yield but with lesser cumulative ash value reduction.

Table 6.2. Processing yield

	Cumulative Yield, %						
	Hydrocyclone Deslimed			Screened	Undeslimed		
Process Flow	Untreated	100Son	100SonCav	+25 μm	Untreated	100Son	100SonCav
15-s flotation	13.83	15.76	9.92	14.28	11.58	17.23	21.24
60-s flotation	23.24	24.60	20.76	25.80	29.25	42.86	42.98
120-s flotation	28.40	28.81	28.65	31.24	45.93	57.96	58.94
240-s flotation	32.30	33.57	33.56	34.53	64.64	74.31	77.63
Desliming only (no flotation)	37.17	41.26	42.27	32.68	-	-	-

Table 6.3. Processing ash reduction

	Cumulative Ash Value Reduction, %						
	Hydrocyclone Deslimed			Screened	Undeslimed		
Process Flow	Untreated	100Son	100SonCav	+25 μm	Untreated	100Son	100SonCav
15-s flotation	70.88	76.37	72.32	90.61	47.63	47.53	38.96
60-s flotation	57.77	68.03	63.94	87.42	39.36	37.16	34.87
120-s flotation	42.00	55.44	48.82	83.97	31.26	27.44	25.62
240-s flotation	31.01	39.88	37.01	80.00	18.67	12.73	10.50
Desliming only (no flotation)	24.17	23.05	24.46	53.06	-	-	-

6.5 Conclusion

The effects on froth flotation of Sample B by two levels of sonication, orifice plate cavitation, and desliming were evaluated. To a great extent, HAC treatment had no or a slightly

negative effect on flotation performance in terms of ash and sulfur values. Desliming improved flotation substantially by reducing the inorganic fines in the feed, which carried over into the froth product. Screening was more effective at desliming compared to cycloning. The ultimate recovery tests with increasing reagent dosage displayed that for cumulative yield, cumulative product ash value was higher following treatment. The rate recovery results indicated that in general, treatment slightly reduced the product ash values for a given collection time.

Undeslimed rate recovery results showed that the 100Son and 100SonCav treatments had marginal to negligible effects on the ash and total sulfur values for the ±25-μm material compared to the untreated test. Proximate attributes of the combined products and tailings for these conditions demonstrated that product yield improved with treatment but at the cost of increased inorganic content and reduced heating value. Overall, HAC treatment had minimal effect on flotation performance of the highly inorganic, Sample B material. Dispersion and surface fine liberation are negated by carryover into the product. Furthermore, desliming is critical to improve flotation performance.

CHAPTER 7

PRESSURE FILTRATION

7.1 Introduction

Filtration primarily refers to the separation of solid particles from liquid through the application of pressure and commonly with the assistance of a semi-permeable filter medium. It is not the filter medium but formation of a filter cake, resulting from deposition of solids, that is largely responsible for the separation and generation of liquid filtrate. In the mineral processing industry, the filter feed consists of suspensions more so than colloids or solutions.

There are several filtration devices utilized to dewater coal including vacuum filters, belt presses, and centrifuges (Lockhart and Veal, 1996). More recently, plate filter presses have been applied. The plate filter press operates by pumping slurry into a fixed-cavity that is lined with a semi-permeable filter medium, which collects the filter cake, while allowing filtrate to pass through the membrane into peripheral exit ports. Operating pressures of up to 2 MPa (290 psi) can be achieved and industrially, units can consist of over 100 flush plates, with frames that are 25 to 150 mm deep (Gösele and Christian, 2005). Slurries of over 10% solids by weight consisting of at least 90% -10-μm particles are commonly treated (Svarovsky, 1985). In addition, pressure plate filters are desirable as they produce dense cakes of low moisture content (typically less than 25%), have an insensitivity to feed fluctuations, and offer simple operation (Gösele and Christian, 2005; White, 2013).

Plate filter press operation is a batch process in which the filter cycle includes loading of the cavity with slurry, a ramping pressure period in which cake formation and filtrate production begins, constant pressure operation, and discharge of the cake. Prior to discharge, processes are often implemented to remove additional moisture to improve cake handleability further and to lessen subsequent thermal drying time when used. Flexible membrane units that squeeze the cake

of moisture are used, but this is more frequently accomplished through post-filtration gas (usually air) blowing. However, dewatering by gas blowing is most practical for cakes consisting of coarser particles due to high capillary forces encountered with small pore sizes (Buscall and White, 1987). Typically, the effective range for application is a cake permeability of 10^{-11} to 10^{-15} m^2 (Carleton and Salway, 1993).

Feed characteristics directly affect filtration performance and cake qualities. As described by Wakeman (2007), feed size distribution primarily controls cake porosity, with wider size ranges producing cakes with greater resistance to fluid flow (i.e., higher cake specific resistance) because particles pack more tightly. The amount of fine particles, particularly those less than 10 μm, have the greatest effect on filtration. Fines contribute most to bleeding or the passage of fine particles through the filter medium into the filtrate, cause blinding of filter medium pores, lead to higher specific resistance of the cake, making washing and dewatering difficult, and interact most strongly with ions and polymers. The large surface area of fines is problematic in dewatering operations. Also, coal slime coatings are detrimental in filtration, increasing cake moisture (Tao and Parekh, 2000). Flocculation prior to filtration is usually necessary in alleviating issues arising from fines (Alam et al., 2011). In addition, particle shape can affect porosity and specific resistance of the cake. Notably, fibrous particles tend to produce porous cakes with low specific resistance to fluid flow (Wakeman, 2007).

7.2 Experimental Circuit

Pressure filtration testing was conducted on Sample B utilizing a pilot-scale, plate-and-frame filter press manufactured by T.H. Minerals, Spain, and distributed by PrepTech, Inc (Fig. 7.1). The unit is loaded via a 120-L feed tank equipped with a variable-speed mixer. The main control panel display serves to control filter press operation and the alternate display controls the feed tank mixer. There are two hydraulically driven filter plates forming the pressure chamber, each 0.63 m by 0.63 m with a filtration surface area of 0.4 m by 0.4 m. Heat set, calendered

polypropylene monofilament cloth with satin weave covers the inside of each plate. Each cloth possesses a permeability of 0.25 m/s and 0.051 mm diameter pores. Two diaphragm pumps, hydraulically driven by two ABB M2AA 090 S (480 V, 1690 rpm) motors, feed slurry into the chamber to maintain an operating pressure of approximately 125 psi. Filtrate enters a collection tank seated below the unit, which is fitted with a conductivity probe. The probe height may be adjusted within the tank to optimize cycle duration as the unit will cease pumping if filtrate does not reach the probe. Filtrate exits and is collected via a discharge line protruding from the collection tank. A manual, 2-way valve between the slurry feed line and filter plates serves to discharge residual slurry prior to cake discharge to prevent dilution of the final cake. Solenoid valves are controlled via compressed house air delivered at approximately 60 psi, and air for the dry cycle supplied via a portable air compressor operating at 100 psi. Upon test completion, slurry drainage was accomplished using the feed tank side- and base-drain valves.

7.3 Experimental Procedures

To determine the effects of hydroacoustic cavitation pretreatment on dewatering of Sample B via filter press, laboratory testing was conducted for a variety of experimental conditions. In order to subject the slurry to hydroacoustic treatment, the material was first loaded into the HAC circuit (Chapter 3). The volume of water necessary to dilute 5-gal bucket samples of Sample B to 20% solids by weight for a target total feed volume of 100 L was calculated. The water was added to the HAC feed tank and recirculated within the circuit. Sample B material was then added. After 1 min of recirculation to ensure slurry homogenization, HAC treatment was engaged. Treatment conditions included no treatment, Son, and SonCav, as discussed in Section 3.3. Sonication was set to 100% power for all filter press testing. After treating the material for 0, 1, or 5 min depending on experimental batch, the slurry was diverted to the filter press feed tank via the HAC circuit T-port, 3-way sampling valve (Fig. 3.1).

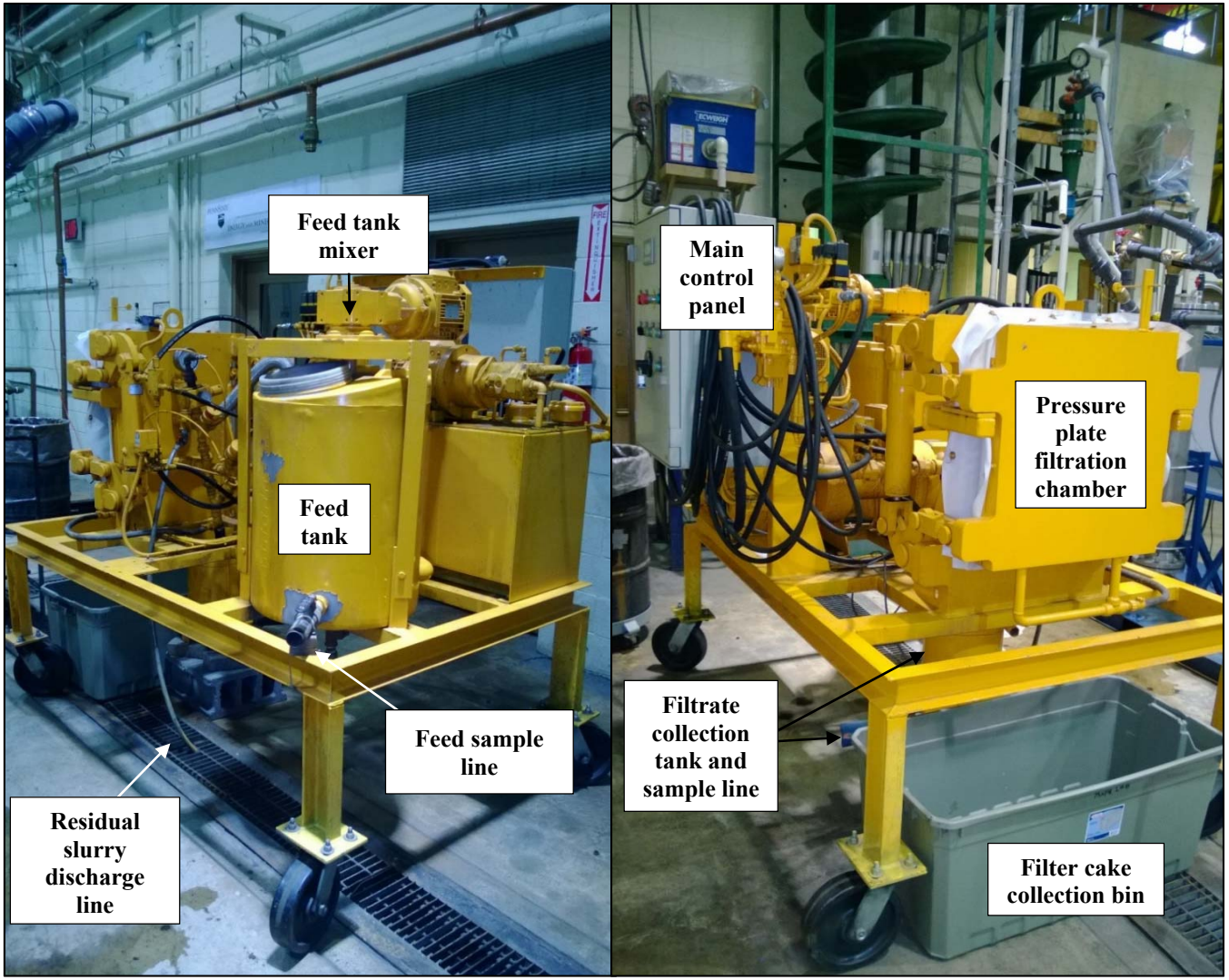

Figure 7.1. Pilot-scale pressure filtration unit

Once in the feed tank, the slurry was continuously agitated by adjusting mixer speed to limit settling without strong vortexing. A 1-L feed sample was taken from the feed tank side 2-way valve near the base of the tank and tested for pH with an Oakton WD-35634-20 pH meter. The wet sample weight was recorded and then the sample was dried for 24 hr in a 217ºF oven to determine dry weight and calculate feed solids concentration. Prior to cycle start, several cycle parameters were set using the main control panel including a 60-s maximum chamber fill time, 700-s maximum filter time, 120-s drying or air blow time, and 60-s pause time between drying time and cake release. Maximum filter time was increased to a total of 40 min for some tests as discussed in Section 7.4. At this point, the filter press cycle was initiated. If the filtrate collection tank conductivity probe did not detect filtrate at the end of the 60-s fill period, the cycle ceased and was manually reinitiated. Following the loading period, filtrate was collected in preweighed buckets. Collection occurred in 30-s intervals from 0-3 min, 60-s intervals from 3-10 min, 120-s intervals from 10-20 min, and 180-s intervals thereafter, depending on total cycle time. Pore fluid released from the cake during the 120-s air blowing period at the cycle end was collected and weighed separately. After air blowing completed, the filter plates retracted and the cake was released, falling into a preweighed, double-handled steel tray (30 in by 18 in by 12 in; not pictured in Fig. 7.1).

All timed filtrate samples and the air blow sample were individually weighed, then combined and transferred into 18 in by 18 in by 3 in stainless steel pans and dried in an oven at 217ºF for at least 24 hrs. The dried filtrate solids were then weighed to determine total filtrate solids concentration. In addition, the wet cake was weighed and then dried in an oven at 217ºF for at least 24 hr. The dry weight was recorded and the moisture content calculated. Once all wet weights were recorded, the remaining filter press feed slurry characteristics were modified either by pH reduction or flocculation. Reduction of pH was achieved by addition of hydrochloric acid of 31.45% purity, or what is industrially known as muriatic acid. Preliminary testing had

indicated that higher filtration rates were possible at lower pH values. The acid was added in 1-L increments and allowed to mix with the slurry for 3 to 5 min before a 1-L feed sample was taken from the feed tank side 2-way valve for pH measurement. This process was repeated until the slurry reached a pH of about 4, at which time the filter press cycle was engaged and the above process repeated. It should be noted that reduction of pH required an approximately 0.02 v/v ratio of muriatic acid to the 20% solids by weight feed slurry.

The next series of filter tests were carried out using flocculated slurry. Preliminary testing of addition of 16 different 200 ppm flocculant solutions to 1-L samples of 20% solids by weight Sample B slurry at natural slurry pH (~8) was conducted prior to testing in the circuit. Testing demonstrated that a proprietary anionic polyacrylamide flocculant, Cytec Superflow A-130 high molecular weight (HMW), provided the greatest visual floc development and so it was utilized for filter press flocculation testing. The flocculant was added as a 600 ppm solution in 1-L increments to the natural pH slurry within the feed tank and allowed to mix with the slurry for 3 to 5 min before a 1-L feed sample was taken from the feed tank side 2-way valve. Samples were taken in clear containers and allowed to settle for qualitative observation of flocculant effects. At about a 0.16 v/v ratio of flocculant addition to 20% solids by weight feed slurry, floc development was visible and settling noticeably affected, thus the filter press cycle was engaged and the experimental filter press procedure repeated. For certain tests, the slurry pH was reduced following the natural pH flocculation filter press test run. All experimental conditions as well as filter time, cake moisture, and solids recovery, have been summarized in Table 7.1. There were a total of 11 filter press runs using five batches of feed slurry.

Ash analysis was performed on all dried cake and filtrate solids. Because the filtrate contained a very low mass of solids, a single replicate was performed, but a triplicate ash analysis was performed on the cake. Three approximately 5-g portions of the dried cake were randomly sampled for analysis. Also, filtrate solids were sized with a Microtrac S3500 loaded with distilled

water. Size distribution variation of the fine material capable of passing through the filter cloth was assumed to be low and for this reason, triplicate analysis was performed for Micotrac sizing on filtrate solids for only select experimental conditions.

Table 7.1. Filter press experimental conditions and results

Batch	Test run	HAC pretreatment	Slurry conditions	Filter time, s	Cake moisture, %	Solids recovery, %
1	1	Untreated	Natural pH	360	-	-
	2		Reduced pH	700	50.09	96.02
2	3	1 min Son	Natural pH	638	40.69	97.21
	4		Reduced pH	1,200	58.02	98.35
3	5	1 min SonCav	Natural pH	830	45.31	96.26
	6		Reduced pH	1,200	61.12	97.27
4	7	Untreated	Natural pH; flocculated	1,200	55.63	98.62
	8		Reduced pH; flocculated	1,800	64.03	99.22
5	9	5 min SonCav	Natural pH	1,080	50.64	98.31
	10		Natural pH; flocculated	2,095	56.78	97.59
	11		Reduced pH; flocculated	2,400	63.92	99.16

7.4 Results and Discussion

The average pH of the six tests performed under natural (unadjusted pH) conditions was 8.01±0.29, and the average pH of the five tests performed at reduced pH was 4.17±0.17. Across all 11 tests, solids concentration of the feed slurry was 19.56±1.57%, and filtrate solids concentration was 0.62±0.36%. Solids recovery was 97.80±1.12%. The average filtrate solids particle top size was about 296 μm with 50% passing 13.1 μm. Cake and filtrate ash values were very consistent across all tests, measured at 64.61±1.57% for the filtrate and 52.71±0.58% for the cake. It should be noted that solids concentration and ash value were not determined for the untreated, natural pH condition (Test 1) as the filtration ceased very early on, prior to programmed cycle end of 700 s, as a cake could not be formed from the untreated slurry without pH reduction or flocculation. Filtrate collection was still performed for this test run.

For all tests, filtration progression with time produced filtrate with visibly lower opacity (Fig. 7.2). It should be noted that several tests ended prematurely as total cycle time was set too low to allow for maximum possible cake formation indicated by cycle end due to the ceasing of filtrate production and in turn, an insufficient filtrate collection tank liquid level reading by the conductivity probe. Total filter time was increased for many tests to adjust for this, but only tests 3, 5, 9, and 10, reached optimum cake formation for this reason. Also, despite not stopping due to a low filtrate tank level, filtrate production rate was very minimal and nearly ceased at the cycle end of test 11. Also, across all tests, cake moisture content and structure varied greatly, even visually, depending on test conditions. Figure 7.3 illustrates the visual differences between a low and high moisture filter press cake product.

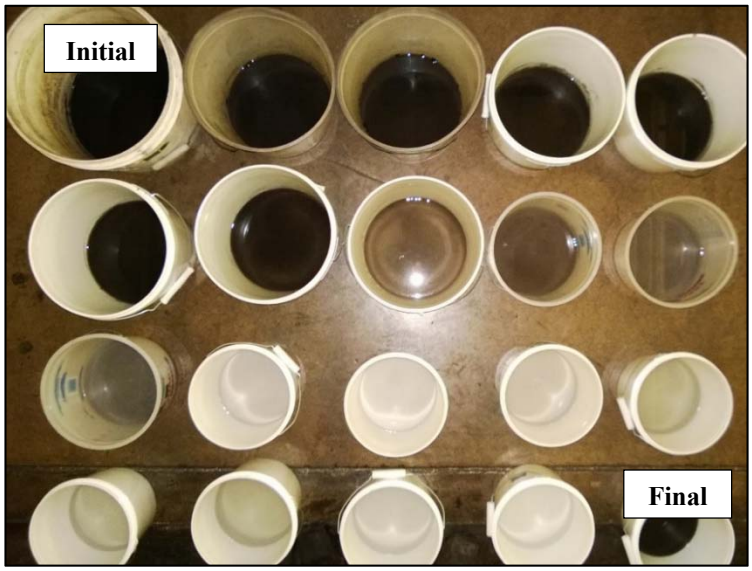

Figure 7.2. Filtrate opacity with cycle progression (final bucket represents air blow liquid)

Though several tests ended early due to a shorter set maximum cycle time, the filtrate rate curves behaved in a parabolic half. Thus, one may make the assumption that should filtration have continued, the filtration curve would have maintained a linear path, having passed the cake formation stage represented by the curvature from about 0-500 s (Fig. 7.4). Based on this fact, comparison of total cycle time between tests cannot be performed, but several observations still

may be drawn. As can be seen in Figure 7.4, feed slurry pH reduction and flocculation had very substantial effects on the filtration rate. For the same HAC treatment conditions, the lower pH tests exhibited higher solids recovery and produced a greater mass of filtrate in less time than their natural pH, unflocculated counterparts. Moreover, lowering pH after flocculation further increased filtration rate. However, this was not observed for the untreated condition as lowering pH following flocculation decreased filtration rate. The untreated, flocculated test run (Test 7) exhibited the best performance of all test runs and extensive SonCav treatment, 5 min in total, exhibited the worst performance at natural pH (Test 9), and improved little after flocculation (Test 10). However, there was a substantial shift in the filtration rate after pH was reduced (Test 11). This was likely a result of particle dispersion and surface fine liberation caused by extensive treatment, the effects of which were not apparent until particle surface charge was reduced as a result of the slurry pH being lowered.

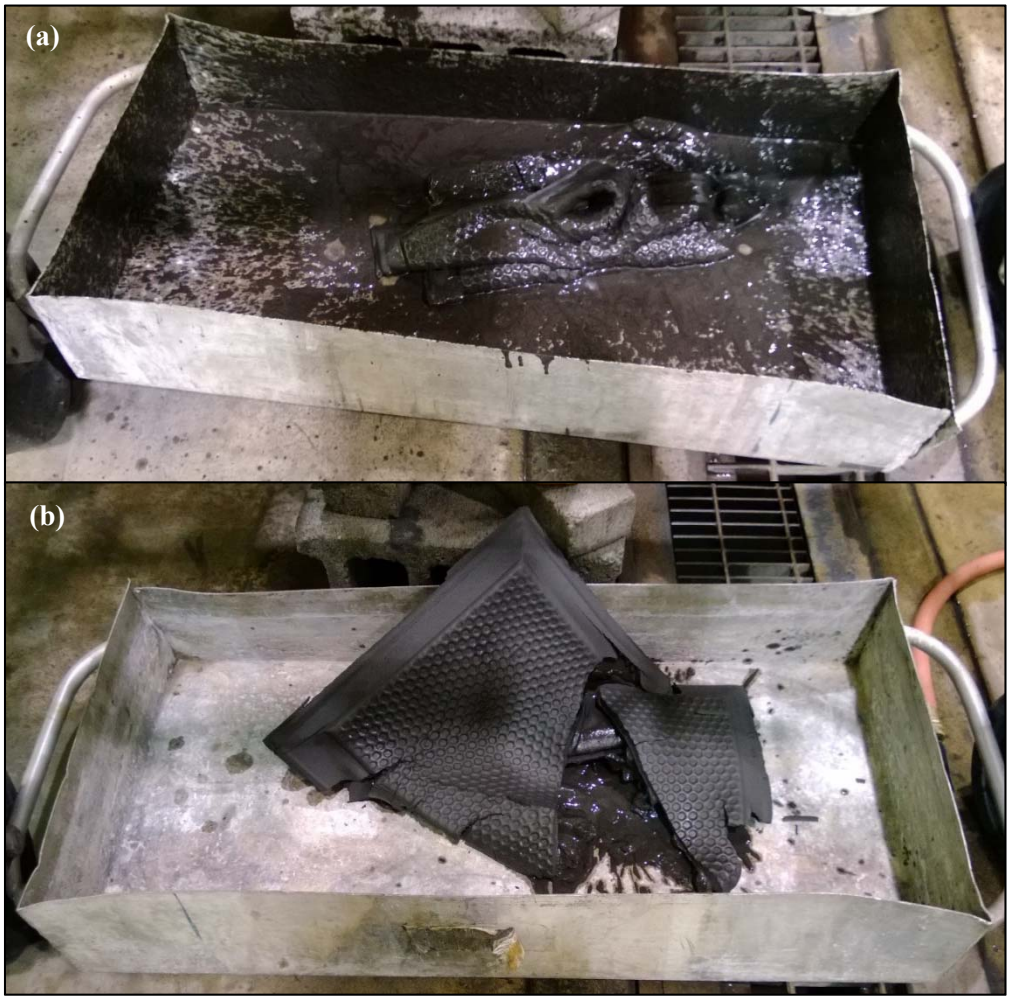

Figure 7.3. High (a) and low moisture (b) filter cakes

Displaying the data in a different manner, Figure 7.5 shows cake moisture as filtration progressed with time. This plot was generated utilizing the cake moisture content determined by oven-drying and the filtrate mass at a given time. Cake moisture percentage by weight ($M_{w,cake(t_i)}$) at time t_i was calculated by

$$M_{w,cake(t_i)} = 100 * \left[1 - \frac{m_{cake,dry(t_f)}}{m_{cake,wet(t_f)} + m_{filtrate(t_f)} - \sum_0^{t_i} m_{filtrate(t_i)}}\right] \quad (7.1)$$

where $m_{cake,dry(t_f)}$ is the final dry cake weight, $m_{cake,wet(t_f)}$ is the final wet cake weight, $m_{filtrate(t_f)}$ is the final total filtrate weight including air blow cake pore liquid, and $\sum_0^{t_i} m_{filtrate(t_i)}$ represents the total filtrate weight up to time t_i.

Overall, treatment of the filter press feed slurries appeared to have had minimal effects on cake moisture with time as many of the curves resembled each other very closely. The effects of reagent addition were more apparent. From the plot, we can see that the flocculated, reduced pH condition for no treatment (Test 8) and 5 min of SonCav treatment (Test 11) possessed the lowest final cake moisture percentage at about 36%. Also, the steepness of the curve for the untreated, reduced pH test (Test 2) demonstrated that the cake formed more quickly than in other test runs. Furthermore, three of the four flocculated tests appeared as the uppermost curves in Figure 7.5. This indicates that at a given filtration time, the cakes formed from flocculated particles contained more moisture than unflocculated cakes. This may be a result of the nature of flocs, which have a greater porosity and tendency to hold water than discrete solid particles. This extended filtration times. In addition, the curves for flocculated slurry with 5 min of SonCav treatment at natural and reduced pH, Tests 10 and 11, respectively, behave much differently than the initial unflocculated, natural pH test of batch 5. Cake moisture declined much more gradually after flocculation, likely due to the porous flocs, as previously explained.

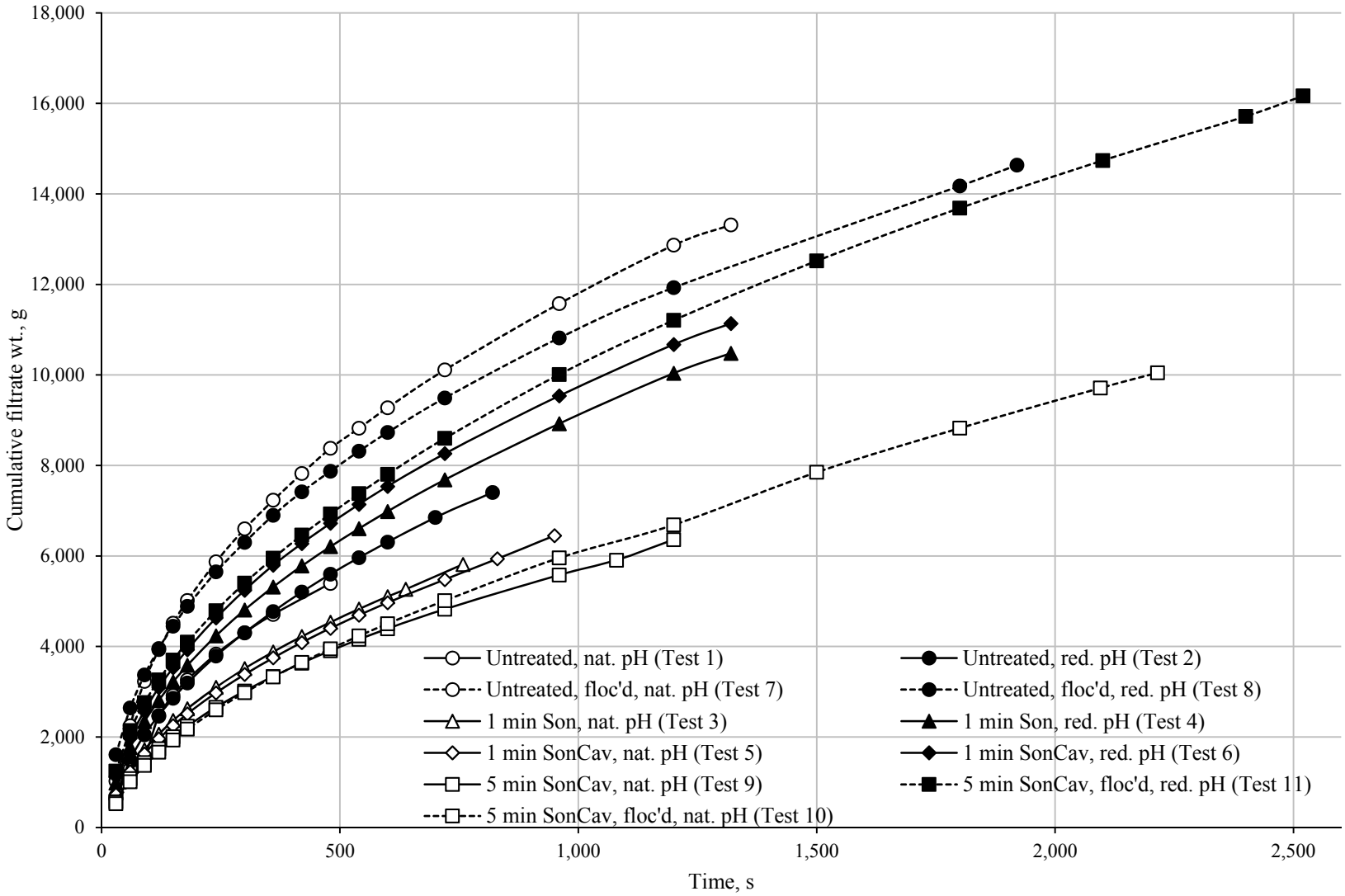

Figure 7.4. Filtrate rate for different test conditions

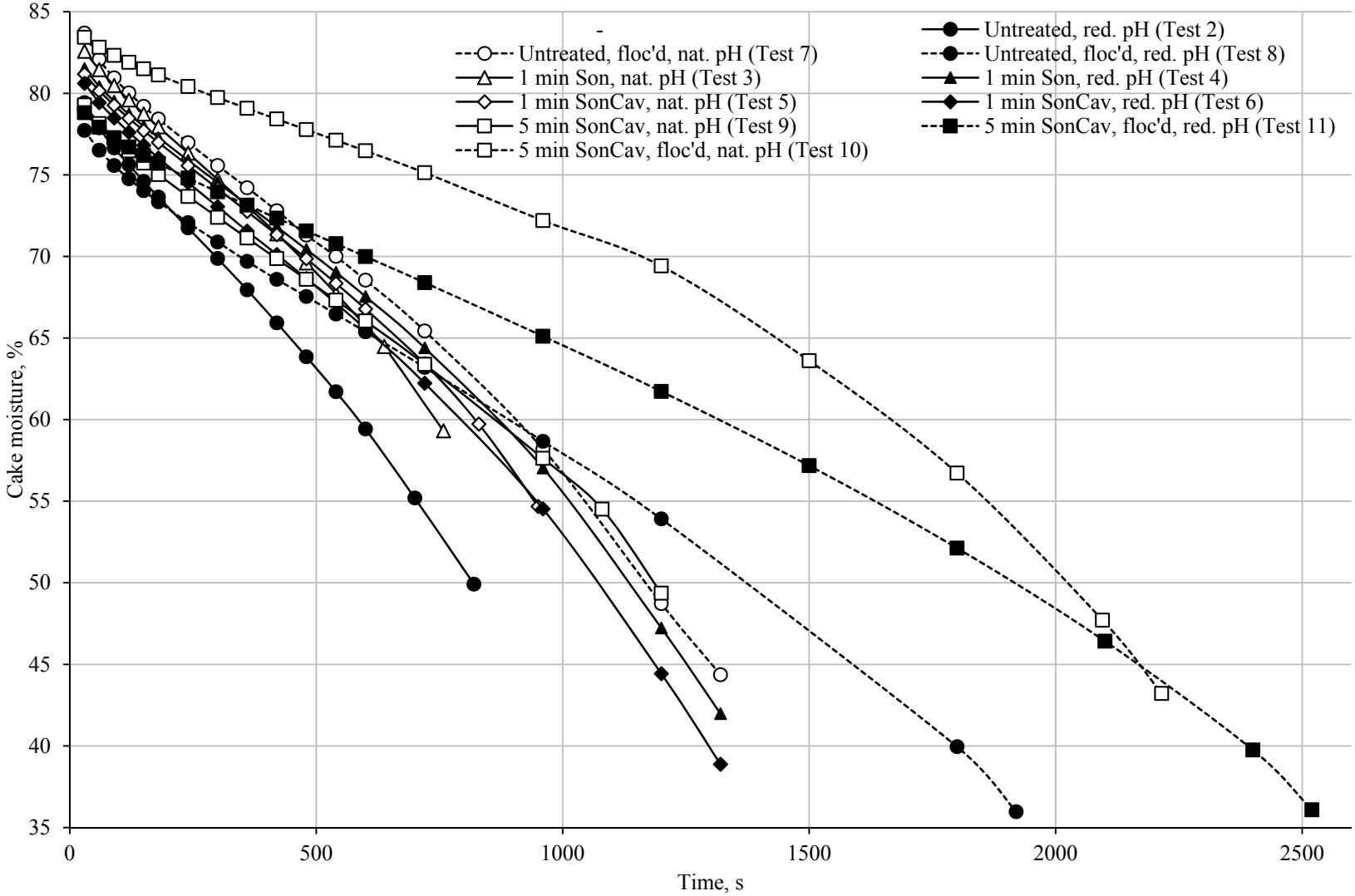

Figure 7.5. Filter cake moisture for different test conditions

7.5 Conclusion

Pressure filtration by plate filter press was effective at consolidating Sample B. Flocculation prior to filtration by addition of an anionic high molecular weight polymer, A-130 HMW, and reduction of slurry pH through addition of muriatic acid, increased the effectiveness of filter press dewatering. Decreasing pH had a more noticeable effect on the results, producing lower moisture cakes, increasing solids recovery, and increasing filtration rate. HAC treatment appeared to have minimal effects; however, application of the higher intensity SonCav treatment for a total of 5 min exhibited the lowest cake moisture following flocculation and pH reduction. This is likely due to greater levels of surface fine liberation and slurry dispersion which were negated by reagent addition. The untreated, flocculated, reduced pH test run (Test 8) produced very similar results. Flocculation was partly detrimental in that it extended filtration times but reduced the moisture of the filter cake.

CHAPTER 8

CONCLUSIONS

This study was conducted to evaluate the effects of HAC treatment on two types of bituminous coal slurries and the performance impacts on subsequent separation processes. Thorough discussion of results can be found in preceding chapters. Summary of the overarching details and conclusions drawn are presented hereafter.

8.1 HAC Treatment

HAC treatment of Sample A resulted in size reduction of primarily the +850-µm particles with SonCav treatment producing more intense size degradation effects than the Son treatment. The size reduction of coarser particles led to an increase in the weight percentage of fines. Extending treatment time appeared to increase these size effects but no strong conclusion can be made as recirculation without treatment led to significant size reduction of coarser particles due to the pump impeller. In addition, 5 s of HAC treatment achieved these size effects while reducing the ash values of the +300-µm particles, in some size fractions over 5% from untreated to SonCav treatment, suggesting that perhaps selective liberation of inorganic fines occurred.

8.2 Hydrocyclone Separation

Combining HAC treatment with hydrocyclone desliming for Sample A, separation of inorganic matter to the overflow stream increased, especially with treatment. For Sample A, underflow stream ash values were reduced by up to 16% after treatment compared to 7% without treatment. However, HAC treatment did not reduce the ash values of Sample B any further. Sulfur increased in the underflow stream and cut size decreased from untreated to Son and then SonCav treatment for both sample types. Less fine material bypassed to the underflow stream (a-bypass) for Sample A as treatment intensified (i.e., Son to SonCav) and increased very slightly for Sample B. Yield was relatively unaffected by treatment. Dispersion of the slurry and

liberation of inorganic surface fines as a result of treatment improved the de-ashing ability of the hydrocyclone.

8.3 Spiral Concentration

Hydrocyclone desliming of Sample A followed by spiral concentration improved yield as well as ash and sulfur reduction. The 26.6 gpm flow rate performed best and treatment increased clean coal yield for this condition. The SonCav treatment at 26.6 gpm flow decreased overall (i.e., as-received to final product) yield by only ~30% with a ~60% and ~6% reduction in ash and total sulfur values, respectively. The spiral improved ash reduction and negated the effects of sulfur concentration by the hydrocyclone. Screening and ash analysis of various size fractions of the clean coal demonstrated that further processing by removal of the -106-μm particles could decrease the ash value an additional 12% with only a 10-15% reduction in product yield. Liberation of the dense, inorganic surface fines prior to size and density separation allowed for greater performance as compared to the untreated condition.

8.4 Froth Flotation

Froth flotation of the -0.15-mm Sample B material was poor due to the high concentration of fine inorganic matter and increased slurry dispersion caused by treatment. Hydrocyclone desliming prior to flotation had minimal effects on initial (i.e., 30 s of froth product recovery) product yield compared to the undeslimed tests and reduced product ash values by up to ~30%. Treatment had minimal or detrimental effects on results in terms of yield and ash and sulfur reduction. Wet screening of the material at 25 μm prior to flotation resulted in ash reduction of ~91% after only 15 s of flotation but had a cumulative (i.e., as-received to product) yield of only ~14%. This demonstrated that the inorganic fines greatly hindered flotation and that an efficient desliming operation would be needed if flotation were to be used.

8.5 Pressure Filtration

Pressure filtration of Sample B by plate-and-frame filter press required addition of HMW flocculant, reduction of slurry pH to ~4, or both to effectively dewater the material and produce a lower moisture cake. Peak test performance was a cake moisture content of ~36%, achieved for two test runs which involved filtration of a pH reduced, untreated slurry and a flocculated, pH reduced slurry which received 5 min of SonCav treatment. Due to the high levels of dispersion generated by treatment and the large percentage of -25 μm material in the Sample B feed, reagent addition was required. Reduction of feed slurry pH increased solids recovery and filtration rate while decreasing cake moisture. Flocculation increased filtration rate and decreased cake moisture but extended filtration times.

8.6 Future Work

Due to circuit construction, testing was limited in that the pump was fixed-speed and possessed a relatively small impeller compared to the top size of the feed material. It may be beneficial to explore the HAC effects with a larger, variable-speed pump so that any impact flow rate may have on ultrasonic cavitation as well as size degradation caused by the pump impeller can be eliminated.

REFERENCES

Alam, N., Ozdemir, O., Hampton, M.A., Nguyen, A.V., 2011. Dewatering of coal plant tailings: Flocculation followed by filtration. *Fuel*, 90: 26-35. doi: 10.1016/j.fuel.2010.08.006

Ambedkar, B., 2012. Ultrasonic coal-wash for de-ashing and de-sulfurization: experimental investigation and mechanistic modeling (Doctoral dissertation). Indian Institute of Technology Madras, Chennai, India. doi: 10.1007/978-3-642-25017-0

Ambedkar, B., Nagarajan, R., Jayanti, S., 2011. Ultrasonic coal-wash for de-sulfurization. *Ultrasonics Sonochemistry*, 18(3): 718-726. Retrieved from http://dx.doi.org/10.1016/j.ultsonch.2010.09.006

American Coal Ash Association, 2012. *Coal combustion products (CCP) production and use survey report*. Retrieved from http://www.acaa-usa.org/Publications/ProductionUseReports.aspx

Archer, P.L., 1979. *Illinois Basin Report: Pennsylvanian Geology and coal and coalbed methane resources of the Illinois Basin, Illinois, Indiana and Kentucky*. TRW Energy Systems Group, Contract No. DE-AC21-78MC08089.

Arnold, B. J., 1989. Flotation rate and residence time distribution in continuous coal froth flotation circuits and an evaluation of reagents and circuit variations for pyritic sulfur removal (Doctoral dissertation). The Pennsylvania State University, University Park, PA.

Arnold, B.J., Aplan, F.F., 1986. The effect of clay slimes on coal flotation, part I: The nature of the clay. *International Journal of Mineral Processing*, 17 (3–4): 225-242. Retrieved from http://dx.doi.org/10.1016/0301-7516(86)90058-X

Atasoy, Y., Spottiswood, D.J., 1995. A study of particle separation in a spiral concentrator. *Minerals Engineering* 8 (10): 1997-1208.

Bagnold, R.A., 1954. Experiments on a gravity-free dispersion of large spheres in a Newtonian fluid under shear. *Proceedings of the Royal Society*, London, Set. A, 225: 49-53.

Benusa, M., 2007. An evaluation of a two-stage spiral processing fine and ultra-fine bituminous coal and anthracite refuse (M.S. thesis). The Pennsylvania State University, University Park, PA.

Borio, R.W., Levasseur, A.A., 1986. Coal Ash Deposition in Boilers. *Mineral Matter and Ash in Coal*, 21: 288-302. doi: 10.1021/bk-1986-0301

Bradley, D., 1965. *The Hydrocyclone*. London: Pergamon Press.

Braun, T., Bohnet, M., 1990. Influence of feed solids concentration on the performance of hydrocyclones. *Chemical Engineering and Technology,* 13 (1): 15-20. Retrieved from http://dx.doi.org/10.1002/ceat.270130104.

Brennen, C.E., 1995. *Cavitation and bubble dynamics.* New York: Oxford University Press.

Bürger, R., Concha, F., Karlsen, K.H., 2001. Phenomenological model of filtration processes: Cake formation and expression. *Chemical Engineering Science,* 56: 4537–4553.

Buscall, R., White, L.R., 1987. The consolidation of concentrated suspensions part 1: The theory of sedimentation. *Journal of the Chemical Society, Faraday Transactions,* 83 (3): 873–891.

Buttermore, W.H., Slomka, B.J., Dawson, M.R., 1989. Sonic enhancement of physical and chemical cleaning of coal. *U.S. Department of Energy Report No. IS-5021*. Retrieved from http://www.osti.gov/scitech/biblio/6502424

Carleton, A.J., Salway, A.G., 1993. Dewatering of cakes. *Filtration and Separation*, 30(7): 641-646.

Celik, M.S., 1989. Effect of Ultrasonic Treatment on the floatability of coal and galena. *Separation Science and Technology*, 24(14): 1159-66. doi: 10.1080/01496398908049894

Criner, H.E., 1950. The Vortex Thickener. *International Conference on Coal Preparation*. Paris.

Driessen, M.G., 1951. Theory of flow in a cyclone. *Review of Industrial Mining*, Special Issue No. 4: 449-461.

EIA, 2013a. *Annual Energy Outlook with Projections to 2040*. Retrieved from http://www.eia.gov/forecasts/aeo/pdf/0383(2013).pdf

EIA, 2013b. *Electric Power Monthly with Data for December 2012*. Retrieved from http://www.eia.gov/electricity/monthly/current_year/february2013.pdf

EIA, 2013c. *Quarterly Coal Report October-December 2012*. Retrieved from http://www.eia.gov/coal/production/quarterly/pdf/0121124q.pdf

EIA, 2013d. *Short Term Energy Outlook)*. Retrieved from http://www.eia.gov/forecasts/steo/archives/jul13.pdf

Fahlstrom, P.H., 1960. Discussion on hydrocyclone. In: *Proceedings of the International Mineral Processing Congress,* 632-643. Westminster: Institute of Mining and Metallurgy.

Fairbanks, H.V., Morton, W.E., Wallis, J.W., 1990. Mineral recovery enhanced by ultrasonic treatment. In: *Proceedings of the Society for Mining, Metallurgy and Exploration Annual Meeting*, Preprint No. 90-21. Salt Lake City: Society for Mining, Metallurgury, and Exploration, Inc.

Frederick, J.R., 1965. *Ultrasonic Engineering*. New York: Wiley and Sons.

Geer, M.R., Yancey, H.F., Allyn, C.L., Eckhouse, R.H., 1950. Laboratory performance tests of the Humphrey spiral as a cleaner of fine coal. *Minerals Engineering*, 187 : 1057-1067.

Gluskoter, H.J., Ruch, R.R., Miller, W.B., Cahill, R.A., Dreher, G.B., Kuhn, J.K., 1977. Trace elements in coal: Occurrence and distribution. *Illinois State Geological Survey*, 499.

Gösele, W., Christian, A., 2005. Filtration. In: *Ullmann's Encyclopedia of Industrial Chemistry* (7^{th} ed.)**.** Pelc, H., Elvers, B., Hawkins, S., Harrer, R., Pikart-Müller, M. (eds), 2011. Weinheim: Wiley-VCH Verlag GmbH and Co. KGaA.

Holland-Batt, A.B., 1995. The dynamics of sluice and spiral separations. *Minerals Engineering*, 8 (1–2): 3-21. Retrieved from http://dx.doi.org/10.1016/0892-6875(94)00098-W

Hsu, C.Y., Wu, S.J., Wu, R.M., 2011. Particles separation and tracks in a hydrocyclone. *Tamkang Journal of Science and Engineering*, 14 (1): 65-70.

Izquierdo, M., Querol, X., 2012. Leaching behaviour of elements from coal combustion fly ash: An overview. *International Journal of Coal Geology*, 94: 54-66.

Kawatra, S. K, Eisele, T.C., 2001. *Coal desulfurization: High-efficiency preparation methods*. New York: Taylor and Francis.

Klimpel, R.R., 1979. Estimation of weight ratios given component make-up analyses of streams. *Transactions of the American Institute of Mining, Metallurgical, and Petroleum Engineers*, 266: 1882-1886.

Klimpel, R.R., 1995. The influence of frother structure on industrial coal flotation. In: *High-Efficiency Coal Preparation: An International Symposium*, 141-151. Littleton: Society for Mining, Metallurgy, and Exploration.

Kuhn, J.K., Fiene, F.L., Cahill, R.A., Gluskoter, H.J., Shimp, N.F., 1980. Abundance of trace and minor elements in organic and mineral fractions of coal. *Environmental Geology Notes*, 88. Illinois Institute of Natural Resources. Retrieved from https://archive.org/details/abundanceoftrace88kuhn

Leighton, T.G., 1994.*The Acoustic Bubble*. London: Academic Press.

Lockhart, N.C., Veal, C.J., 1996. Coal dewatering: Australian R&D trends. *Coal Preparation*, 17(1–2): 5–24. doi: 10.1080/07349349608905254

Lynch, A.J., Bush, P.D., 1977. *Mineral crushing and grinding circuits: Their simulation, optimisation, design and control*. Amsterdam: Elsevier.

Lynch, A.J., Johnson, N.W., Manlapig, E.V., Thorne, C.G., 1981. *Mineral and coal flotation circuits: Their simulation and control* (Vol. 3). New York: Elsevier. Retrieved from http://library.dmr.go.th/library/TextBooks/3435.pdf

Majumder, A.K., Barnwal, J.P., 2011. Processing of coal fines in a water-only cyclone. *Fuel*, 90 (2): 834-837. Retrieved from http://dx.doi.org/10.1016/j.fuel.2010.10.038

Mason, T.J., Lorimer, J.P., 1988, *Sonochemistry: Theory, applications and uses of ultrasound in chemistry*. New York: John Wiley and Sons.

Miller, J.W., 2014. The future of coal: Scrubbing technology revives Midwest Mines. *The Wall Street Journal*. Retrieved from http://online.wsj.com/news/articles/SB10001424052702303332904579228161981168296

Ozkan, S.G., 2011. Effects of simultaneous ultrasonic treatment on flotation of hard coal slimes. *Fuel*, 93: 576-580.

Radovic, L.R., Schobert, H.H. 1997. *Energy and fuels in society: Analysis of bills and media reports* (2nd ed.). New York: McGraw-Hill.

Reinecke, C.F., Nierop, P.V., Keyser, N.M., Schneider, M., 1993. The influence of slime coating on the beneficiation behavior of a high ash South African coal. In: *Proceedings of the 10th Annual International Pittsburgh Coal Conference*, 144-148.

Rietema, K., 1961a. Performance and design of hydrocyclones (Part I and IV). *Chemical Engineering Science,* 15: 298-325

Rietema, K., 1961b. The mechanism of the separation of finely dispersed solids in cyclones. In: *Cyclones in Industry.* Rietema, K., Verver, C.G. (eds.), 1961. Amsterdam: Elsevier.

Shchukin, D. G., Skorb, E., Belova, V., Möhwald, H., 2011. Ultrasonic cavitation at solid surfaces. *Advanced Mater*ials, 23: 1922–1934. doi: 10.1002/adma.201004494

Sivamohan, R., Forssberg, E., 1985. Principles of spiral concentration. *International Journal of Mineral Processing*, 15: 173-181.

Slechta, J., Firth, B.A., 1984. Classification of fine coal with a hydrocyclone. *International Journal of Mineral Processing*, 12(4): 213-237. Retrieved from http://dx.doi.org/10.1016/0301-7516(84)90030-9

Slomka, B.J., Buttermore, W.H., 1991. Sonically enhanced beneficiation of Illinois No. 6 coal. *Fuel Processing Technology,* 29(1–2): 133-142. Retrieved from http://dx.doi.org/10.1016/0378-3820(91)90023-6

Smith, A.E., Bernstein, P.M., Bloomberg, S.J., Mankowski, S.M., Tuladhar, S.D., 2012. An Economic Impact Analysis of EPA's Mercury and Air Toxics Standards Rule. NERA Economic Consulting. Retrieved from http://www.nera.com/nera-files/PUB_MATS_Rule_0312.pdf

Smitham, J., Firth, B.A., 1982. The distribution of an insoluble flotation collector on fine coal particles. In: *Proceedings of the Australasian Institute of Mining and Metallurgy*, No. 283: 29-35. Australasian Institute of Mining and Metallurgy.

Suslick, K.S., Didenko, Y., Fang, M.M., Hyeon, T., Kolbeck, K.J., McNamara III, W.B., Mdleleni, M.M., Wong, M., 1999. Acoustic cavitation and its chemical consequences. *Philosophical Transactions of the Royal Society A.,* 357: 335-353.

Suslick, K.S., Price, G.J., 1999. Applications of ultrasound to materials chemistry. *Annual Review of Materials Science*, 29: 295-326.

Svarovsky, L., 1984. *Hydrocyclones*. New York: Technomic Publishing Co.

Svarovsky, L., 1985. *Solid-liquid separation process and technology: Handbook of powder technology* (Vol. 5). Amsterdam: Elsevier.

Tao, D., Parekh, B.K., 2000. Enhanced fine coal beneficiation using ultrasonic energy. *Minerals and Metallurgical Processing*, 17(4): 252-258.

Thompson, J.V., Welker, M., 1990. The Humphreys Companies: Development and application of Humphreys spiral concentrator. *Skillings' Mining Review*, 79(8): 4-15.

Vorres, K.S., 1986. Chemistry of mineral matter and ash in coal: An overview. In: *Mineral Matter and Ash in Coal*, 301: 1-8. American Chemical Society. Retrieved from http://pubs.acs.org/doi/pdf/10.1021/bk-1986-0301.ch001

Wakeman, R., 2007. The influence of particle properties on filtration. *Separation and Purification Technology*, 58 (2): 234-241.

Wang, T., Wang, J., Tang, Y., Shi, H., Ladwig, K., 2009. Leaching characteristics of arsenic and selenium from coal fly ash: Role of calcium. *Energy and Fuels*, 23 (6): 2959-2966.

Wang, W., Cannon, F.S., Voigt, R.C., Komarneni, S., 2006. Effects of advanced oxidation on green sand properties via iron casting into green sand molds. *Environmental Science and Technology*, 40: 3095-3101.

Wen-ze, K., Hai-xin, X., Jun-tao, C., 2007. Study of enhanced fine coal de-sulphurization and de-ashing by ultrasonic flotation. *Journal of China University of Mining and Technology*, 17(3): 0358-0362.

Wen-ze, K., Hai-xin, X., Hu, J., 2008. Study of the effect of ultrasonic treatment on the surface composition and the flotation performance of high-sulfur coal. *Fuel Processing Technology*, 89: 1337-1344. doi:10.1016/j.fuproc.2008.06.003.

White, J., 2013. Assessment of plate and frame presses in fine coal refuse disposal. *Coal Age News*. Retrieved from http://www.coalage.com

Wills, B.A., Napier-Munn, T., 2006. *Wills' Mineral Processing Technology: An Introduction to the Practical Aspects of Ore Treatment and Mineral Recovery*. Oxford: Butterworth-Heinemann.

Zeilinger, J., Deurbrouck, A.W., 1976. Physical desulfurization of fine-size coals on a spiral concentrator. *Report of Investigations # 8152*. Washington: U.S. Bureau of Mines.

APPENDIX A

OPERATING PROCEDURES

Microtrac

1. Turn on the power to the Dell Optiplex 760 desktop PC, attached Dell monitor, Microtrac Sample Delivery Controller, and Microtrac S3500.
2. Ensure adequate supply of distilled water and sample hose is in container.
3. Ensure device rinse/flush tube stemming from the rear of the Sample Delivery Controller is in the sink and within a beaker so that solids are not deposited in the drain but allowed to settle in the beaker for proper disposal.
4. Ensure sample material which is being Microtrac'd is less than 0.15 mm in diameter. Brush through US 70 Mesh screen if particles are agglomerated from drying.
5. Start program Microtrac FLEX 10.5.2.
6. Navigate to and click the "Auto" function button at the top left of the program window located just below the dropdown menu for "Data Retrieval" and to the right of the "Run" function button.
    a. The program will perform a fill then "wet Setzero" and then a sample "Identifiers" prompt will appear.
    b. If "No Setzero" is indicated and device continues rinsing and does not prompt to add sample within 2-3 min then lines are clogged. Contact Tom Motel.
7. In "Title" box enter sample ID. Ignore "Sample Id's" box.
8. Click OK and add sample.
9. "Sample Loading" prompt "Status" box says "Add sample".
10. Lift sample port cover at the top front of Sample Delivery Controller and add sample to port containing water.
11. Device will now automatically dilute and ultrasonicate sample to ensure proper loading factor for effective laser reading then read size distribution, rinse, and complete auto sequence cycle.
12. When prompt disappears navigate to Start, Computer, OS (C:), Program Files, Microtrac FLEX 10.5.2, ExportData, sort files by date by clicking "Date modified" tab so most recent date is first then you should see four files saying MTData then your sample ID from the Title box.
    a. The program actually gathers data three times so three of the files will be those runs and the fourth, most recent file when sorted by data modified will be an average of the three.
    b. Size distribution data will be located within the files.
13. Entire process should take 5-10 min depending on loading and necessity for device to dilute.
14. Check distilled water supply and maintain if performing multiple runs.

Spiral

1. Remove sump drain plug and close the sump drain ball valve (red handle) under the base of the sump and ensure bypass ball valve (yellow handle) is closed so that the system will direct flow to head tank.
2. Remove plastic cover from the ABB HVAC pump control panel and plug the motor for 15HP Westinghouse centrifugal pump/panel into a 480 V receptacle.
    a. Turn on main power on wall mounted panel then switch second wall panel downward to send power to 480 V receptacle .
3. Ensure power switch off and plug in Balford motor for Lightnin model EV5P75 mixer.
4. Fill sump with water.

5. Turn on pump by pressing green power on button on control panel and adjust pump speed so that water passes through the head tank and flows down the spiral to flush any solids from the system. This speed should range from 21-22 Hz. Direct drain line into floor trench.
6. Turn off pump by pressing red power off button and open sump drain ball valve to drain the system.
7. Rinse out head tank by pulling away outlet pipe at head tank flow control orifice. Rinse sump and spiral turns and open then close bypass valve to rinse of solids.
8. Repeat steps 4-7 until system is free of solids.
9. Close sump drain valve.
10. Remove head tank outlet line and insert desired head tank flow control orifice.
11. Determine makeup water needed to ensure at least 50 gallons of slurry at desired solids concentration will fill sump. This sump slurry volume will help prevent vortexing. Fill sump with makeup water..
12. Turn on pump and circulate makeup water through the system. Ensure water is passing through head tank overflow line.
13. Turn on mixer if water level is above impeller otherwise wait until adequate slurry volume. Adjust mixer to desired speed without vortexing.
14. Add desired quantity of feed slurry to sump at a pace which will prevent system clogging. This will depend on feed slurry solids concentration. Continuously monitor head tank level by observing flow from head tank overflow line and adjust pump speed as necessary.
15. Operate spiral for 10 min to ensure slurry is well-mixed and flow across spiral turns is completely developed.
16. Take simultaneous samples for desired sampling time across all sample ports (i.e., splitter box ports and center column port) with appropriately sized containers.
    a. Simultaneous sampling ensures that the feed slurry characteristics will not be compromised.
    b. Select containers based on observed volumetric flow from ports and desired sampling time.
17. Sample from head tank overflow line if desired.
18. Open bypass valve and direct bypass line into sump. Reduce pump speed using control panel so that slurry no longer pumps to head tank (~19 Hz).
19. Change head tank flow control outlet orifice if desired. Dilute feed slurry solids concentration if desired.
    a. Drain slurry from bypass line into a 50-gal drum following dilution if sump level too high to ensure adequate room for sampling.
20. Close bypass valve, return pump speed to original level, and repeat steps 16-18 if necessary.
21. Upon completion of sampling, divert remaining slurry into 50-gal drum(s) via bypass line.
22. When the sump is empty, shut off the pump.
23. Turn off and unplug the mixer.
24. Repeat steps 4-7 until the system is clear of solids. However, continue to divert the slurry into 50-gal drum(s) via the bypass line until the system appears mostly clear of solids. At this point it is acceptable to divert remaining slurry/system flushing water into the trench drain via the sump drain line.
25. Once the system is thoroughly rinsed, place both wall power panels to the off position, unplug the pump, and replace the plastic cover on the pump control panel.

Hydroacoustic Cavitation Circuit

Circuit Loading

1. Plug circuit power cord stemming from main control panel box into 208 V wall socket
2. Place the 2-way ball valve controlling flow to the trench drain at the base of circuit feed tank in the closed position .
3. Ensure the six other 2-way ball valves are in the open position.
4. Ensure the gate valve on the recirculation pipe is open.
5. Ensure the two 3-way ball valves are positioned to recirculate flow.
6. Ensure the 2-way ball valve at the bottom of the hydroacoustic vessel is closed and the stopcock (red handle) at the top of the hydroacoustic vessel is open.
    a. The stopcock at the top of the vessel should never be closed.
7. Fill feed tank with at least 20 gal of water.
    a. This amount will prevent vortexing and suction of air by the pump.
    b. The system piping and hydroacoustic vessel hold nearly 10 gal of fluid.
8. Ensure pump and ozone control knob are in the off position and then flip the power lever on the main control panel box upward to turn on.
9. Turn pump control knob on the main control panel to on.
10. Allow the water to recirculate to rinse solids from the system then turn the pump control knob to the off position.
11. Empty the water from the circuit using the valve from step 2 and the valve at the bottom of the hydroacoustic vessel in step 6 and return them to the closed position once emptied.
12. Repeat steps 7-11 until the system is clear of solids.
13. Ensure both 2-way ball valves at the base of the feed tank are closed and load the circuit with the desired amount of dilution water if dilution of feed solids is necessary.
    a. Ensure the system is not underloaded (see step 7).
14. Place the 2-way ball valve controlling flow from the base of the feed tank to the pump in the open position.
15. Turn the pump control knob to on.
16. Slowly introduce feed solids into the feed tank while the dilution water is recirculating.
    a. If no dilution water is necessary, follow steps 13-15 but utilize the mixer mounted to the feed tank to minimize settling and begin recirculating flow as soon as 15 gal of slurry is within the feed tank. Additional feed slurry can be introduced while the initial 15 gal is recirculating.

Depending on the objective, several options are now available

Ultrasonic Treatment (cont. from 16)
Note: The ultrasonic treatment must only be running when water/slurry is in the system. Running the ultrasonics in air will damage the resonator and thus should never be performed.

1. Supply power to the ultrasonic unit by pressing the switch on the right-front of the ultrasonic generator control panel to on.
    a. Occasionally the ultrasonics will turn on immediately and will be audibly apparent. If this occurs quickly press the “start/stop” button.
2. Adjust the power, time, and turn sweep on or off if desired.

a. Adjustment is intuitive as the buttons are “power -” to decrease power, “power +” to increase power, “time -”, “time +”, and “sweep”.

3. Press the “start/stop” button to treat as desired.

Cavitation Treatment (cont. from 16)

17. Simultaneously open the two 2-way ball valves which direct flow to and from the cavitation plate.
18. Simultaneously close the two 2-way ball valves which direct flow from the pump to the hydroacoustic vessel to direct all flow from the pump through the cavitation plate only.

Ultrasonic and cavitation treatment

Follow the steps for the *Cavitation treatment* section followed by the steps for the *Ultrasonic treatment* section.

Circuit Sampling

1. Prepare sample containers in advance of utilizing the circuit.
2. Locate the T-port 3-way ball valve between where the slurry exits the piping into the feed tank during recirculation and the L-port 3-way ball valve which directs flow from the base of the hydroacoustic vessel to either recirculation or to the hydrocyclone.
3. Gradually turn the T-port 3-way ball valve and collect the desired amount of sample material then return the valve to the closed position.

Hydrocyclone

1. Prepare sample and waste containers for the hydrocyclone underflow and overflow in advance of utilizing the circuit.
    a. Due to the large volumetric flow rate of overflow in comparison to the underflow, it may be prudent to position a 55-gal drum on a dolly for waste collection.
2. Follow steps 1-16 to ready the circuit and recirculate the feed slurry.
3. If any circuit treatment (i.e., ultrasonics & cavitation) is desired, perform those steps prior to hydrocyclone use.
    a. Treatment can run while the hydrocyclone is in use.
4. Locate the L-port 3-way ball valve which directs flow from the base of the hydroacoustic vessel to either recirculation or to the hydrocyclone.
5. Position waste containers below the underflow and overflow outlets.
6. Gradually turn the L-port 3-way ball valve to direct flow to the hydrocyclone until the desired inlet pressure is achieved as indicated on the in-line pressure gauge at the inlet.
7. Switch out the waste containers and collect the desired quantity of sample material.
    a. Be wary that the pressure may drop at the hydrocyclone inlet if the feed tank slurry level gets too low.
8. Once the sample is collected or pressure begins to drop at the hydrocyclone inlet, immediately replace the waste containers below the underflow and overflow and return the L-port 3-way ball valve in step 3 to the recirculation position.

a. Allowing the sample containers to remain below the underflow and overflow is not recommended as any slurry remaining in the lines will run into the containers (largely out of the underflow) and distort results.

Circuit Drainage/Cleaning/Shutdown

1. If ultrasonic treatment is on, shut it off immediately by pressing the switch on the ultrasonic generator control panel to off as it is unnecessary to continue treatment at this point in the operation.
2. Position a 55-gal drum below the T-port 3-way ball valve mentioned in *Circuit Sampling* step 2.
3. Gradually turn the T-port 3-way ball valve and collect slurry remaining in the circuit in the 55-gal drum.
4. The pump may be unable to transport the slurry when the feed tank level gets too low. This will be audibly and visibly apparent from reduced flow from the T-port 3-way ball valve. At this point, return the T-port 3-way ball valve to the recirculation position and shut off the pump by turning the pump control knob off.
5. Fill the feed tank with at least 20 gal of water then recirculate the water through the system via the pump and repeat steps 3 and 4. Continue doing this until the system appears clear of most solids.
6. Now follow steps 7-12 in the *Circuit loading* section.
7. Shut down the system by flipping the power lever on the main control panel box downward.
8. Unplug the main control panel power cord.

Filter Press

1. Label, weigh, and record the weights of all filtrate and feed collection buckets/beakers as well as the cake collection pan.
2. Adjust the probe level in the filtrate tank as per the filter time requirements. Higher values of filter time would be obtained by lowering the probe.
3. Move the air compressor from Room 27A to the highbay area, adjacent to the small hindered-settling column. Plug in the unit.
4. Connect the filter press power cable to the specified electric outlet located on the wall behind the small hindered-settling column. Switch the unit on by turning the central black round knob counter clockwise.
5. Ensure that the filter cloth on the filter plates is clean. If necessary, hose the cloth to remove any solids attached to the cloth.
6. Locate the connection for the air line of the pneumatic system on the right hand side of the control panel. Attach the air hose from the house air line located on the wall near the steps to the pneumatic system connection. Open the house air ball valve.
7. Attach the air hose from the compressor to the air inlet behind the filter plate. Switch the compressor to auto. If necessary, adjust the air pressure to approximately 100 psi by turning the control knob next to the air inlet. The air pressure must never exceed 150 psi.
8. Place the collection pan under the plate opening to collect the filter cake.
9. Close the residual slurry valve. Place the discharge hose in a clean 5-gallon bucket.
10. Carefully close both drain valves on the side and on the bottom of the feed tank. Hold the valve securely so that you do not damage the tank threads when moving the valve lever.

11. Depending on desired slurry treatment prior to filtration, follow the appropriate **Hydroacoustic Cavitation Circuit** operating procedures.
12. Using the T port 3-way valve of the HAC circuit, adjust flow direction and fill the filter press feed tank. A slurry volume greater than ~70 liters should be used to ensure that the feed pump will work properly when feeding the slurry to the filter plates.
13. Turn on the mixer using the control knob located on the mixer control panel located to the left of the main control panel. Increase the mixer speed using the other knob. Adjust the mixer speed if necessary but avoid producing a strong vortex in the feed tank. Continue mixing throughout all tests. Do not shut off the mixer until the test has been completed and the feed tank is empty.
14. Ensure that the feed sample beaker is held under the side discharge valve of the feed tank. Slowly open the side drain valve slightly, and collect ~500 mL of slurry. Close the valve when completed. Set aside the beaker for desired feed testing (e.g., solids %, ash %, etc.) at a later time.
15. Perform desired feed adjustments (e.g., dilution, pH adjustment, flocculation) within the filter press feed tank. Add the desired waster/reagents to the slurry while continually mixing. Continue to sample ~500 mL of slurry from the side drain valve and test the sample until the desired effects are observed.
16. Once the filter press feed slurry reaches the desired conditions, arrange the labeled filtrate collection buckets/beakers near the filtrate discharge tank. Ensure that one bucket is under the filtrate discharge line
17. On the control panel, press ► to enter the “Maximum fill time”, “Maximum filter time”, “Pause time”, and “Dry time” to the desired values in seconds. Use the MOD button to move between parameters. Use the ▲ and ▼ keys to increase and decrease the values. Press ENTER to confirm the values.
18. Set the Pause time between the Dry Cycle and Discharge to at least 60 seconds to allow sufficient time for residual slurry collection from the residual slurry valve between these steps. Press ENTER to confirm. Press ESC twice to go back to the proper screen.
19. After the slurry is well mixed, set the MAN – AUTO switch to MAN. Have a stop watch ready.
20. Press the MAN button twice. The plate will start closing.
21. Start timing as soon as filtrate begins to discharge the filtrate tank. If the maximum fill time is exceeded the pump will stop. If this happens, it will be necessary to press the MAN button twice to restart the cycle.
22. Collect filtrate at desired predefined time intervals in the labeled buckets.
23. While the pump is running, record the feed slurry pressure indicated on the pressure gauge located behind the filter plate.
24. The Filter Cycle is determined by the probe height inside the filtrate tank. If the filtrate level falls below the bottom of the probe, the pump stops and no more feeding is done. If this occurs, record the time when the filtration cycle stopped.
25. As soon as the Filter Cycle is completed, the machine pauses for 5 seconds and then automatically switches to the Dry Cycle for air blow.
26. During this cycle, air from the compressor is blown in the filter plates, removing additional filtrate. Continue collecting the filtrate in the buckets at the desired time intervals.
27. When the Dry Cycle is complete and during the Pause Cycle, slowly open the residual slurry valve while holding and directing the hose into the bucket to drain excess slurry. This prevents slurry from mixing with the dried cake. This step must be done within the defined pause time.

28. After the Pause Cycle ends, the plates open and the filter cake drops into the collection pan. Ensure that there are no solids sticking to the filter. Do not scrape the cloth.
29. Weigh a large stainless steel pan. Transfer the wet filter cake to the pan and weigh the cake. Record the weight. Dry the sample in the convection oven. Weigh the dried solids. Record the weight.
30. Weigh the beaker with the feed slurry to determine the slurry weight. Record the weight. Transfer to a preweighed stainless steel pan, dry the sample in the convection oven, and weigh the dried solids. Record the weight.
31. Weigh the filtrate samples (beginning with the last sample). Record the total weight of each.
32. Weigh a large stainless steel pan. Combine all filtrate samples in the pan. Dry the combined filtrate in the convection oven and weigh and record the dry solids weight.
33. With the mixer in the feed tank running, carefully open the side drain valve on the feed tank and collect the slurry in the feed buckets. Change buckets as needed. If desired, take an additional sample to determine the final pH and solids concentration of the slurry. Transfer unwanted slurry into a waste drum.
34. When the flow from side drain valve stops, carefully close the valve. Place another bucket under the drain valve at the bottom of the tank. Turn off the mixer in the feed tank.
35. Open the drain valve at the bottom of the tank and allow the slurry to drain into the feed bucket. Change buckets as needed. Seal each bucket when completed. Transfer unwanted slurry into a waste drum.
36. When the feed tank is empty, place an empty bucket under the drain valve, and hose the tank thoroughly. Drain the tank, changing buckets as needed, and repeat until no solids remain.
37. Hose the filter cloth until the cloth is clean. Carefully hose the filter plates and filter unit to ensure that all parts are clean. It will be necessary to run the entire filter cycle to flush all solids from the feed lines.
38. Fill the feed tank to ~¾ full with water. Ensure that at least two, 2-gallon buckets are available to collect the filtrate. Close the residual slurry valve.
39. To start the filter cycle, press the MAN button twice. After the filtrate is collected, the bucket can be emptied. Continue filling and emptying the filtrate buckets over the entire filter cycle. After the filter plates have opened, hose the filter cloth to remove any solids. Open the residual slurry valve.
40. If any solids are on the filter cloth, it will be necessary to repeat the filter cycle. Before beginning the filter cycle, ensure that sufficient water is in the feed tank and that the residual slurry valve is closed.
41. Turn off the power by turning the central knob clockwise on the main control panel. Unplug the electrical and air line connections and clean the work area. Return the compressor to Room 27A.

Flotation

Cell Loading

1. Depending on desired flotation feed treatment, follow the appropriate **Hydroacoustic Cavitation Circuit** operating procedures. Follow the *Circuit Sampling* subsection if an undeslimed test is to be conducted or the *Hydrocyclone* subsection if a deslimed test is desired.

    a. Load the HAC circuit at the desired solids concentration but be aware that dilution may be required if hydrocyclone desliming is performed as the hydrocyclone underflow is more concentrated than the hydrocyclone feed.
2. Lower the impeller shaft into the flotation cell.
3. Add the slurry sample collected in item 1 until the level reaches the top of the stator.
    a. Ensure that the slurry is at the desired test solids concentration prior to introduction to the flotation cell.
4. Ensure that the air valve is closed. Turn on the motor. Record the impeller speed from the tachometer. Mix the pulp for three minutes. During this time, record the slurry pH.

Ultimate recovery testing (cont. from Cell Loading)

5. Using a microliter syringe, add 40-µL of MIBC to the cell.
6. Condition for 1 min.
7. Open the air valve and allow 5 s for the froth to develop.
8. Begin timing. Using the paddle, collect the froth product in a preweighed, labelled pan until minimal solids are observed in the froth. 'Pull' only the froth from the surface, while minimizing the collection of the cell contents. Use a wash water bottle or faucet spray hose to rinse solids from the cell walls and stator shaft and to add water to keep the cell level constant. Close the air valve when completed and record the time.
9. Set the froth product sample aside and add an additional 40-µL of MIBC to the cell.
10. Repeat steps 6-8.
11. Set the froth product sample aside and add an additional 40-µL of MIBC to the cell.
12. Repeat steps 6-8
13. Set the froth product sample aside and add 50-µL of #2 fuel oil to the cell.
    a. Utilize a separate microliter syringe to add the #2 fuel oil.
14. Condition for 4 min.
15. Repeat steps 6-8.
16. Set the froth product sample aside and empty the remaining contents of the cell (i.e., tailings) into a preweighed, labelled pan. Utilize a spray bottle or faucet spray hose to rinse all solids from the cell and stator into the pan.
17. Transfer all froth product samples and the tailings sample into a convection oven.
18. Once dried, individually weigh the pans, record the weight, and remove the material from the pans and bag, individually, for desired subsequent analyses.
    a. Dry weight of the material may be calculated as the difference between the final dry weight including the pan and the pan weight.

Flotation rate testing (cont. from Cell Loading)

5. Using a microliter syringe, add 120-µL of MIBC to the cell.
6. Condition for 1 min.
7. Open the air valve and begin timing. Take note of the time required for the froth to spill onto the cell weir (i.e., induction)
8. Once the froth spill onto the weir, again begin timing and use the paddle and collect the froth product in a preweighed, labelled pan for 15 s. 'Pull' only the froth from the

surface, while minimizing the collection of the cell contents. Use a wash water bottle or faucet spray hose to rinse solids from the cell walls and stator shaft and to add water to keep the cell level constant.

9. Set the pan the pan aside and place an additional preweighed, labelled pan under the cell weird and collect the froth by scraping for an additional 15 s.
10. Repeat steps 8-9 so that froth products are collected in separate pans for time intervals 0-15, 15-30, 30-45, 45-60, 60-90, 90-120, 120-180, and 180-240 s.
11. Close the air valve.
12. Empty the remaining contents of the cell (i.e., tailings) into a preweighed, labelled pan. Utilize a spray bottle or faucet spray hose to rinse all solids from the cell and stator into the pan.
13. Transfer all froth product samples and the tailings sample into a convection oven.
14. Once dried, individually weigh the pans, record the weight, and remove the material from the pans and bag, individually, for desired subsequent analyses.
    a. Dry weight of the material may be calculated as the difference between the final dry weight including the pan and the pan weight.

Screening

1. Riffle the desired weight of sample material for screening.
    a. 30-200 g is preferable for accurate results.
2. Select the desired sizes at which the material is to be screened and obtain the appropriate screens.
3. Ensure that the screens are in the proper order (coarse to fine sizes with a bottom pan). Place the sample on the top screen of the stack and cover with the lid. Place the stack in the Ro-Tap sieve shaker. Place the cover on the stack with the rubber stopper up. If necessary, adjust the height so that that stack cover is flush with the top of the Ro-Tap. Lower the tapping arm. Set the timer and operate for 5 minutes.
4. Remove the screen stack from the Ro-Tap. Taking care not to lose any of the material, check the screens for blinding, i.e., blockage of the screen openings by a layer of particles adhering to the mesh and to each other. If necessary, brush the underside of the screens to break up these layers, allowing the material to pass to the next finer screen. Never use a hard brush on the fine sieves.
5. Replace the screens in the Ro-Tap, and operate for an additional 10-15 minutes.
6. Weigh the material on each screen to two decimal places. Record the weight and bag each size fraction, individually.

Ash Analysis

1. Grind any material that is +140 μm prior to ash analysis.
2. Power on the ash analyzer by flipping the switch on the right side of the device upward.
3. Following power up, open the device by pressing the green button on the face of the unit.
4. Insert a clean, empty crucible is in the “home” position indicated by a small circular hole adjacent to the crucible holder.
5. Using the computer which controls the device, launch the analyzer management program by double clicking the desktop shortcut titled “TGA701 Software.” This will bring up a spreadsheet style screen with several columns.
6. In the “Name” column, enter a designation for each the samples you will be analyzing.

7. In the “Method” column, click the drop down arrow in the rightmost portion of the cell and select “ASTM D5142 Moisture Ash”.
8. Open the valves for the nitrogen and oxygen gas.
    a. Ensure that the gas pressure is to the indicated mark on each respective pressure gauge, or about 4000 kPa. This is the minimum required quantity remaining in the tanks to complete one run.
9. Click the “Analyze” button at the top left of the program screen.
10. Follow the onscreen prompt and load the crucibles then press the green blinking button on the device front face to initiate crucible weighing.
    a. Add the desired quantity of crucibles (one per each sample to be analyzed) into the holder slots on the outer portion of the carousel in a counter clockwise direction starting after the home position.
11. Follow the onscreen prompt and using a ¼ teaspoon laboratory scoop, place a single scoop of each sample into their respective crucibles then once again press the green blinking button.
12. Observe the program screen and wait 5 minutes to see that the analysis begins without a prompt indicating an error.
    a. Full analysis will take approximately four hours and the device should be intermittently checked to ensure it is running properly.
13. Once analysis is complete, turn off the nitrogen and oxygen gas.
14. Observe the temperature at the bottom of the program window and ensure that it is 30°C then press the green button to open the device hood.
15. Discard the analyzed sample then clean and return the crucibles to their holding tray.

APPENDIX B

HAC TREATMENT

	Direct wt. %											
Size interval	Untreated[1]				Son[2]				SonCav[3]			
µm	0 min	1 min	5 min	10 min	0 min	1 min	5 min	10 min	0 min	1 min	5 min	10 min
+1180	9.32	8.88	6.78	4.68	8.43	7.17	4.74	4.47	7.44	6.05	4.06	2.97
-1180+850	10.86	10.38	9.47	9.21	10.14	9.23	8.98	9.15	9.55	8.12	7.75	6.71
-850+600	10.97	10.31	12.00	12.54	9.89	11.48	9.67	9.97	10.07	11.43	11.42	10.74
-600+425	11.54	10.97	11.07	11.66	10.88	11.20	10.66	10.69	11.18	11.40	11.24	10.77
-425+300	9.49	8.97	8.54	8.74	9.16	8.86	8.91	8.71	9.53	9.23	9.11	8.73
-300+212	8.30	7.98	7.39	7.41	8.35	7.87	8.07	7.87	8.73	8.40	8.03	7.89
-212+150	6.76	6.60	6.68	6.48	6.99	7.39	6.86	6.75	7.21	7.69	7.36	7.26
-150+106	5.63	5.74	5.68	5.45	6.10	6.58	6.10	5.75	6.83	7.05	6.45	6.31
-106+75	4.53	4.71	4.87	4.73	4.90	5.01	5.18	4.83	4.67	5.10	5.42	5.53
-75+53	3.57	3.90	3.70	3.60	3.93	3.77	4.28	3.49	4.10	3.82	3.96	4.21
-53+38	3.18	3.65	2.88	2.84	3.37	2.61	3.90	3.02	2.70	2.47	2.97	3.21
-38+25	1.69	2.19	2.54	2.53	3.06	2.46	2.66	1.73	1.95	1.85	2.61	2.64
-25	14.17	15.72	18.38	20.13	14.80	16.39	20.00	23.57	16.02	17.39	19.61	23.02
Total	100	100	100	100	100	100	100	100	100	100	100	100

[1]No ultrasonic treatment without flow being diverted through the cavitation plate

[2]100% power ultrasonication without flow being diverted through the cavitation plate

[3]100% power ultrasonication with all flow being diverted through the cavitation plate

	Ash %											
Size interval	Untreated				Son				SonCav			
µm	0 min	1 min	5 min	10 min	0 min	1 min	5 min	10 min	0 min	1 min	5 min	10 min
+1180	14.14	13.45	12.13	14.25	13.86	9.74	11.74	10.68	12.07	9.12	8.16	9.36
-1180+850	14.36	15.22	10.18	10.79	14.23	11.66	9.26	10.81	13.81	10.19	7.56	9.24
-850+600	19.26	18.76	15.41	15.91	19.09	14.24	12.31	13.37	16.76	10.72	8.76	9.71
-600+425	25.53	25.91	20.89	19.24	24.68	14.27	14.97	15.82	20.08	14.72	10.4	12.25
-425+300	29.02	26.83	20.16	25.07	28.63	23.35	22.46	17.99	26.12	20.87	17.44	13.31
-300+212	33.34	30.02	24.00	27.92	34.26	27.15	24.19	24.21	30.28	27.42	22.33	16.67
-212+150	37.87	33.01	30.31	31.71	35.52	35.41	31.11	28.01	33.62	30.51	24.4	23.4
-150+106	38.24	36.02	35.48	33.08	39.67	39.93	30.95	29.18	39.61	34.61	31.32	26.93
-106+75	39.99	39.59	38.96	37.22	37.21	40.32	36.83	33.23	42.59	38.89	36.26	34.25
-75+53	43.16	43.93	43.09	39.48	44.54	43.53	42.26	34.07	42.55	46.67	39.9	35.6
-53+38	48.67	46.35	45.38	42.05	46.88	44.67	43.86	44.12	50.97	48.33	43.15	41.37
-38+25	59.14	57.71	53.34	49.58	53.54	56.08	53.72	54.78	58.34	57.17	51.69	49.02
-25	74.71	74.10	74.54	74.1	75.01	75.99	74.56	70.91	73.86	73.61	72.98	71.82
Head (Calculated)	34.65	34.78	33.34	34.56	35.46	33.11	33.91	33.32	34.50	32.12	30.77	31.69

APPENDIX C

HYDROCYCLONE SEPARATION

	Sample A, Direct Wt. %						
Size interval	Untreated[1]		Son[2]		SonCav[3]		Actual
µm	UF	OF	UF	OF	UF	OF	Feed
-3350+1180	15.00	0.00	5.66	0.00	6.42	0.00	9.32
-1180+850	12.55	0.00	9.91	0.00	9.82	0.00	10.86
-850+600	12.36	0.00	13.95	0.00	11.05	0.00	10.97
-600+425	11.70	0.00	13.35	0.00	12.31	0.00	11.54
-425+300	9.63	0.00	10.63	0.00	10.73	0.00	9.49
-300+212	8.26	0.00	9.45	0.00	10.02	0.00	8.30
-212+150	7.05	0.49	8.38	0.04	8.67	0.00	6.76
-150+106	5.87	1.43	7.08	0.30	7.40	0.11	5.63
-106+75	4.59	2.05	5.30	0.93	6.19	0.65	4.53
-75+53	3.20	3.77	4.38	2.12	4.47	1.56	3.57
-53+38	2.42	7.09	3.06	4.66	3.47	4.77	3.18
-38+25	1.60	8.89	2.25	7.60	2.57	8.02	1.69
-25+18.5	1.68	10.22	2.01	9.44	1.40	9.42	2.17
-18.5+13.08	1.34	11.34	1.42	10.74	2.88	10.90	1.93
-13.08+9.25	0.82	9.82	1.00	10.74	0.68	10.69	1.88
-9.25+6.54	0.60	10.73	0.69	12.63	0.92	12.54	1.45
-6.54+4.62	0.47	9.35	0.51	10.57	0.65	10.94	1.28
-4.62+3.27	0.35	8.32	0.42	9.24	0.07	9.71	1.21
-3.27+2.31	0.21	3.84	0.24	4.36	0.07	4.20	1.08
-2.31+1.64	0.22	6.93	0.23	8.68	0.14	8.51	0.94
-1.64+1.16	0.10	3.91	0.10	4.61	0.07	4.66	0.76
-1.16+0.82	0.00	0.51	0.00	0.60	0.00	0.58	0.55
-.82+.58	0.00	0.00	0.00	0.00	0.00	0.00	0.39
-.58+.41	0.00	0.13	0.00	1.06	0.00	0.94	0.29
-.41+.29	0.00	1.11	0.00	1.69	0.00	1.78	0.18

[1]No ultrasonic treatment without flow being diverted through the cavitation plate

[2]100% power ultrasonication without flow being diverted through the cavitation plate

[3]100% power ultrasonication with all flow being diverted through the cavitation plate

	Sample A, Klimpel								
							Wt. % Feed Recon. ($p'(x_i)$)		
Size interval	Untreated		Son		SonCav		Untreated	Son	SonCav
µm	$\lvert p(x_i)-q(x_i)\rvert$	$\lvert t(x_i)-p(x_i)\rvert$	$\lvert p(x_i)-q(x_i)\rvert$	$\lvert t(x_i)-p(x_i)\rvert$	$\lvert p(x_i)-q(x_i)\rvert$	$\lvert t(x_i)-p(x_i)\rvert$			
-3350+1180	9.32	5.69	9.32	3.66	9.32	2.89	13.78	4.99	5.65
-1180+850	10.86	1.69	10.86	0.95	10.86	1.04	11.53	8.73	8.64
-850+600	10.97	1.39	10.97	2.98	10.97	0.08	11.36	12.29	9.72
-600+425	11.54	0.17	11.54	1.81	11.54	0.77	10.75	11.76	10.83
-425+300	9.49	0.14	9.49	1.14	9.49	1.23	8.84	9.36	9.43
-300+212	8.30	0.04	8.30	1.14	8.30	1.72	7.59	8.32	8.81
-212+150	6.27	0.29	6.72	1.62	6.76	1.91	6.51	7.39	7.62
-150+106	4.20	0.25	5.32	1.45	5.51	1.77	5.51	6.27	6.52
-106+75	2.49	0.06	3.60	0.77	3.88	1.65	4.38	4.78	5.52
-75+53	0.20	0.37	1.45	0.81	2.00	0.91	3.24	4.11	4.12
-53+38	3.92	0.76	1.48	0.12	1.60	0.29	2.80	3.25	3.63
-38+25	7.20	0.09	5.92	0.57	6.33	0.88	2.19	2.89	3.23
-25+18.5	8.05	0.50	7.27	0.17	7.25	0.77	2.38	2.89	2.37
-18.5+13.08	9.42	0.58	8.82	0.51	8.98	0.96	2.16	2.53	3.85
-13.08+9.25	7.93	1.06	8.85	0.89	8.80	1.20	1.55	2.16	1.89
-9.25+6.54	9.27	0.86	11.17	0.76	11.09	0.54	1.42	2.11	2.32
-6.54+4.62	8.07	0.81	9.29	0.77	9.67	0.63	1.19	1.71	1.89
-4.62+3.27	7.11	0.86	8.03	0.78	8.51	1.13	1.00	1.47	1.23
-3.27+2.31	2.76	0.87	3.27	0.84	3.11	1.01	0.51	0.73	0.57
-2.31+1.64	5.99	0.73	7.73	0.72	7.57	0.80	0.76	1.23	1.15
-1.64+1.16	3.15	0.67	3.85	0.67	3.90	0.70	0.41	0.63	0.62
-1.16+0.82	0.05	0.55	0.04	0.55	0.03	0.55	0.04	0.07	0.07
-.82+.58	0.39	0.39	0.39	0.39	0.39	0.39	0.00	0.00	0.00
-.58+.41	0.16	0.29	0.77	0.29	0.65	0.29	0.01	0.13	0.11
-.41+.29	0.93	0.18	1.51	0.18	1.60	0.18	0.09	0.20	0.21
Σ	137.18	12.18	143.94	19.46	146.11	20.00	100	100	100
C=T/Q	11.27		7.40		7.30				
C/(1+C)=T/P	0.92		0.88		0.88				

	Sample A, Size Selectivity											
Geometric mean size	$S_a(x_i)$			$c(x_i)$			$s_f(x_i)$			$(s_a(x_i)-s_f(x_i))^2$		
µm	Untreated	Son	SonCav	Untreated	Son	SonCav	Untreated	Son	SonCav	Untreated	Son	SonCav
1988.22	1.00	1.00	1.00	1.00	1.00	1.00	1.00	1.00	1.00	7.04E-07	4.79E-08	2.48E-07
1001.50	1.00	1.00	1.00	1.00	1.00	1.00	1.00	1.00	1.00	5.38E-06	5.65E-07	2.12E-06
714.14	1.00	1.00	1.00	0.99	1.00	1.00	1.00	1.00	1.00	1.47E-05	1.90E-06	6.08E-06
504.98	1.00	1.00	1.00	0.99	1.00	1.00	0.99	1.00	1.00	4.08E-05	6.61E-06	1.79E-05
357.07	1.00	1.00	1.00	0.99	0.99	0.99	0.99	1.00	0.99	1.13E-04	2.29E-05	5.26E-05
252.19	1.00	1.00	1.00	0.98	0.99	0.99	0.98	0.99	0.99	3.12E-04	7.92E-05	1.54E-04
178.33	0.99	1.00	1.00	0.96	0.98	0.98	0.97	0.98	0.98	5.29E-04	2.52E-04	4.48E-04
126.10	0.98	0.99	1.00	0.94	0.96	0.96	0.95	0.97	0.96	6.91E-04	5.96E-04	1.14E-03
89.16	0.96	0.98	0.99	0.90	0.93	0.94	0.92	0.95	0.94	1.45E-03	9.78E-04	2.08E-03
63.05	0.91	0.94	0.95	0.84	0.88	0.89	0.88	0.90	0.90	5.96E-04	1.21E-03	2.79E-03
44.88	0.79	0.83	0.84	0.76	0.80	0.83	0.82	0.84	0.84	7.89E-04	9.37E-05	6.31E-06
30.82	0.67	0.69	0.70	0.64	0.67	0.73	0.74	0.73	0.75	4.40E-03	2.25E-03	2.67E-03
21.51	0.65	0.61	0.52	0.51	0.52	0.61	0.64	0.61	0.64	8.31E-05	6.49E-06	1.35E-02
15.56	0.57	0.49	0.66	0.39	0.37	0.49	0.55	0.49	0.52	3.41E-04	2.38E-06	1.89E-02
11.00	0.49	0.41	0.32	0.28	0.24	0.36	0.47	0.39	0.40	2.76E-04	4.53E-04	6.55E-03
7.78	0.38	0.29	0.35	0.19	0.15	0.24	0.40	0.31	0.29	2.66E-04	3.69E-04	3.08E-03
5.50	0.36	0.26	0.30	0.12	0.08	0.16	0.35	0.26	0.21	6.87E-05	2.68E-05	7.93E-03
3.89	0.32	0.25	0.05	0.08	0.05	0.10	0.32	0.23	0.16	7.62E-08	6.62E-04	1.12E-02
2.75	0.38	0.29	0.11	0.05	0.03	0.06	0.30	0.21	0.12	7.10E-03	6.30E-03	1.56E-04
1.94	0.26	0.16	0.11	0.03	0.01	0.04	0.28	0.20	0.10	6.23E-04	1.52E-03	1.04E-04
1.37	0.22	0.13	0.10	0.02	0.01	0.02	0.28	0.20	0.09	3.49E-03	3.67E-03	1.19E-04
0.97	0.00	0.00	0.00	0.01	0.00	0.01	0.27	0.19	0.08	7.32E-02	3.70E-02	5.92E-03
0.69	0.00	0.00	0.00	0.01	0.00	0.01	0.27	0.19	0.07	7.15E-02	3.64E-02	5.20E-03
0.49	0.00	0.00	0.00	0.00	0.00	0.00	0.27	0.19	0.07	7.06E-02	3.61E-02	4.81E-03
0.34	0.00	0.00	0.00	0.00	0.00	0.00	0.26	0.19	0.07	7.00E-02	3.59E-02	4.58E-03
									Σ	2.12E-02	1.85E-02	7.09E-02

	Sample B, Direct Wt. %						
Size interval	Untreated[1]		Son[2]		SonCav[3]		Actual
µm	UF	OF	UF	OF	UF	OF	Feed
-1184+837	0.00	0.00	0.00	0.00	0.00	0.00	0.00
-837+591.9	0.20	0.00	0.33	0.00	0.20	0.00	0.00
-591.9+418.6	0.98	0.00	1.06	0.00	0.95	0.00	0.00
-418.6+296	1.84	0.00	2.01	0.00	1.86	0.00	0.18
-296+209.3	3.38	0.00	4.35	0.00	3.59	0.00	0.94
-209.3+148	4.27	0.00	5.89	0.04	4.69	0.04	1.53
-148+104.6	5.06	0.36	5.91	0.12	5.21	0.12	2.14
-104.6+73.99	7.07	0.96	6.83	0.24	6.64	0.24	3.08
-73.99+52.32	10.05	1.74	9.43	0.97	9.72	1.00	4.71
-52.32+37	12.25	3.63	11.73	3.11	12.44	3.09	6.83
-37+26.16	11.57	6.50	11.05	5.57	11.66	5.53	8.10
-26.16+18.5	8.93	8.73	8.56	7.38	8.97	7.33	8.24
-18.5+13.08	7.24	9.57	6.98	10.19	7.30	10.17	8.21
-13.08+9.25	5.92	9.50	5.68	11.22	5.96	11.22	8.17
-9.25+6.54	4.52	9.41	4.36	10.50	4.56	10.46	7.67
-6.54+4.62	3.53	9.56	3.42	10.03	3.54	9.97	7.16
-4.62+3.27	2.93	9.52	2.85	9.68	2.91	9.63	6.63
-3.27+2.31	2.51	8.87	2.45	8.86	2.51	8.82	6.02
-2.31+1.64	2.21	7.89	2.15	7.88	2.19	7.88	5.43
-1.64+1.16	1.91	6.12	1.80	6.27	1.85	6.32	4.60
-1.16+0.82	1.54	3.91	1.39	4.06	1.44	4.16	3.55
-.82+.58	1.15	2.22	1.02	2.31	1.06	2.39	2.73
-.58+.41	0.83	1.19	0.73	1.23	0.76	1.29	2.19
-.41+.29	0.10	0.32	0.00	0.33	0.00	0.34	1.48

[1]No ultrasonic treatment without flow being diverted through the cavitation plate

[2]100% power ultrasonication without flow being diverted through the cavitation plate

[3]100% power ultrasonication with all flow being diverted through the cavitation plate

	Sample B, Klimpel								
							Wt. % Feed Recon. ($p'(x_i)$)		
Size interval	Untreated		Son		SonCav		Untreated	Son	SonCav
µm	$\lvert p(x_i)-q(x_i)\rvert$	$\lvert t(x_i)-p(x_i)\rvert$	$\lvert p(x_i)-q(x_i)\rvert$	$\lvert t(x_i)-p(x_i)\rvert$	$\lvert p(x_i)-q(x_i)\rvert$	$\lvert t(x_i)-p(x_i)\rvert$			
-1184+837	0.00	0.00	0.00	0.00	0.00	0.00	0.00	0.00	0.00
-837+591.9	0.00	0.20	0.00	0.33	0.00	0.20	0.08	0.14	0.08
-591.9+418.6	0.00	0.98	0.00	1.06	0.00	0.95	0.37	0.44	0.40
-418.6+296	0.18	1.66	0.18	1.83	0.18	1.68	0.69	0.83	0.79
-296+209.3	0.94	2.45	0.94	3.42	0.94	2.65	1.26	1.80	1.52
-209.3+148	1.53	2.73	1.49	4.35	1.49	3.16	1.59	2.45	2.01
-148+104.6	1.78	2.92	2.03	3.76	2.03	3.07	2.11	2.51	2.27
-104.6+73.99	2.12	3.99	2.84	3.76	2.84	3.57	3.23	2.96	2.95
-73.99+52.32	2.97	5.34	3.74	4.72	3.72	5.00	4.83	4.46	4.68
-52.32+37	3.19	5.43	3.72	4.91	3.74	5.61	6.84	6.67	7.04
-37+26.16	1.60	3.48	2.53	2.95	2.56	3.56	8.38	7.83	8.12
-26.16+18.5	0.49	0.69	0.86	0.32	0.91	0.73	8.80	7.87	8.02
-18.5+13.08	1.36	0.97	1.98	1.23	1.96	0.90	8.70	8.87	8.96
-13.08+9.25	1.32	2.26	3.05	2.49	3.05	2.21	8.17	8.94	9.00
-9.25+6.54	1.75	3.15	2.83	3.31	2.80	3.10	7.59	7.97	7.97
-6.54+4.62	2.39	3.63	2.86	3.74	2.80	3.62	7.32	7.30	7.25
-4.62+3.27	2.89	3.71	3.05	3.79	3.00	3.73	7.07	6.86	6.79
-3.27+2.31	2.85	3.51	2.84	3.57	2.80	3.51	6.51	6.22	6.15
-2.31+1.64	2.46	3.22	2.46	3.27	2.45	3.23	5.78	5.52	5.48
-1.64+1.16	1.52	2.69	1.67	2.80	1.72	2.75	4.56	4.43	4.43
-1.16+0.82	0.36	2.01	0.51	2.16	0.61	2.11	3.03	2.96	3.01
-.82+.58	0.51	1.58	0.42	1.71	0.34	1.67	1.82	1.78	1.83
-.58+.41	1.00	1.36	0.96	1.46	0.90	1.43	1.05	1.03	1.06
-.41+.29	1.16	1.38	1.16	1.48	1.14	1.48	0.24	0.19	0.20
Σ	31.35	52.99	39.05	55.60	38.98	53.24	100	100	100
C=T/Q	0.59		0.70		0.73				
Coarse yield= C/(1+C)=T/P	0.37		0.41		0.42				

	Sample B, Size Selectivity											
Geometric mean size	$S_a(x_i)$			$c(x_i)$			$s_f(x_i)$			$(s_a(x_i)-s_f(x_i))^2$		
μm	Untreated	Son	SonCav	Untreated	Son	SonCav	Untreated	Son	SonCav	Untreated	Son	SonCav
995.49	1.00	1.00	1.00	1.00	1.00	1.00	1.00	1.00	1.00	6.45E-06	1.36E-07	1.69E-07
703.96	1.00	1.00	1.00	0.99	1.00	1.00	1.00	1.00	1.00	2.16E-05	6.30E-07	7.51E-07
497.73	1.00	1.00	1.00	0.99	1.00	1.00	0.99	1.00	1.00	7.21E-05	2.91E-06	3.33E-06
351.97	1.00	1.00	1.00	0.98	1.00	1.00	0.98	1.00	1.00	2.38E-04	1.34E-05	1.47E-05
248.90	1.00	1.00	1.00	0.97	0.99	0.99	0.97	0.99	0.99	7.79E-04	6.15E-05	6.45E-05
176.00	1.00	0.99	0.99	0.94	0.98	0.98	0.95	0.98	0.98	2.48E-03	4.74E-05	2.39E-05
124.45	0.89	0.97	0.97	0.90	0.96	0.96	0.91	0.96	0.97	4.43E-04	5.72E-05	1.96E-05
87.98	0.81	0.95	0.95	0.83	0.91	0.92	0.85	0.93	0.93	1.54E-03	6.02E-04	4.95E-04
62.21	0.77	0.87	0.88	0.72	0.83	0.84	0.76	0.86	0.87	1.00E-04	1.72E-04	1.19E-04
44.00	0.67	0.73	0.75	0.59	0.69	0.71	0.65	0.75	0.76	3.30E-04	4.05E-04	2.06E-04
31.11	0.51	0.58	0.61	0.44	0.51	0.54	0.52	0.60	0.62	4.39E-05	1.90E-04	1.54E-04
22.00	0.38	0.45	0.47	0.30	0.33	0.36	0.40	0.44	0.47	5.63E-04	3.59E-05	1.14E-05
15.56	0.31	0.32	0.34	0.19	0.19	0.21	0.31	0.32	0.35	4.09E-06	1.36E-06	9.04E-06
11.00	0.27	0.26	0.28	0.11	0.10	0.11	0.24	0.25	0.27	7.09E-04	1.78E-04	1.45E-04
7.78	0.22	0.23	0.24	0.06	0.05	0.06	0.20	0.21	0.22	3.60E-04	2.96E-04	3.64E-04
5.50	0.18	0.19	0.21	0.04	0.02	0.03	0.18	0.19	0.20	1.04E-06	2.67E-05	4.86E-05
3.89	0.15	0.17	0.18	0.02	0.01	0.01	0.16	0.18	0.19	1.16E-04	5.01E-05	4.84E-05
2.75	0.14	0.16	0.17	0.01	0.00	0.01	0.16	0.17	0.18	1.82E-04	1.16E-04	1.03E-04
1.94	0.14	0.16	0.17	0.01	0.00	0.00	0.15	0.17	0.18	1.13E-04	1.10E-04	1.08E-04
1.37	0.16	0.17	0.18	0.00	0.00	0.00	0.15	0.17	0.18	2.82E-05	5.41E-06	4.61E-06
0.97	0.19	0.19	0.20	0.00	0.00	0.00	0.15	0.17	0.18	1.56E-03	5.87E-04	6.01E-04
0.69	0.23	0.24	0.24	0.00	0.00	0.00	0.15	0.17	0.18	7.36E-03	4.50E-03	4.46E-03
0.49	0.29	0.29	0.30	0.00	0.00	0.00	0.15	0.17	0.18	2.09E-02	1.56E-02	1.54E-02
0.34	0.16	0.00	0.00	0.00	0.00	0.00	0.15	0.17	0.18	1.23E-04	2.88E-02	3.14E-02
									Σ	8.13E-03	2.37E-03	1.94E-03

APPENDIX D

SPIRAL CONCENTRATION

	Untreated, 12.2 gpm							
Size interval	FEED		CC		MID		REF	
µm	Wt. %	% Ash	Wt. %	% Ash	Wt. %	% Ash	Wt. %	% Ash
+1180	13.80	21.91	30.08	16.24	13.51	64.38	9.21	82.02
-1180+850	13.26	25.73	20.66	9.01	12.99	50.63	12.44	84.32
-850+600	14.63	33.36	17.50	6.32	14.17	33.07	14.77	83.08
-600+425	13.14	30.61	10.20	5.25	15.44	16.59	15.53	78.53
-425+300	9.43	39.03	4.75	4.63	11.93	12.40	13.01	75.15
-300+212	8.10	40.47	3.14	4.20	9.01	12.24	10.87	71.59
-212+150	6.57	45.59	2.55	5.32	6.29	13.88	8.13	69.25
-150+106	5.10	41.62	2.21	5.63	4.35	18.67	5.60	70.40
-106+75	3.75	42.68	1.80	10.75	3.15	29.81	3.60	72.45
-75+53	2.74	50.88	1.32	24.74	2.38	53.13	1.98	78.24
-53+38	1.87	66.63	0.94	49.09	1.88	70.74	1.43	82.34
-38+25	1.37	76.66	0.59	63.73	0.88	76.95	0.55	83.41
-25	6.24	86.53	4.28	84.76	4.02	86.17	2.89	90.52
Head	-	37.59	-	15.64	-	35.29	-	79.01
Head (Calculated)		38.11		13.98		34.46		78.04

	Son, 12.2 gpm							
Size interval	FEED		CC		MID		REF	
µm	Wt. %	% Ash	Wt. %	% Ash	Wt. %	% Ash	Wt. %	% Ash
+1180	7.41	21.22	13.25	19.14	6.93	62.96	6.29	81.45
-1180+850	12.71	25.24	17.18	8.80	8.90	50.89	10.10	80.14
-850+600	13.94	21.80	19.20	6.97	10.99	32.10	12.44	78.82
-600+425	12.77	28.76	12.30	6.11	14.90	14.75	13.58	74.37
-425+300	10.06	29.18	6.02	5.23	13.00	10.15	12.51	66.16
-300+212	8.37	37.17	4.11	5.35	10.54	9.54	11.42	60.09
-212+150	6.79	35.16	3.30	5.93	7.22	10.25	9.35	58.52
-150+106	5.42	34.81	2.95	7.63	5.06	14.06	7.03	61.75
-106+75	4.20	40.36	2.66	10.65	3.77	26.91	4.87	65.16
-75+53	2.80	44.51	2.46	19.39	3.31	45.13	2.90	66.99
-53+38	2.03	52.65	2.00	33.13	2.54	55.72	1.84	70.45
-38+25	1.48	65.35	1.20	52.43	1.55	68.61	1.31	76.70
-25	12.01	82.00	13.37	80.21	11.30	82.45	6.39	85.20
Head	-	35.64	-	18.28	-	31.16	-	69.85
Head (Calculated)		36.64		19.87		32.70		70.92

	SonCav, 12.2 gpm							
Size interval	FEED		CC		MID		REF	
µm	Wt. %	% Ash	Wt. %	% Ash	Wt. %	% Ash	Wt. %	% Ash
+1180	4.15	12.88	7.87	10.80	2.06	42.66	1.03	68.17
-1180+850	9.00	11.58	17.40	8.20	4.97	33.03	2.88	66.39
-850+600	13.71	11.59	19.83	6.84	8.99	21.97	6.08	64.87
-600+425	13.02	15.22	14.61	6.43	13.33	15.44	9.56	60.25
-425+300	9.95	17.93	9.12	5.90	14.43	11.47	11.96	56.32
-300+212	8.62	19.57	5.78	5.75	13.09	10.01	14.50	52.80
-212+150	7.57	22.78	3.73	6.05	9.94	9.84	13.44	52.86
-150+106	5.89	30.29	3.07	6.95	6.45	11.39	11.80	54.02
-106+75	4.76	28.47	2.58	9.28	4.69	18.58	8.71	61.63
-75+53	4.00	34.09	1.95	14.11	4.02	31.93	5.36	62.87
-53+38	3.64	32.22	1.79	23.66	3.31	39.34	3.80	64.06
-38+25	1.71	48.73	1.70	37.63	2.11	58.51	2.62	66.21
-25	13.97	76.91	10.56	76.16	12.61	76.61	8.27	80.12
Head	-	26.51	-	15.20	-	23.74	-	61.31
Head (Calculated)		27.60		15.50		25.58		59.71

	Untreated, 26.6 gpm					
Size interval	CC		MID		REF	
µm	Wt. %	% Ash	Wt. %	% Ash	Wt. %	% Ash
+1180	23.34	16.36	8.58	69.79	7.52	83.48
-1180+850	17.44	12.93	13.54	65.42	10.57	85.66
-850+600	13.98	9.32	12.47	51.80	14.99	84.77
-600+425	10.40	8.85	12.64	33.05	16.29	84.41
-425+300	6.88	8.00	12.16	20.88	12.65	80.99
-300+212	5.05	8.71	10.32	17.11	11.38	79.47
-212+150	4.15	8.38	8.11	19.94	9.01	74.36
-150+106	3.59	11.86	5.77	35.11	6.19	78.49
-106+75	3.02	19.95	4.61	51.18	3.83	78.47
-75+53	2.09	38.39	3.09	67.30	2.42	80.36
-53+38	2.09	56.60	2.49	74.59	1.53	82.81
-38+25	0.86	73.32	0.99	78.75	0.72	84.83
-25	7.12	83.89	5.24	86.50	2.90	89.30
Head	-	17.86	-	45.08	-	83.27
Head (Calculated)		19.25		45.03		82.05

	Son, 26.6 gpm					
Size interval	CC		MID		REF	
µm	Wt. %	% Ash	Wt. %	% Ash	Wt. %	% Ash
+1180	10.60595	20.45	6.54	69.36	5.02	84.14
-1180+850	15.1031	9.73	9.91	58.43	9.74	82.96
-850+600	14.75121	8.24	10.87	44.47	12.46	82.44
-600+425	11.732	7.48	12.75	28.37	14.30	80.56
-425+300	8.03716	7.11	12.18	17.91	13.16	75.88
-300+212	5.932859	7.10	10.99	15.69	12.22	73.24
-212+150	4.729397	8.04	7.97	18.34	10.25	71.02
-150+106	4.074882	10.70	5.93	30.05	7.63	72.19
-106+75	3.561123	18.43	4.88	45.75	4.78	72.57
-75+53	2.822155	26.57	3.92	55.55	2.56	71.96
-53+38	2.216905	38.76	2.49	62.13	1.53	74.69
-38+25	1.787599	58.20	1.76	71.54	1.03	78.72
-25	14.64565	81.25	9.80	82.23	5.32	85.52
Head	-	20.41	-	40.58		76.00
Head (Calculated)		22.75		41.21		77.63

	SonCav, 26.6 gpm					
Size interval	CC		MID		REF	
µm	Wt. %	% Ash	Wt. %	% Ash	Wt. %	% Ash
+1180	5.60	10.89	1.80	56.22	0.77	73.40
-1180+850	11.94	8.35	3.95	47.26	2.31	73.86
-850+600	16.96	7.58	7.27	36.76	5.92	73.25
-600+425	14.35	6.92	10.76	25.83	9.92	70.69
-425+300	9.50	6.71	12.67	17.97	11.31	68.42
-300+212	7.03	6.60	13.64	15.23	13.30	67.50
-212+150	5.57	7.24	11.86	16.16	14.50	66.98
-150+106	4.18	8.93	8.55	22.11	11.85	66.46
-106+75	3.45	11.91	6.73	36.82	8.37	67.40
-75+53	3.17	20.53	5.63	49.77	5.45	67.34
-53+38	3.22	21.86	4.57	48.81	3.79	61.70
-38+25	1.31	46.02	2.19	65.03	1.28	68.60
-25	13.73	76.34	10.38	76.69	11.22	80.31
Head	-	15.37	-	32.31	-	70.23
Head (Calculated)		18.62		33.39		69.47

	Untreated, 31.6 gpm					
Size interval	CC		MID		REF	
µm	Wt. %	% Ash	Wt. %	% Ash	Wt. %	% Ash
+1180	21.88	14.79	6.67	68.00	7.69	84.42
-1180+850	17.89	11.00	11.40	64.19	10.02	85.85
-850+600	14.53	10.04	13.69	54.89	14.87	85.98
-600+425	10.99	9.27	14.02	37.90	15.82	83.92
-425+300	7.29	8.21	11.93	23.53	12.50	81.22
-300+212	5.32	8.38	10.70	19.64	11.18	78.89
-212+150	4.38	9.28	8.04	24.38	8.92	78.61
-150+106	3.70	12.08	6.39	38.06	6.27	77.69
-106+75	2.94	21.60	4.94	54.95	3.90	79.21
-75+53	1.98	35.49	3.79	66.22	2.51	79.83
-53+38	1.82	57.15	2.34	76.16	1.56	83.12
-38+25	0.86	73.23	1.63	80.38	0.61	83.54
-25	6.41	86.92	4.45	86.72	4.16	90.39
Head	-	20.66	-	46.80	-	83.21
Head (Calculated)		18.16		46.17		82.66

	Son, 31.6 gpm					
Size interval	CC		MID		REF	
µm	Wt. %	% Ash	Wt. %	% Ash	Wt. %	% Ash
+1180	9.20	21.53	5.97	38.24	4.18	81.82
-1180+850	13.24	10.61	9.96	33.61	8.12	82.81
-850+600	16.72	8.59	12.87	30.49	11.21	81.06
-600+425	13.35	7.41	13.06	32.08	13.89	79.43
-425+300	8.29	7.08	10.68	22.96	13.78	76.70
-300+212	6.29	7.13	9.66	22.81	12.90	72.58
-212+150	4.76	8.03	7.46	27.05	11.06	70.85
-150+106	3.96	11.97	5.80	31.08	8.38	71.04
-106+75	3.34	17.36	4.60	41.89	5.34	73.77
-75+53	2.99	25.39	3.68	47.67	2.89	71.27
-53+38	2.04	38.67	2.14	52.83	1.74	73.14
-38+25	1.76	57.84	2.03	66.87	1.11	77.76
-25	14.07	80.80	12.09	81.14	5.40	85.33
Head	-	20.94		36.03	-	77.19
Head (Calculated)		22.21		38.20		76.73

	SonCav, 31.6 gpm					
Size interval	CC		MID		REF	
µm	Wt. %	% Ash Dry	Wt. %	% Ash	Wt. %	% Ash
+1180	6.30	12.94	2.07	57.67	1.47	76.62
-1180+850	13.67	8.73	5.11	48.60	3.63	76.40
-850+600	15.49	7.59	7.34	38.28	7.85	76.04
-600+425	12.95	7.21	9.64	29.08	11.59	74.31
-425+300	9.73	6.77	12.17	19.94	11.84	70.41
-300+212	7.51	6.91	13.38	16.75	13.68	68.89
-212+150	5.43	7.50	10.72	19.05	14.40	67.70
-150+106	4.56	9.33	8.90	27.32	11.22	68.43
-106+75	3.87	14.06	7.12	40.14	7.64	69.20
-75+53	2.96	20.79	5.15	49.37	5.03	67.17
-53+38	2.58	31.93	4.01	54.88	3.07	61.24
-38+25	2.27	43.79	3.11	60.34	1.64	68.90
-25	12.67	76.25	11.29	77.11	6.94	80.73
Head	-	16.01	-	37.04	-	70.20
Head (Calculated)		18.77		36.61		70.95

Untreated, 26.6 gpm						
Size Interval	CC		MID		REF	
µm	Wt. %	% Sulfur	Wt. %	% Sulfur	Wt. %	% Sulfur
+300	72.43	3.15	59.23	4.91	64.87	6.96
-300+106	13.55	2.74	24.19	3.31	25.81	9.73
-106	14.02	4.62	16.58	6.12	9.32	8.97
Head (Calculated)	100	3.30	100	4.72	100	7.86
Head	-	3.33	-	4.62	-	8.71

Son, 26.6 gpm						
Size Interval	CC		MID		REF	
µm	Wt. %	% Sulfur	Wt. %	% Sulfur	Wt. %	% Sulfur
+300	61.18	2.99	52.25	4.79	56.40	7.48
-300+106	16.11	2.90	24.90	3.21	31.43	9.18
-106	22.71	3.08	22.84	5.38	12.17	9.62
Head (Calculated)	100	3.00	100	4.53	100	8.27
Head	-	-	-	-	-	-

SonCav, 26.6 gpm						
Size Interval	CC		MID		REF	
µm	Wt. %	% Sulfur	Wt. %	% Sulfur	Wt. %	% Sulfur
+300	60.67	2.88	36.45	4.63	33.88	6.69
-300+106	18.25	2.70	34.06	3.31	40.93	7.70
-106	21.09	4.03	29.50	5.35	25.19	8.74
Head (Calculated)	100	3.09	100	4.39	100	7.62
Head	-	-	-	-	-	-

APPENDIX E

FROTH FLOTATION

Ultimate Flotation Recovery											
Treatment	40 µL MIBC (0.5 lb/ton)		80 µL MIBC (1.0 lb/ton)		120 µL MIBC (1.5 lb/ton)		120 µL MIBC (1.5 lb/ton) and 50 µL #2 fuel oil (0.7 lb/ton)		Tailings		Total Cell (Calculated)
	Wt. %	% Ash	Wt. %	% Ash	Wt. %	% Ash	Wt. %	% Ash	Wt. %	% Ash	% Ash
As-received	30.74	35.27	24.31	35.58	11.03	56.11	10.97	51.24	18.18	90.94	51.30
Screened +500 Rep1	39.20	11.35	24.35	14.07	9.04	28.50	16.52	36.80	10.89	87.52	26.06
Screened +500 Rep2	63.19	8.44	21.50	17.21	6.91	22.30	4.11	32.19	4.27	84.86	15.53
Deslimed 50Son	57.82	29.56	8.33	52.77	5.09	62.40	19.62	35.68	9.13	90.50	39.93
Deslimed 100Son	63.59	34.09	7.59	40.16	3.80	47.08	17.14	61.26	7.88	90.85	44.17
Deslimed Cav	56.52	29.11	11.37	49.12	5.88	58.26	18.48	38.85	7.75	89.64	39.59
Deslimed 50SonCav	49.00	29.63	15.98	42.92	5.58	44.68	19.35	23.13	10.10	91.25	37.56
Deslimed 100SonCav	51.38	30.30	10.66	31.04	3.25	52.17	23.67	26.06	11.04	87.73	36.43
Undeslimed 50Son	55.68	46.37	22.40	47.44	6.10	61.97	6.19	58.27	9.62	85.78	52.09
Undeslimed 100Son	57.38	44.72	21.90	51.53	4.38	63.45	6.11	53.55	10.23	84.15	51.60
Undeslimed Cav	65.88	49.63	22.07	47.21	3.03	58.10	3.64	54.56	5.38	86.31	51.50
Undeslimed 50SonCav	62.46	49.62	22.23	44.25	4.32	57.30	4.09	47.84	6.90	85.07	51.13
Undeslimed100SonCav	65.00	50.79	18.79	47.60	3.32	62.24	3.65	44.57	9.25	85.37	53.54
Deslimed Untreated	58.33	25.93	18.92	41.30	9.58	69.51	6.41	56.75	6.76	89.98	39.32

Flotation Rate Tests			
Test ID	Test Description	Induction Time, s	Initial pH
RT1	Undeslimed, 50Son	15	8.05
RT2	Undeslimed, 100Son	12	8.15
RT3	Undeslimed, Cav	15	8.22
RT4	Deslimed, 50Son	14	8.05
RT5	Deslimed, 100Son	5	8.08
RT6	Undeslimed, 50SonCav	18	8.12
RT7	Undeslimed, 100SonCav	12	8.13
RT8	Deslimed, 50SonCav	6	7.93
RT9	Deslimed, 100SonCav	12	7.99
RT10	Undeslimed, Untreated	20	7.95
RT11	+25 μm (wet screened)	15	8.04
RT12	Undeslimed, 5 min 100SonCav	9	8.3
RT13	Deslimed, Untreated	5	8.15

Flotation Rate Tests													
Collection End Time	Wt. %												
s	RT1	RT2	RT3	RT4	RT5	RT6	RT7	RT8	RT9	RT10	RT11	RT12	RT13
15	17.75	17.23	15.84	20.93	38.19	15.78	21.24	34.84	23.47	11.58	34.60	25.91	37.20
30	8.94	11.01	7.23	12.33	11.57	7.33	8.60	12.37	9.64	6.49	10.93	10.61	12.90
45	8.38	7.65	8.82	12.73	6.03	7.37	7.14	6.11	8.29	6.16	10.03	8.11	7.30
60	7.11	6.97	6.70	6.70	3.84	5.54	6.00	4.91	7.70	5.01	6.96	6.09	5.12
90	12.24	9.62	10.05	8.26	6.28	11.45	9.13	7.30	11.45	9.98	8.99	9.60	8.25
120	7.29	5.48	7.51	4.49	3.93	7.28	6.83	4.68	7.21	6.70	4.20	6.52	5.62
180	9.33	8.85	12.52	5.50	6.30	9.85	12.06	6.40	8.30	10.80	5.00	7.83	6.46
240	6.74	7.50	7.69	3.72	5.24	8.24	6.63	4.90	3.33	7.91	2.98	5.73	4.04
Tails	22.22	25.69	23.65	25.35	18.63	27.17	22.37	18.47	20.59	35.36	16.30	19.59	13.10
Total	100	100	100	100	100	100	100	100	100	100	100	100	100

Flotation Rate Tests													
Collection End Time	% Ash												
s	RT1	RT2	RT3	RT4	RT5	RT6	RT7	RT8	RT9	RT10	RT11	RT12	RT13
15	26.04	27.22	20.40	11.87	12.26	25.21	31.67	13.39	14.36	27.17	4.87	21.57	15.11
30	31.16	32.63	21.86	13.82	17.37	26.11	32.71	18.80	18.62	33.40	7.52	31.32	23.59
45	35.59	35.12	31.88	22.45	28.78	28.65	35.41	28.21	20.89	35.64	8.51	41.20	35.68
60	42.53	43.11	37.78	26.60	38.17	36.87	40.93	40.49	29.72	33.71	10.33	50.62	47.40
90	50.81	50.25	48.58	36.00	56.77	48.85	48.23	58.77	41.52	42.77	14.35	66.75	62.34
120	57.13	54.92	54.89	45.55	68.45	54.42	55.89	71.62	56.17	43.43	22.04	73.89	73.77
180	67.60	68.03	70.57	61.24	78.07	65.42	69.15	77.34	67.50	53.64	29.65	80.36	76.17
240	75.67	77.40	78.36	72.07	82.35	74.39	74.85	79.41	70.56	64.48	30.34	84.86	79.05
Tails	76.75	81.39	79.61	83.35	81.65	79.08	79.78	64.84	67.95	78.41	45.20	82.76	75.02
Feed (calculated)	52.26	54.55	52.84	41.02	40.59	53.65	53.89	39.17	39.94	55.00	16.05	53.93	40.93

Flotation Rate Tests							
Condition	Collection Time	+25 µm			-25 µm		
	s	Interval Wt. %	Overall Wt. %	% Ash	Interval Wt. %	Overall Wt. %	% Ash
Undeslimed, Untreated	0-15	28.91	3.35	7.18	71.09	8.23	34.09
Undeslimed, 100Son		36.62	6.31	7.37	63.38	10.92	37.16
Undeslimed, 100SonCav		34.87	7.41	8.86	65.13	13.84	42.26
Undeslimed, Untreated	15-30	29.34	2.38	8.15	70.66	4.12	42.42
Undeslimed, 100Son		34.83	3.84	8.55	65.17	7.17	44.75
Undeslimed, 100SonCav		34.56	2.52	9.97	65.44	6.08	45.03
Undeslimed, Untreated	45-60	30.86	1.47	9.80	69.14	3.54	44.85
Undeslimed, 100Son		31.04	2.43	13.94	68.96	4.54	55.98
Undeslimed, 100SonCav		33.81	2.07	14.33	66.19	3.93	53.43

Flotation Rate Tests						
	Wt. %					
Collection Time	Undeslimed, Untreated		Undeslimed, 100Son		Undeslimed, 100SonCav	
s	-25 µm	+25 µm	-25 µm	+25 µm	-25 µm	+25 µm
0-15	8.23	3.35	10.92	6.31	13.84	7.41
15-30	4.59	1.91	7.18	3.84	5.63	2.97
30-45	4.20	1.97	3.72	3.92	4.22	2.92
45-60	3.47	1.55	4.81	2.16	3.97	2.03
60-120	10.81	5.87	8.77	6.33	9.06	6.90
120-240	12.66	6.06	10.35	6.00	10.15	8.54
Tails	27.62	7.73	16.89	8.79	14.07	8.30
Total Interval	71.58	28.42	62.65	37.35	60.93	39.07
Total Cell	100		100		100	

Flotation Rate Tests						
	% Ash					
Collection Time	Undeslimed, Untreated		Undeslimed, 100Son		Undeslimed, 100SonCav	
s	-25 µm	+25 µm	-25 µm	+25 µm	-25 µm	+25 µm
0-15	34.09	7.18	37.16	7.37	42.26	8.86
15-30	42.42	8.15	44.75	8.55	45.03	9.97
30-45	42.97	8.63	49.39	13.94	47.27	11.11
45-60	44.85	9.80	55.98	17.37	53.43	14.33
60-120	57.68	11	66.26	29.45	64.7	25.96
120-240	73.7	22.18	81.04	35.28	81.43	52.64
Tails	87.31	32.69	89.67	40.95	89.56	56.9

Flotation Rate Tests						
	% Total Sulfur					
Collection Time	Undeslimed, Untreated		Undeslimed, 100Son		Undeslimed, 100SonCav	
s	-25 µm	+25 µm	-25 µm	+25 µm	-25 µm	+25 µm
0-15	1.81	2.28	1.86	2.14	1.67	2.25
15-30	1.74	2.12	1.78	2.11	1.56	2.05
30-45	-	-	1.89	1.96	1.64	2.03
45-60	1.73	2.09	1.64	2.09	-	-
60-120	1.66	2.05	1.72	1.9	1.55	1.88
120-240	1.5	2.06	1.41	2	1.29	1.69
Tails	1.15	3.66	0.95	2.45	1.07	2.24

	Flotation Rate Test Tailings Analysis					
Condition	Ash %	Total Sulfur %	Pyritic %	Sulfate %	Organic %	Heating Value Btu/lb
Undeslimed, Untreated	74.80	1.66	1.36	0.04	0.26	2909
Undeslimed, 100Son	75.32	1.62	1.15	0.07	0.4	2685
Undeslimed, 100SonCav	75.74	1.51	1.26	0.05	0.2	273 5

APPENDIX F

PRESSURE FILTRATION

			Filter press feed slurry					
Batch ID	Test ID	Treatment Condition	pH at cycle start	pH at cycle end	Pressure, psi	Wet wt., g	Dry wt., g	% Solids by wt.
1	1	Untreated, nat. pH	7.88	-	125	No sample collected		
	2	Untreated, red. pH	4.34	4.88		1,542	296	19.21
2	3	1 min Son, nat. pH	8.11	-		820	145	17.74
	4	1 min Son, red. pH	4.3	5.25		756	145	19.18
3	5	1 min SonCav, nat. pH	7.54	-		792	147	18.58
	6	1 min SonCav, red. pH	4.03	-		902	156	17.33
4	7	Untreated, floc'd, nat. pH	7.91	-		894	187	20.90
	8	Untreated, floc'd, red. pH	3.95	5.26		944	191	20.18
5	9	5 min SonCav, nat. pH	8.28	-		744	161	21.69
	10	5 min SonCav, floc'd, nat. pH	8.32	-		909	199	21.89
	11	5 min SonCav, floc'd, red. pH	4.22	5.54		878	166	18.89

		Filter cake			Filtrate			
Batch ID	Test ID	Wet wt., g	Dry wt., g	% Solids by wt.	Wet wt., g	Dry wt., g	% Solids by wt.	% Ash
1	1	Failed to produce cake			5,394	Discarded		
	2	4,674	2,341	50.09	7,402	97	1.31	64.91
2	3	3,775	1,536	40.69	5,814	44	0.76	64.81
	4	4,438	2,575	58.02	10,479	43	0.41	65.17
3	5	4,065	1,842	45.31	6,449	72	1.11	62.47
	6	4,650	2,842	61.12	11,138	80	0.72	63.13
4	7	5,256	2,924	55.63	13,317	41	0.31	65.29
	8	6,950	4,450	64.03	14,637	35	0.24	67.69
5	9	4,011	2,031	50.64	6,362	35	0.55	65.94
	10	3,922	2,227	56.78	10,050	55	0.55	63.01
	11	7,400	4,730	63.92	16,168	40	0.25	63.71

Test 1		Test 2		Test 3		Test 4		Test 5		Test 6	
Sample time, s	Filtrate wt., g	Sample time, s	Filtrate wt., g	Sample time, s	Filtrate wt., g	Sample time, s	Filtrate wt., g	Sample time, s	Filtrate wt., g	Sample time, s	Filtrate wt., g
30	1,026	30	695	30	774	30	982	30	725	30	1,128
60	272	60	798	60	535	60	786	60	510	60	844
90	281	90	556	90	409	90	575	90	392	90	601
120	880	120	425	120	343	120	464	120	332	120	520
150	457	150	383	150	304	150	409	150	292	150	438
180	347	180	338	180	260	180	368	180	260	180	399
240	569	240	594	240	473	240	651	240	463	240	701
300	467	300	515	300	414	300	571	300	410	300	610
360	409	360	467	360	369	360	509	360	367	360	555
480	686	420	433	420	340	420	467	420	337	420	479
-	-	480	395	480	315	480	425	480	314	480	448
-	-	540	363	540	293	540	396	540	292	540	418
-	-	600	344	600	274	600	380	600	275	600	395
-	-	700	545	638	161	720	701	720	508	720	727
-	-	820	551	758	550	960	1,240	830	463	960	1,275
-	-	-	-	-	-	1,200	1,114	950	509	1,200	1,136
-	-	-	-	-	-	1,320	441	-	-	1,320	464
-	-	-	-	-	-	-	-	-	-	-	-
-	-	-	-	-	-	-	-	-	-	-	-
-	-	-	-	-	-	-	-	-	-	-	-
-	-	-	-	-	-	-	-	-	-	-	-
Total	5,394	-	7,402	-	5,814	-	10,479	-	6,449	-	11,138

Test 7		Test 8		Test 9		Test 10		Test 11	
Sample time, s	Filtrate wt., g	Sample time, s	Filtrate wt., g	Sample time, s	Filtrate wt., g	Sample time, s	Filtrate wt., g	Sample time, s	Filtrate wt., g
30	639	30	1,609	30	570	30	528	30	1,249
60	1,609	60	1,034	60	511	60	483	60	896
90	982	90	728	90	355	90	362	90	617
120	703	120	583	120	306	120	294	120	501
150	582	150	494	150	265	150	267	150	438
180	503	180	441	180	234	180	241	180	396
240	854	240	760	240	417	240	427	240	696
300	729	300	651	300	358	300	379	300	609
360	632	360	600	360	322	360	347	360	551
420	589	420	517	420	295	420	321	420	510
480	558	480	457	480	272	480	302	480	469
540	445	540	442	540	254	540	285	540	447
600	452	600	415	600	233	600	269	600	427
720	836	720	762	720	433	720	510	720	795
960	1,465	960	1,326	960	755	960	945	960	1,411
1,200	1,292	1,200	1,112	1,080	328	1,200	730	1,200	1,197
1,320	447	1,800	2,245	1,200	454	1,500	1,162	1,500	1,313
-	-	1,920	461	-	-	1,800	974	1,800	1,166
-	-	-	-	-	-	2,095	887	2,100	1,052
-	-	-	-	-	-	2,215	337	2,400	977
-	-	-	-	-	-	-	-	2,520	451
-	13,317	-	14,637		6,362		10,050		16,168

Test ID	Filter Cake % Ash
1	No sample collected
2	52.05
	52.33
	52.38
3	52.95
	53.47
	52.81
4	51.42
	52.21
	51.85
5	52.9
	52.75
	53.17
6	51.99
	51.81
	52.03
7	53.57
	53.51
	53.48
8	52.67
	52.6
	52.6
9	52.59
	52.44
	53.03
10	53.75
	53.98
	52.63
11	52.92
	52.89
	52.64

	Filtrate % Passing														
Size, µm	Test 2			Test 3			Test 4			Test 5			Test 6		
	Rep1	Rep2	Rep3	Rep1	Rep2	Rep3	Rep1	Rep2	Rep3	Rep1	Rep2	Rep3	Rep1	Rep2	Rep3
352	100	100	100	100	100	100	100	100	100	100	100	100	100	100	100
296	100	100	100	100	100	100	100	100	100	100	99.88	99.88	100	100	100
248.9	100	100	100	100	100	100	100	100	100	100	99.62	98.96	100	100	100
209.3	100	100	100	100	100	100	100	100	100	100	99.38	96.38	100	100	100
176	100	100	100	100	100	100	100	100	100	100	99.38	95.52	100	100	100
148	100	100	100	100	100	100	100	100	100	100	99.38	95.52	100	100	100
124.4	100	100	100	100	100	100	100	100	100	100	99.38	95.52	100	100	100
104.6	100	100	100	100	100	100	99.9	100	100	100	99.38	95.52	99.9	99.52	100
87.99	100	100	100	100	100	100	99.34	100	99.66	100	99.38	95.52	99.29	98.75	100
73.99	100	100	100	100	100	100	98.2	99.49	99.16	100	99.38	95.52	97.95	97.6	100
62.22	100	100	100	100	100	100	96.3	98.43	98.4	100	99.38	95.52	95.62	95.94	99.52
52.32	100	100	100	100	100	100	93.73	96.38	97.12	99.52	98.96	95.32	92.24	93.42	97.25
44	100	100	100	99.37	100	98.59	90.77	93.29	95.07	97.15	97.64	94.65	88.06	89.73	92.8
37	100	100	100	98.01	100	95.41	87.28	89.49	92.11	92.76	95.56	93.63	83.31	85.14	88.01
31.11	100	99.52	98.8	96.32	99.15	92.99	83.13	85.51	88.56	88.17	92.22	91.73	78.58	80.43	84.04
26.16	100	97.55	93.11	92.22	94.08	89.76	77.96	81.02	84.37	82.85	86.52	86	73.72	75.66	79.99
22.00	99.83	85.68	78.78	80.23	77.16	82.09	72.37	76.08	79.63	75	75.59	71.2	68.84	70.95	75.19
18.50	92.8	56.8	62.75	62.63	60.82	66.67	66.74	70.52	74.4	64.31	60.59	55.3	63.31	65.75	68.7
15.55	42.39	43.87	55.08	52.5	54.75	51.92	61.15	64.62	68.58	53.97	49.68	47.91	57.22	59.82	61.47
13.08	34.18	40.95	51	46.98	52.07	43.2	55.96	59.1	62.72	46.38	42.95	43.42	51.42	53.92	55.48
11.00	33.35	38.61	44.98	39.73	48.75	35.94	50	52.82	55.85	40.19	35.31	36.09	45.36	47.51	49.87
9.25	32.36	31.24	29.43	28.34	40.29	28.2	43.41	45.84	48.42	33.25	25.14	23.32	39.31	41.24	43.92
7.78	20.81	19.27	20.66	23.12	28.95	23.45	37.94	40.09	42.51	26.85	20.34	19.06	34.55	36.39	38.54
6.54	16.91	16.9	19.07	21.96	24.54	21.12	32.16	34.27	36.76	22.99	19.13	18.42	29.71	31.4	32.45
5.50	16.56	16.9	18.56	21.43	23.26	19.35	23.35	25.7	29.33	20.42	18.51	18.09	22.9	23.37	23.79
4.62	16.56	16.9	18.1	21.33	22.21	18.87	20.59	23	26.36	18.61	18.17	18.09	20.33	20.57	21.43
3.89	16.56	16.9	17.52	21.33	20.96	18.52	19.06	21.43	24.56	17.49	18.06	18.09	18.81	18.93	20.15
3.27	16.56	16.9	15.72	20.53	19.66	17.57	16.47	18.74	21.5	16.16	17.26	17.32	16.26	16.23	17.82
2.750	16.56	15.92	12.91	18.58	17.31	15.58	12.56	14.64	16.91	14.16	15.43	15.41	12.47	12.35	13.94
2.312	16.56	12.87	10.1	15.08	13.44	12.02	8.08	9.87	11.71	11.14	12.31	12.35	8.24	8.03	9.21
1.944	15.9	8.08	6.7	10.8	9.56	7.53	4.92	6.28	7.78	7.68	8.36	8.61	5.16	4.82	5.77
1.635	10.33	4.5	3.1	7.85	6.97	4.2	3.43	4.39	5.63	5.07	5.39	5.76	3.55	3.12	4.03
1.375	5.19	3.22	1.62	6.65	5.77	2.64	2.88	3.65	4.73	3.9	4.21	4.63	2.89	2.42	3.36
1.156	4.37	2.88	1.46	6.17	5.31	1.99	2.88	3.65	4.38	3.6	3.91	4.36	2.89	2.42	3.36
0.972	4.37	2.88	1.46	5.82	5.31	1.6	2.88	3.65	4.38	3.6	3.91	4.36	2.89	2.42	3.36
0.817	4.37	2.88	1.46	5.35	5.31	1.22	2.88	3.65	4.38	3.6	3.66	4.12	2.89	2.42	3.36
0.687	4.03	2.46	1.46	4.45	4.95	0.72	2.88	3.65	4.27	3.6	3.1	3.53	2.89	2.42	3.36
0.578	1.63	1.01	0.67	1.8	3.33	0.21	1.76	2.35	2.61	2.82	1.38	1.58	1.84	1.48	2.58
0.486	0.4	0	0	0.22	1.2	0	0.5	0.62	0.69	1.15	0.28	0.28	0.56	0.41	0.83
0.409	0	0	0	0	0	0	0	0	0	0.23	0	0	0	0	0